AN ABSTRACT OF THE THESIS OF

JEROME STANLEY BLANK for the Ph. D. in Chemistry
(Name) (Degree) (Major)

Date thesis is presented August 12, 1964

Title A STRUCTURE INVESTIGATION OF NITROGEN DIOXIDE:

I. GEOMETRY AND AMPLITUDES OF VIBRATION

II. QUADRATIC POTENTIAL CONSTANTS.

Abstract approved ▮▮▮▮▮▮▮▮▮▮▮▮▮▮▮
(Major professor)

The molecular structure and root-mean-square amplitudes of

vibration of gaseous nitrogen dioxide have been investigated by elec-

tron diffraction at a nozzle temperature of 380° K. The results are

$r_{N-O} = 1.202 \pm 0.0013$ Å, $r_{O \cdots O} = 2.213 \pm 0.0050$ Å, $< O-N-O =$

$134.02 \pm 0.65°$, $l_{N-O} = 0.0382 \pm 0.0025$ Å and $l_{O \cdots O} = 0.0470 \pm 0.0050$ Å.

The interatomic distances given are r_a values from the third cycle

of least-squares refinement of intensity curves and differ from the

equilibrium values r_e by small amounts; the l_a values correspondingly

differ from the l_e values. The estimated standard errors include

standard deviations derived from least-squares, deviations of the

individual photographic plates at a given camera distance, estimates

of correlation among the data, uncertainty in the constants of the

experiment, and uncertainty in the factors employed in the data reduc-

tion. These errors are clearly conservative estimates.

By combining the mean-square-amplitudes (described above) with the normal vibrational frequencies, a reasonable set of values have been obtained for the potential constants of the general quadratic function

$$2V = f_r[(\Delta r_1)^2 + (\Delta r_2)^2] + 2f_{rr}(\Delta r_1)(\Delta r_2) + f_a(r_e \Delta a)^2$$
$$+ 2f_{ra}(\Delta r_1 + \Delta r_2)(r_e \Delta a).$$

The values in millidynes/$\overset{\circ}{A}$ (with estimated standard errors) for the observed fundamental and harmonic frequencies, respectively, are

$f_r = 10.77_1 \pm 0.90_3$ and $11.15_8 \pm 1.00_1$; $f_{rr} = 2.36_8 \pm 0.90_3$ and $2.25_1 \pm 1.00_1$; $f_a = 0.96_9 \pm 0.59_9$ and $1.09_4 \pm 0.67_7$; $f_{ra} = 0.52_0 \pm 0.32_8$ and $0.53_3 \pm 0.38_5$.

In addition to the potential constants described above, various combinations of frequencies and mean-square amplitudes were investigated using a least-squares procedure. These results are expressed in terms of symmetrized compliance constants based on valence force coordinates.

The agreement between the various sets of internal potential constants and compliance constants derived in this work with those of isotopic spectroscopy suggests very strongly that mean-square amplitudes from electron diffraction (at least for small molecules composed of similar atoms) are consistent with spectroscopy data (vibrational frequencies).

A STRUCTURE INVESTIGATION OF NITROGEN DIOXIDE
I. GEOMETRY AND AMPLITUDES OF VIBRATION
II. QUADRATIC POTENTIAL CONSTANTS

by

JEROME STANLEY BLANK

A THESIS

submitted to

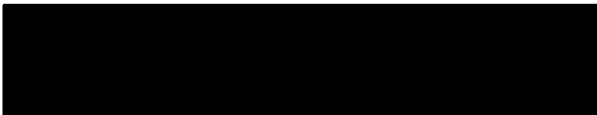OREGON STATE UNIVERSITY
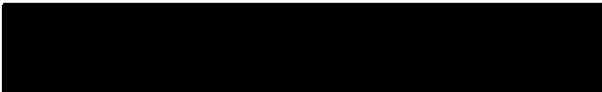
in partial fulfillment of
the requirements for the
degree of

DOCTOR OF PHILOSOPHY

August 1964

APPROVED:

Professor of Chemistry

In Charge of Major

Chairman of Department of Chemistry

Dean of Graduate School

Date thesis is presented ___August 12, 1964___

Typed by Nancy Kerley

ACKNOWLEDGMENT

TABLE OF CONTENTS

TABLE OF CONTENTS (continued)

LIST OF FIGURES

LIST OF TABLES

A STRUCTURE INVESTIGATION OF NITROGEN DIOXIDE

INTRODUCTION

An understanding of the forces operating between atoms in a molecule is one of the principle objectives of vibrational spectroscopy. When applied to simple molecules this technique yields results (vibrational frequencies) which may be interpreted in terms of the values of potential constants defining a vibrational potential function; the values of the potential constants in principle permit one to make deductions concerning bond properties.

The main trouble encountered in the application of vibrational spectroscopy to the elucidation of vibrational potential functions lies not in the experiment itself, but in the physics of the problem. Even in the simpler harmonic cases the 3n-6 (or 3n-5) data (vibrational frequencies) for a single isotopic species generally number fewer than the parameters (potential constants) one would like to determine. The investigator must thus either content himself with an assumed abbreviated potential function, or he must study other isotopic species. The desirable latter alternative is not always possible for molecules due to experimental difficulties and interpretation problems.

Recent work (22, p. 594-598; 37, p. 643-652) indicates that another possible approach to this problem lies in combining the

vibrational amplitudes of electron diffraction with the frequencies of vibrational spectroscopy. The feasibility of this approach for simple molecules constitutes the purpose of this work; that is, this work is an attempt to ascertain the reliability and consistency of the observed vibrational amplitudes of electron diffraction, using the results (quadratic potential constants) of vibrational spectroscopy of isotopic species as the principal reliability criteria. The past thorough studies of nitrogen dioxide, together with the structural simplicity of the molecule from the electron diffraction point of view, make it especially useful as a test case. This structural simplicity involves the facts that (a) there are only two, well-resolved, interatomic distances in the molecule (N-O and O $\cdots$ O), and (b) the atomic number difference of the atoms is very small whick minimizes the complicating phase shift effect (13, p. 667-671).

PART I

GEOMETRY AND AMPLITUDES OF VIBRATION

PREVIOUS STRUCTURAL INVESTIGATIONS OF NITROGEN DIOXIDE

Structural investigations of gaseous nitrogen dioxide by electron diffraction, ultraviolet, infrared and microwave spectroscopy have been carried out over a period in excess of thirty years (see bibliographies given in references cited below[1]). Though some of the early investigations (15, p. 775-784; 31, p. 738-742) indicated a non-linear symmetric structure with a large bond angle, precise values of the equilibrium N-O distance, O-N-O angle, vibrational frequencies, and the quadratic potential constants have only recently been obtained (5 p. 1040-1043; 45, p. 1248-1251; 1, p. 413-427). These recent investigations make nitrogen dioxide an especially favorable example for establishing the reliability of electron diffraction measurements in the determination of potential constants. In order to better acquaint the reader with the structural history of nitrogen dioxide, some of the results referred to above are summarized in Table 1.

---

[1]Through 1945 (19, p. 284), 1948 (9, p. 207-210), 1956 (5, p. 1040-1043), 1958 (1, p. 413-427).

ELECTRON DIFFRACTION METHOD

List of Symbols (In order of appearance in Part I of text)

n	total number of atomic nuclei in the molecule.
λ	electron wavelength of the incident beam.
v	velocity of the incident beam electrons.
c	velocity of light in vacuum.
V	electron accelerating voltage.
θ	one-half the scattering angle.
s	electron diffraction variable. $s = 4\pi\lambda^{-1} \sin \theta$.
$I(s)$	number of electrons scattered per unit solid angle per unit time.
I_o	number of electrons crossing unit area per unit time in the incident beam.
m_e	electronic mass.
ϵ	electronic charge.
h	planck's constant.
Z	atomic number.
F	atomic scattering factor for x-rays.
f_i	atomic scattering factor for electrons. $$f_i = (Z-F)_i / s^2.$$
n_{ij}	the number of times the i, jth distance occurs in

the molecule.

r_{ij} distance between ith and jth atoms in the mole-

cule as measured by electron diffraction.

r_{ij}^i instantaneous distance between ith and jth atoms

in the molecule.

r_{ij}^e equilibrium distance between ith and jth atoms in

the molecule.

l_{ij} root-mean-square vibrational amplitude cor-

responding to the i, jth distance.

$$l_{ij} = <(r_{ij}^i - r_{ij}^e)^2>^{\frac{1}{2}} .$$

S incoherent scattering factor for x-rays tabulated

by Bewilogua (4, p. 470-474) according to a

theory of Heisenberg (18, p. 737-740).

η_i phase coefficient for ith atom.

$\cos|\eta_i - \eta_j|$ phase shift for atomic pair i, j.

M(s) function expressing the effect of molecular vibra-

tions on the theoretically scattered electron

intensity.

$I_E(s)$ modified molecular intensity function.

A_{ij} variable coefficient of i, j distance normalized

with respect to k, lth distance.

$$A_{ij} = (Z-F)_i (Z-F)_j Z_k Z_l / (Z-F)_k (Z-F)_l .$$

r general distance parameter.

c'	$c' = n_{ij}A_{ij}/r_{ij}.$
c''	$c'' = \pi c'/2.$
$rD(r)$	generalized radial distribution function (Fourier sine transform of $I_E(s)$).
$rD'(r)$	experimental radial distribution function (includes the artificial temperature factor), where the improper integral in $rD(r)$ has been replaced by a finite sum.
Δs	increment in s.
$rD'(r)_{Exp}$	same as $rD'(r)$ save for the constant Δs interval which has been factored out.
$rD'(r)_{Theor}$	theoretical radial distribution function corresponding to $rD'(r)_{Exp}$.
x_i	general parameter.
$f(x_1, x_2, \ldots, x_m)$	general non-linear function.
N	number of observations.
m	total number of parameters.
x_i^o	trial value of x_i.
$f(x_1^o, x_2^o, \ldots, x_m^o)$	trial value of $f(x_1, x_2, \ldots, x_m)$.
Δx_i	correction to trial value x_i^o.
$\mathbb{F}_N$	matrix of function corresponding to adjusted values of parameters. $\mathbb{F}_N = \mathbb{F}.$

F_N^O matrix of function corresponding to trial values of parameters. $F_N^O = F^O$.

A_{Nm} matrix of derivatives. $A_{Nm} = A$.

$\overline{X}_m$ matrix of corrections to trial values of parameters. $\overline{X}_m = \overline{X}$.

F_N^{Obs} matrix of observed values of function. $F_N^{Obs} = F^{Obs}$.

V_N matrix of residuals. $V_N = V = F_N - F_N^{Obs}$.

N $N = F^{Obs} - F^O$.

P diagonal weight matrix.

B $B = A'PA$.

Y $Y = A'PN$.

$\sigma(x_i)$ standard error in x_i.

k' amplitude scale factor with respect to the modified experimental intensity function.

b arbitrary constant used in calculation of P.

x_T linear distance on the microdensitometer trace, measured from position of undiffracted beam.

x_p linear distance on photographic plate, measured from position of undiffracted beam.

$I_o(dens)$ intensity of incident microdensitometer light beam.

$I(dens)$ intensity of transmitted microdensitometer light.

μ light absorption coefficient.

D	photographic density.
D'	apparent photographic density determined from amplified trace.
ΔD_1	amplification correction to D'.
ΔD_2	scale correction to D'.
h_k	the kth camera distance (perpendicular distance from photographic plate to scattering point); k = a, b, and c denotes 478.00, 192.07 and 120.00 mm., respectively.
δ	blackness correction.
γ	proportionality constant related to the blackness correction.
$I_p(s)$	electron intensity incident on a flat photographic plate mounted perpendicular to the direction of the undiffracted electron beam.
t	exposure time.
E	exposure.
$I_p^{k(i)}(s)$	$I_p(s)$ function from the ith plate at the kth camera distance.
$I_p^{k}(s)$	composite $I_p(s)$ function from the kth camera distance.
r_s	radius on the sector measured from the undiffracted beam position.

ρ	proportionality factor related to the sector calibration (nearly constant except at small scattering angles).
$a(r_s)$	angular opening of the sector.
$g(\theta)$	sector function.
$I_t^k(s)$	total scattered intensity per unit solid angle corresponding to the kth camera distance.
$B_t^k(s)$	experimental background function corresponding to the kth camera distance.
$I_m^k(s)$	molecular intensity function corresponding to the kth camera distance.
$I_m^T(s)$	composite molecular intensity function from the three camera distances.
$t(s)$	$t(s) = I_p^a(s)/[I_p^a(s) + I_p^b(s)]$
$u(s)$	$u(s) = I_p^b(s)/[I_p^a(s) + I_p^b(s)]$
$v(s)$	$v(s) = I_p^b(s)/[I_p^b(s) + I_p^c(s)]$
$w(s)$	$w(s) = I_p^c(s)/[I_p^b(s) + I_p^c(s)]$
$I_E^T(s)_{Exp}$	experimental modified molecular intensity function (composite) from the three camera distances.
$I_E^T(s)_{Theor}$	theoretical modified molecular intensity function.
$I_E^{k(i)}(s)$	$I_E(s)$ function from the ith plate at the kth camera distance.

$I_E^k(s)$ — composite $I_E(s)$ function from the kth camera distance.

k'' — amplitude scale factor with respect to experimental radial distribution functions $(rD'(r)_{Exp})$.

M — error matrix derived from least-squares refinement.

$\overline{s}^2$ — $\overline{s}^2 = V'P V/(N-m)$.

X — matrix of parameters actually adjusted by least-squares (includes interactomic distances and vibrational amplitudes).

U — matrix of parameters of interest (includes interatomic distances, bond angle and vibrational amplitudes).

D — matrix of coefficients transforming X to U. $U = DX$.

a' — $a' = \partial(<O-N-O)/\partial r_{N-O} = -r_{O\cdots O}/r_{N-O}^2 \cos (<O-N-O/2)$.

b' — $b' = \partial(<O-N-O)/\partial r_{O\cdots O} = [r_{N-O} \cos (<O-N-O/2)]^{-1}$.

σ_i^{LS} — same as $\sigma(x_i)$

$\sigma_2(x_j)$ — standard error derived from variations in the most probable parameters as obtained from the individual photographic plates at a given camera distance.

$x_j^{a(i)}$ — most probable parameters obtained from least-squares analysis of the ith plate at 478.00 mm.

$x_j^{b(i)}$ — most probable parameters obtained from least-squares analysis of the ith plate at 192.07 mm.

x_j^a — most probable parameters obtained from least-squares analysis of the 478.00 mm composite.

x_j^b — most probable parameters obtained from least-squares analysis of the 192.07 mm composite.

$\sigma_2^{a(i)}(x_j)$ — variation in the interatomic distances and vibrational amplitudes derived from the ith plate at the 478.00 mm camera distance.

$\sigma_2^{b(i)}(x_j)$ — variation in the interatomic distances and vibrational amplitudes derived from the ith plate at the 192.07 mm camera distance.

$\sigma_2(<O-N-O)$ — same as $\sigma_2(x_j)$ where the parameter is the bond angle.

$\sigma_T(x_j)$ — overall standard error in the parameter x_j.

Scattering Theory

Since scattering theory applicable to gaseous electron diffraction has been presented by many authors (8, p. 231-239; 13, p. 667-671; 39, p. 19-199), there seems to be no need for more than a brief summary here.

In investigations of the structure of free molecules by gaseous electron diffraction, high velocity electrons[1] are used. The information obtained includes only the number (roughly) and magnitudes of interatomic distances, and their corresponding vibrational amplitudes.

Scattering theory for gaseous electron diffraction is developed by first considering the elastically scattered electrons, and then the aggregate effect of all the various kinds of inelastic scattering.

In the case of elastic scattering, a single atom is treated and then an array of atoms having fixed relative positions (a molecule). In this treatment, a single atom is represented by a small, spherically symmetrical region (a central force field) in which the potential energy of the scattered electrons is different from zero. The distribution of the scattered electrons is assumed to be observed at large

---

[1]Operating voltages fall in the range of 30-50 kilovolts. For example, if λ is equal to 0.06458 A°, one finds by calculation that v/c and V are equal to 0.352 and 34.9 kilovolts, respectively.

distances from the atom, and an asymptotic solution is sought. An important approximation often utilized in this treatment is due to Born (39, p. 116-126), and amounts to an assumption that inside the atom the amplitude of the incident wave is much greater than that of the scattered wave. Further, it is assumed that no phase shift occurs in the scattering process. The solution for a molecule, obtained by summing the scattered waves due to the atoms, is averaged over all possible orientations in order to account for the random phase relations between the waves scattered by different molecules.

Unfortunately, in the case of inelastic scattering a reasonably rigorous theory is still lacking. Therefore, in lieu of treating the aggregate effect of the inelastic scattering by molecules, the atoms are treated separately and then summed over.

The result of these considerations for the intensity of scattering per unit solid angle is

$$I(s) = I_0(8\pi^2 m_e \epsilon^2/h^2)^2 \left({\sum_{i,j}}' n_{ij}f_i f_j (sr_{ij})^{-1} \sin (sr_{ij}) \exp (-l_{ij}s^2/2) \right.$$
$$\left. + \sum_i f_i^2 + \sum_i S_i s^{-4} \right)_{\circ} \quad [1] \qquad (I, 1)$$

Equation (I, 1) is valid in the approximation of harmonic molecular vibrations. The first term on the right-hand side is the molecular structure sensitive part of the total scattered intensity. It can be

---

[1] The effect of apparatus scattering (from aperatures, etc.) is not represented in this equation.

more generally written as

$$I_0(8\pi^2 m_e \epsilon^2/h^2)^2 \sum_{i,j}' n_{ij} f_i f_j \cos|\eta_i - \eta_j| M(s)(sr_{ij})^{-1} \sin(sr_{ij}) , \quad (I, 2)$$

where $\cos|\eta_i - \eta_j|$ denotes the phase shift (13, p. 667-671) which was

assumed to be unity in the Born approximation, and $M(s)$ is some

function expressing the effect of a more general type of molecular

vibration.

Principles of Structural Determination

Several methods are currently in use for elucidation of struc-

tural information from gaseous diffraction data. All of these begin,

essentially, with the diffraction data in a form assumed to be de-

scribed by an analytical function such as equation (I, 1) or (I, 2) or a

convenient modification of them. The process by which the experi-

mental data (the photographic blackening) is converted into the de-

sired form is termed "data reduction" and will be described later in

connection with the nitrogen dioxide work. The data in the chosen

form may be called the "experimental intensity curve" or "function, "

or the "radial distribution curve" or "function, " the latter being the

Fourier sine transform of some experimental intensity curve. Each

of these types of curves has advantages. Some investigators prefer

to work almost entirely with radial distribution curves, fitting

theoretical curves to the experimental one, often by least-squares

techniques (7, p. 705-708); others use radial distribution curves in the early stages of an investigation, and refine the parameters by least-squares fitting based on intensity curves (17, p. 529-533; 24, p. 533-537). The latter approach was used in this thesis work. The radial distribution method was employed for the purpose of obtaining approximate values of the structural parameters, and these approximate values were then used as starting values in a least-squares refinement based on intensity curves.

The concluding portion of this section will be devoted to a brief discussion of the radial distribution method (44, p. 671-690) and of least-squares applied to electron diffraction intensity curves (17, p. 529-533; 24, p. 533-537).

Radial Distribution Method

It is convenient to use the following molecular intensity function

$$I_E(s) = \sum_{i,j}' n_{ij} \, r_{ij}^{-1} \, A_{ij}(s) \, \exp(-1_{ij}^2 \, s^2/2) \, \sin(sr_{ij}) \, . \qquad (I, 3)$$

Further, it is convenient for the initial discussion to treat the A_{ij}'s as constants.

In order to gain some insight as to the appearance of the distance spectrum for a molecule, it suffices to treat the contribution of a single[1] i, j pair to $I_E(s)$. Consider the integral

---

[1]Analogous to considering a diatomic molecule.

$$\int_0^\infty [I_E(s)]_{ij} \sin(rs)\, ds = c' \int_0^\infty \exp(-1_{ij}^2\, s^2/s) \sin(r_{ij}\, s)$$

$$\times \sin(rs)\, ds \ . \qquad (I, 4)$$

Using the trigonometric identity

$$\sin x \sin y = 2^{-1} [\cos(x-y) - \cos(x+y)] , \qquad (I, 5)$$

the right-hand side of equation (I, 4) can be written as

$$c'/2 \int_0^\infty \exp(-1_{ij}\, s^2/2) \cos[(r-r_{ij})s]\, ds$$

$$-c'/2 \int_0^\infty \exp(-1_{ij}\, s^2/2) \cos[(r+r_{ij})s]\, ds . \qquad (I, 6)$$

Evaluating (I, 6) by standard methods, it is found that

$$\int_0^\infty [I_E(s)]_{ij} \sin(rs)\, ds = [c''/1_{ij}(2\pi)^{1/2}] [\exp(-(r-r_{ij})^2/2\, 1_{ij}^2)$$

$$- \exp(-(r+r_{ij})^2/2\, 1_{ij}^2)] . \qquad (I, 7)$$

It is clear that the second exponential term can be neglected with respect to the first one, so that

$$\int_0^\infty [I_E(s)]_{ij} \sin(rs)\, ds \simeq [c''/1_{ij}(2\pi)^{1/2}]$$

$$\times \exp[-(r-r_{ij})^2/2\, 1_{ij}^2] . \qquad (I, 8)$$

The right-hand side of equation (I, 8) is seen to be the normal

Gaussian distribution. Each i, j pair in the molecule will make such

a contribution and hence the curve representing the entire distance

spectrum will be composed either of distinct Gaussian peaks (one for

each i, j pair in the molecule), or when two or more r_{ij}'s are approxi-

mately equal in magnitude, of composites of Gaussian peaks.

Letting $rD(r)$ represent the theoretical radial distribution

function [in the literature, $\sigma(r)/r$ is often used to denote $4\pi rD(r)$], it

is clear from the preceding that $I_E(s)$ can be written as[1]

$$I_E(s) = (2/\pi)^{1/2} \int_0^\infty r\, D(r) \sin(sr)\, dr \ . \qquad (I, 9)$$

In the derivation of equation (I.7), the A_{ij}'s were assumed to be

independent of s. Since this is not usually the case, all but one of

the peaks[2] in the theoretical radial distribution function will be

slightly distorted from the ideal Gaussian form. Further distortion

results from anharmonic instead of harmonic vibrations.

In practice, $I_E(s)$ as obtained experimentally is rarely

available outside of the range $2 \leq s \leq 60$. The effect of not evaluating

the integral in equation (I, 9) over the whole range in which the in-

tegrand is different from zero is the introduction of ripples (diffrac-

tion rings) in the experimental $rD(r)$ curve, which, of course, contri-

butes to skewing of the true peaks. For this reason, the factor

$\exp(-as^2)$, often referred to as the artificial temperature factor, is

usually introduced in the integrand to compensate for the finite upper

limit, and the experimental radial distribution curve takes the form

---

[1]The constant $(2/\pi)^{1/2}$ has been arbitrarily included for nor-
malization purposes.

[2]The multiplication of $(Z-F)_i(Z-F)_j$ by $Z_k Z_l/(Z-F)_k(Z-F)_l$
exactly eliminates the dependence of A_{kl} on the parameter s.

$$r\,D'(r) = \sum_{s(min)}^{s(max)} I_E(s)\,\exp\,(-as^2)\,\sin\,(rs)\,\Delta s\,, \qquad (I,\,10)$$

where the integral has been replaced by a summation. The finite

lower limit is often handled by the introduction of a theoretical in-

tensity curve in the interval from zero to s(min). Further, since

$I_E(s)$ is usually obtained experimentally at a constant Δs interval,

Δs can be factored out of the summation and the equation actually used

for evaluating $rD'(r)$ is

$$r\,D'(r)_{Exp} = \sum_{s\,=\,0}^{s(max)} I_E(s)\,\exp\,(-as^2)\,\sin\,(rs)\,. \qquad (I,\,11)$$

The theoretical radial distribution curve corresponding to $r\,D'(r)_{Exp}$

can be calculated from the expression

$$r\,D'(r)_{Theor} = \sum_{i,\,j}{}' n_{ij}\,Z_i\,Z_j\,(r_{ij})^{-1}\,(1_{ij}^2 + 2a)^{-1/2}$$
$$\times\,\exp\,[\,-(r-r_{ij})^2/2(1_{ij}^2+2a)]\,. \qquad (I,\,12)$$

Least-Squares Method

The problem of refinement by least-squares based on intensity

curves is that of fitting a theoretical curve (which is a function of the

molecular parameters) to an appropriate experimental curve. Since

the adjustment is linear only for small ranges of parameter changes,

it is necessary to have fairly good starting parameter values. As

indicated earlier, such a starting model can be obtained from the

$r \, D'(r)_{Exp}$ curve.

The principles of least-squares curve-fitting in matrix form will be summarized in the following. Suppose $f(x_1, x_2, \cdots, x_m)$ is a non-linear function representing a curve which consists of N experimental data. If approximate values for $x_1, x_2, \cdots, x_m$ are known, $f(x_1, x_2, \cdots, x_m)$ may be expanded as

$$f(x_1, x_2, \cdots, x_m) = f(x_1^o, x_2^o, \cdots, x_m^o) + \sum_{i=1}^{m} \left(\frac{\partial f}{\partial x_i} \right)_o \Delta x_i \; . \quad (I, 13)$$

We have N such equations corresponding to the N observed points. If matrix notation is introduced,

$$\mathbb{F}_N = \mathbb{F}_N^o + \mathbb{A}_{Nm} \bar{X}_m \; ; \quad (I, 13')$$

equation (I, 13') is usually referred to as the conditional equations. Since $\mathbb{F}_N$ and $\mathbb{F}_N^{Obs}$ differ by V_N, equation (I, 13') gives (dropping subscripts)

$$\mathbb{F}^{Obs} + V = \mathbb{F}^o + \mathbb{A} \bar{X} \quad (I, 14)$$

$$V = \mathbb{F}^o - \mathbb{F}^{Obs} + \mathbb{A} \bar{X} \quad (I, 15)$$

$$= -\mathbb{N} + \mathbb{A} \bar{X} \; . \quad (I, 15')$$

The least-squares criterion may be expressed as

$$V' \, \mathbb{P} \, V \longrightarrow \text{minimum,} \quad (I, 16)$$

from which one finds

$$(\partial / \partial \bar{X}) (V' \, \mathbb{P} \, V) = \mathbb{A}' \, \mathbb{P} \, V = 0 \quad (I, 17)$$

Combination of equations (I, 15') and (I, 17) give the normal equations

$$\mathbb{B} \, \overline{X} = Y \qquad\qquad (I, 18)$$

where

$$\mathbb{B} = A' \mathbb{P} A \qquad\qquad (I, 19)$$

and

$$Y = A' \mathbb{P} \mathbb{N} \, . \qquad\qquad (I, 20)$$

The solutions are

$$\overline{X} = \mathbb{B}^{-1} Y, \qquad\qquad (I, 21)$$

and the standard errors are

$$\sigma(x_i) = [(\mathbb{B}^{-1})_{ii} \, V' \, \mathbb{P} \, V/(N-m]^{\frac{1}{2}} \qquad (I, 22)$$

$$= [(\mathbb{B}^{-1})_{ii} \, (\mathbb{N}' \, \mathbb{P} \, \mathbb{N} - \overline{X}' \, Y)/(N-m)]^{\frac{1}{2}} \, . \quad (I, 23)$$

In the case of electron diffraction, $f(x_1, x_2, \cdots, x_m)$ may be identified with an intensity function, say $I_E(s)$, the parameters of which are k' (scaling factor), some of the r_{ij}'s, and the l_{ij}'s. Therefore, the columns of the A matrix are $\partial I_E/\partial k'$, $\partial I_E/\partial r_{ij}, \cdots$, $\partial I_E/\partial r_{kl}$, $\partial I_E/\partial l_{ij}, \cdots, \partial I_E/\partial l_{kl}$, et cetera. The elements of the diagonal weight matrix, $\mathbb{P}$, are often calculated using the analytical expression

$$(\mathbb{P})_{ii} = \text{const } s_i \exp(-bs_i^2), \qquad\qquad (I, 24)$$

which simply reflects general experience regarding the quality of the data.

DETERMINATION OF MOLECULAR STRUCTURE

Experimental

The electron diffraction photographs of gaseous nitrogen dioxide were taken with the Oslo sector apparatus (3, p. 232-238); the electron source being a hot cathode gun similar to that used in electron microscopes [see (14, p. 40-46; 20, p. 12-22) for discussions relating to the performance characteristics of such electron guns and the general problem of resolution in electron diffraction cameras, respectively].

The preparation of the nitrogen dioxide sample proceeded essentially as follows. Powdered $Pb(NO_3)_2$ was dried at temperatures ranging from 110° to 120° C. The powder was then transferred to a pyrex tube and slowly heated in the presence of a stream of O_2. The reaction proceeds according to the equation

$$2Pb(NO_3)_2 \longrightarrow 2PbO_{(s)} + 4NO_{2(g)} + O_{2(g)} . \qquad (I, 25)$$
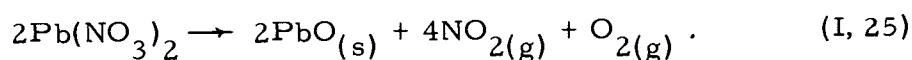
The water vapor liberated during the heating process was condensed with a cold trap (5° - 20° C). The nitrogen dioxide was passed over PbO_2 and Pb_2O_5, and condensed in a dry ice bath. Finally, the nitrogen dioxide was purified by distillation.

Several photographic plates (Kodak B-40 lantern slide plates) were exposed at each of the three camera distances, 478.00, 192.07

and 120. 00 mm, from which four plates per distance were subse-

quently selected for analysis (twelve plates in all); the exposure times

ranged from about one-half minute to five minutes in duration.

The average nozzle temperature and electron wavelength for

each of the runs were determined as 107° C and 0. 06458 Å, respec-

tively. The temperatures were read from a thermocouple placed in

contact with the input gas nozzle a short distance from the tip. The

wavelength associated with the electron beam was determined in

separate experiments by diffraction from gold foil (8, p. 242).

The rotating sector, which must be used to even out the steeply

falling background for photographic purposes, was spiral in shape

(with a maximum radius of approximately 11 cm) such that its angular

opening was proportional to the cube of the radius save for very small

s values where the opening was larger in order to give a more uniform

background.[1] The mounting of the sector in the diffraction chamber

was such that its rotational axis (perpendicular to the plane of the

sector) coincided with the direction of the undiffracted electron beam;

the distance between sector and photographic plate was approximately

16 mm. The sector described above acted effectively as an s^3 screen

(for the better part of the s range), which tended to offset the char-

acteristic inverse square fall-off of intensity with distance from the

----

[1]Such a sector is usually referred to as an "r^3 sector. "

scattering point, and therefore, to accentuate the oscillating features of the diffraction pattern. In other words, without a sector, the photographic plate would be over exposed at small s values and under exposed at large s values.

Data Reduction

Though it is usual to refer to the experimental diffraction curve as that which corresponds to a suitable molecular intensity function, it is only the information contained on the photographic plates which can be properly referred to as the experimental data. The microdensitometery of the plates and the various mathematical operations performed on the experimental data, eventually leading to the isolation of a suitable molecular intensity function, constitute the data reduction process.

Exposed photographic plates from gaseous electron diffraction show well-defined rings such that as the scattering angle increases, the blackening of the photographic emulsion appears to pass through successive maximum and minimum values. It has been pointed out (41, p. 868) that these maxima and minima are not real, but correspond to small fluctuations in the density superimposed on a monotonically falling background (see discussion of sector).

The photographic plates from the nitrogen dioxide experiments were traced with a Leeds and Northrup recording microdensitometer

along a direction corresponding to a ring diameter, chosen to be as free as possible from photographic defects. During the tracing, the plates were oscillated about their centers in order to average out emulsion irregularities arising from graininess. This was accomplished by mounting a plate on an oscillating device which itself was mounted on the microdensitometer carriage. Since the diffraction pattern on the photographic plate was radially symmetric, the corresponding microdensitometer tracing consisted of two branches (left and right branch) separated by a narrow region corresponding to the position of the beam stop image which coincided with that of the undiffracted beam.

In practice, two traces corresponding to two different microdensitometer carriage speeds and amplifier gains[1] were actually made of a given plate. The slower carriage speed and higher amplifier gain had the advantage of spreading out and magnifying the individual undulations and hence facilitating the reading off of the photographic densities. The traces clearly showed the desired broad maxima and minima, which became progressively weaker as the scattering angle increased, and less easy to detect in the presence of the low level

---

[1] In subsequent discussions, "unamplified" and "amplified" trace will refer to the tracings obtained with the faster carriage speed and lower amplifier gain, and the slower carriage speed and higher amplifier gain, respectively. In both of these cases, the chart speeds were the same and greater than the corresponding carriage speeds.

noise present in the traces. In addition to this noise, occasional spike-like absorption minima (equivalent to transmission maxima) occurred in the traces and were credited to dust on the surface of the photographic plate during the diffraction experiment and to emulsion defects.

The procedure employed in reading photographic densities from a trace involved the following steps.

First, a continuous smooth pencil line was drawn on each branch of a trace in an attempt to visually average out the effect of noise in the recorded signal. When the spikes described above were encountered, the line was drawn so as to correspond to the curvature of the trace on each side of the spike. A center line corresponding to zero scattering angle was then located on the amplified trace by averaging the center positions between corresponding maxima and minima on each of the two branches. The effective position of a given maximum or minimum was located by constructing tangents to the peak (one on the up side and one on the down side), and then locating the point of intersection of these two tangents. This tangent technique was also employed in locating the effective peak positions on the unamplified trace.

Second, an s scale, graduated in one-quarter s units, was

placed along the bottom of the amplified trace.[1] Since the amplified

trace was recorded at a chart speed greater than that of the corre-

sponding carriage speed, it was necessary to relate distances on the

amplified trace to those on the plate. This was done by simply

tracing an accurately calibrated, etched glass scale under the same

conditions used with the diffraction plates. The result (often called

the "paper factor") was $x_T/x_P = 5.2350$. The value of the paper

factor actually used in calculating the x_T's was 5.2415, which was

the value determined from the calibration trace in the Oslo laboratory

before mailing to Oregon. The discrepancy between these two values

was probably due to shrinkage of the chart paper caused by differ-

ences in humidity. This discrepancy was eventually taken account of

by multiplying the final distance parameters of nitrogen dioxide by

the factor $1.0012 = 5.2415/5.2350$. A correction to the mean ampli-

tudes is also required in principle, however it is so small in value

that it was neglected.[2]

---

[1]Since there were two branches per trace, each trace re-
quired two s scales using the previously determined center line as a
common zero point relative to s. Obviously, the s scales differed
in spacing and range for the different camera distances.

[2]For example the correction is about 2×10^{-6} Å for $l(N-O)$:

$$I \propto I_O \exp(-l^2 s^2/2),$$
$$0 = -s^2 dl - sl^2 ds,$$
$$dl = -l^2 (ds/s) = -(0.038)^2(1.2 \times 10^{-3}).$$

The third and final step of this procedure involved the actual

reading of the photographic densities from the microdensitometer

traces. Since the absorption of light by the photographic emulsion

follows the exponential law

$$I(dens)/I_o(dens) = \exp(-\mu D), \qquad (I, 26)$$

it was convenient to use a logarithmically scaled "T" square to read

the photographic densities from the traces. The scale of the "T"

square was in density units,

$$D = \log[I_o(dens)/I(dens)], \qquad (I, 27)$$

with the zero and infinity points at positions corresponding to the

edges of the chart paper. It was necessary, of course, to scale the

readings obtained from the amplified trace to the actual densities (D)

as defined in equation (I, 26). Further, since the functional relation-

ship of exposure (scattered electron intensity x time)[1] and density is

known, a determination of the desired scattered electron intensity is

possible. The scaling procedure was as follows. The only essential

difference between the unamplified and amplified traces was that of

amplifier gain. Clearly one correction to the apparent density (as

read from the amplified trace) must consist of determining the in-

creased amplification of the amplified trace in "T" square density

units. This was accomplished by measuring the average difference

---

[1] E = It is termed the reciprocity law.

in readings between corresponding maxima and minima on the un-
amplified and amplified traces, and then adding this term to the ap-
parent density reading of the amplified trace. A second minor cor-
rection term was also necessary because of slight differences be-
tween the scale of the "T" square and the 0 to 100 percent transmis-
sion scale of the unamplified traces. This term was either subtracted
or added to the apparent density described above, depending on
whether the 100 percent transmission line of the "T" square fell above
or below that of the unamplified trace.

An algebraic formulation of this procedure is as follows (see
Figure 1 for the meaning of the various symbols). Let

$$D = \log \left[I_O' (\text{dens})/I'(\text{dens}) \right] = \log \left[I_O'' (\text{dens})/I''(\text{dens}) \right] \qquad (\text{I}, 28)$$

and

$$D' = \log \left[I_O(\text{dens})/I'(\text{dens}) \right] , \qquad (\text{I}, 29)$$

then

$$\Delta D = D - D' = \log \left[I_O'(\text{dens})/I'(\text{dens}) \right] - \log \left[I_O(\text{dens})/I'(\text{dens}) \right] \qquad (\text{I}, 30)$$

or

$$\Delta D = \log \left[I_O''(\text{dens})/I''(\text{dens}) \right] - \log \left[I_O(\text{dens})/I'(\text{dens}) \right] . \qquad (\text{I}, 30')$$

Rearrangement of equation (I, 30') yields

$$\Delta D = \log \left[I'(\text{dens})/I''(\text{dens}) \right] - \log \left[I_O(\text{dens})/I_O''(\text{dens}) \right] , \qquad (\text{I}, 31)$$

where

$$\log \left[I'(\text{dens})/I''(\text{dens}) \right] = \log \left[I_O(\text{dens})/I''(\text{dens}) \right]$$
$$- \log \left[I_O(\text{dens})/I'(\text{dens}) \right] . \qquad (\text{I}, 32)$$

Letting $\Delta D_1 = \log [I'(dens)/I''(dens)]$ and $\Delta D_2 = \log [I_o(dens/I_o''(dens)]$, then

$$\Delta D = \Delta D_1 - \Delta D_2 \qquad\qquad (I, 33)$$

or

$$D = D' + \Delta D_1 - \Delta D_2 . \qquad\qquad (I, 34)$$

ΔD_1 and ΔD_2 may be identified with the first and second corrections, respectively, as discussed in the previous paragraph.

The recorded diffraction patterns covered the following scattering ranges:

$$h_a; \quad 2.50 \leq s \leq 20.75$$

$$h_b; 10.25 \leq s \leq 42.00$$

$$h_c; 18.50 \leq s \leq 49.75 .$$

Following the reading of the densities from the plates, as described above, the densities were corrected for non-linearity of photographic response according to the relation[1]

$$I_p = \gamma(D + \delta) . \qquad\qquad (I, 35)$$

The values of δ actually used in this work (see Table 10) were obtained from the Oslo laboratory.[2] δ was taken as zero for $D < 0.62$,

---

[1]The proportionality constant γ (in units of reciprocal time) was arbitrarily taken as unity.

[2]The Oslo calibration of photographic densities with electron intensities was based on a series of investigations extending over a period of some fourteen years, employing the procedure developed by Karle and Karle (27, p. 961).

for densities less than this value, the density-exposure curve was
found to be linear. All twelve of the photographic plates used were
sufficiently light in exposure that only data occurring in the following
scattering ranges were actually blackness corrected:[1]

$$h_b; \quad 10.25 \leq s \leq 18.00$$

$$h_c; \quad 18.50 \leq s \leq 35.00 \ .$$

The relevancy of this fact will be seen later in the discussion of un-
certainties in the final mean square vibrational amplitudes.

As a check on the Oslo blackness correction, a blackness
correction was constructed in this laboratory using two plates made
at the 478 mm distance. As in the Oslo correction, the method of
Karle and Karle (27, p. 961) was employed in this analysis. The
applicability of this method rests on the validity of the reciprocity
law

$$E = It \ , \qquad\qquad (I, 36)$$

for fast electrons. From equation (I. 36), it is seen that it is pos-
sible to interpret the difference in two exposures as due to differ-
ences in electron intensity at constant time. This interpretation,
combined with the assumption that D is proportional to I for $D \leq 0.25$
(for contrast lantern slide plates), constitute the basis of the method.

A comparison of the two corrections (Oregon and Oslo)

---

[1] The 478 mm plates did not require blackness correcting.

indicated that δ (Oregon) was somewhat greater than δ (Oslo) [for

example, δ (Oregon) - δ (Oslo) $\simeq$ 0.010 density units at D = 0.480].

This difference may or may not be significant; but because the two

plates used in deriving the Oregon correction did not differ quite

enough in density for optimal results, and because the blackness cor-

rection in any event was not great, it was decided to use the Oslo cor-

rection.

The $I_p(s)$ (or D) data (see Tables 2, 3, and 4) were plotted on

large-scale graph paper in order to locate possible reading errors.

A composite function for each of the camera distances was then ob-

tained by summing the I_p data from each of the four plates at cor-

responding points of s:

$$I_p^k(s) = \sum_{i=1}^{4} I_p^{k(i)}(s) . \tag{I, 37}$$

This composite intensity function is related to the total scat-

tered intensity per unit solid angle $[I_t^k(s)]$ by the equation

$$I_p^k(s) = I_t^k(s) \, g(\theta) , \tag{I, 38}$$

where $g(\theta)$ incorporates the effect of the sector and that of using a

flat plate perpendicular to the undiffracted beam instead of a cylin-

drical film with an axis perpendicular to the undiffracted beam and a

surface everywhere equidistant from the scattering point. Recalling

the screening effect of the rotating sector, it is clear that one part

of $g(\theta)$ will take the form $a(r_s) = \rho \, r_s^3$. The second factor of $g(\theta)$ is

$\cos^3 2\theta$. Two powers of this factor are derived from the inverse fall-off of intensity with distance from the scattering point, and one power from the angle of inclination of the element of area on the flat plate with respect to the scattered electron rays striking it. Equation (I, 38) thus becomes

$$I_t^k(s) = I_p^k(s)/a\,(r_s)\,\cos^3 2\theta. \qquad (I.39)$$

For the purpose of extracting the molecular sensitive part of the scattered intensity, it is convenient to multiply both sides of equation (I, 39) by s^4, giving

$$s^4 I_t^k(s) = s^4 I_p^k(s)/a(r_s)\,\cos^3 2\theta. \qquad (I, 40)$$

For each camera distance, $s^4 I_t^k(s)$ curves were obtained by performing the multiplications indicated in equation (I, 40) and plotted on large-scale graph paper. Values of the calibration function $a(r_s)$ were obtained from the Oslo Laboratory.[1] It would now seem that the desired molecular intensity function $I_m^k(s)$ could be obtained by subtracting the last two terms in equation (I, 1) from $s^4 I_t^k(s)$; these two terms constitute the theoretical background and can be calculated. As has been pointed out, however, the theory of incoherent scattering is on poor ground and, even more important, there inevitably exists on any exposed plate a superposed experimental background derived

---

[1] See Tables 11, 12, and 13 for $s^4/a(r_s)\,\cos^3 2\theta$ values actually used. These values correspond to a value of λ equal to 0.06449 Å; values calculated with $\lambda_{exp} = 0.06458$ would differ inconsequentially from these.

from apparatus scattering. In practice, therefore, since little is
known about the apparatus background other than it is monatonically
declining with increasing angle, one simply draws a background
curve through the undulations of the experimental intensity and sub-
tracts it. The result is the desired function,

$$I_m^k(s) = s^4 I_t^k(s) - B_t^k(s). \tag{I, 41}$$

The initial background often contains errors which manifest them-
selves by negative values of $rD(r)$ calculated from $I_m(s)$, or small
peaks in $rD(r)$ at $r < 1.00 \overset{\circ}{A}$. These errors are usually corrected by
changing the background. Throughout this work, experimental back-
ground functions were used instead of theoretical functions.

Following subtraction of the background, the three $I_m^k(s)$
functions were placed on a common amplitude scale by comparing
corresponding maxima and minima in the following overlap regions:

$$I_m^a(s) \text{ and } I_m^b(s); \quad 10.25 \le s \le 20.75$$

$$I_m^b(s) \text{ and } I_m^c(s); \quad 28.75 \le s \le 42.00.$$

A single composite function, $I_m^T(s)$, was then obtained by combining[1]
$I_m^a(s)$, $I_m^b(s)$ and $I_m^c(s)$ now normalized as follows:

---

[1]The data available from the $I_m^c(s)$ curve in the range
$18.50 \le s < 28.75$, was not used in forming the composite curve $I_m^T(s)$.

$$2.50 \leq s \leq 10.00; \quad I_m^T(s) = I_m^a(s)$$

$$10.25 \leq s \leq 20.75; \quad I_m^T(s) = t(s)\, I_m^a(s) + u(s)\, I_m^b(s)$$

$$21.00 \leq s \leq 28.50; \quad I_m^T(s) = I_m^b(s)$$

$$28.75 \leq s \leq 42.00; \quad I_m^T(s) = v(s)\, I_m^b(s) + w(s)\, I_m^c(s)$$

$$42.25 \leq s \leq 49.75; \quad I_m^T(s) = I_m^c(s).$$

The weighting factors $t(s)$, $u(s)$, $v(s)$ and $w(s)$ were obtained from the

$I_p^k(s)$ data. The overall range of the composite $I_m^T(s)$ was

$2.50 \leq s \leq 49.75$.

The composite curve $I_m^T(s)$ resulting from the procedures

just described is in theory represented by the expression

$$s I_m^T(s) = k' \sum_{i,j}{}' \; n_{ij}(Z-F)_i(Z-f)_j\, r_{ij}^{-1}$$
$$\cos |\Delta \eta_{ij}| \; \exp(-1_{ij}s^2/2) \sin(r_{ij}s), \quad (I, 42)$$

which is, in fact, equation $(I, 2)$ multiplied by s^5. In order to replace

the variable coefficients of $I_m^T(s)$ in equation $(I, 42)$ by essentially

constant coefficients, as is necessary for obtaining an easily inter-

preted radial distribution curve, the modified molecular intensity

function $I_E^T(s)_{Exp}$ was calculated according to the equation

$$I_E^T(s)_{Exp} = s I_m^T(s)\, Z_N Z_O / (Z-F)_N (Z-F)_O. \quad (I, 43)$$

The values of $F_N(s)$ and $F_O(s)$ were obtained by combining those

published by Hoerni and Ibers (21, p. 745) with those of Viervoll

and Ögrim (43, p. 279). In the former case the $F_i(s)$'s were com-

puted from Hartree-Fock radial wave functions, and in the latter an

interpolation method was used to extend the calculations of James and

Brindley (25, p. 81-111) to s equal to 30. Since the nitrogen dioxide

data extended well-beyond s = 30, it was necessary to extrapolate the

F_i curves to obtain values in this region. The values of $(Z-F/Z)_O$

and $(Z-F/Z)_N$ used are given in Table 14. Values of $I_E^T(s)_{Exp}$ are

given in Table 5 and the curve is ploted in Figure 2.

Reference to equations (I, 42) and (I, 43) reveals that $I_E^T(s)_{Exp}$

for nitrogen dioxide corresponds to the theoretical scattering equa-

tion (if the relatively important $\cos |\Delta\eta_i|$ term is ignored[1])

$$I_E^T(s)_{Theor} = k'[2Z_N Z_O r_{N-O}^{-1} \exp(-l_{N-O}s^2/2) \sin(sr_{N-O})$$
$$\text{(I, 44)}$$
$$+ Z_N Z_O(Z-F)_O((Z-F)_N r_{O...O})^{-1} \exp(-l_{O...O}s^2/2) \sin(sr_{O...O})] .$$

The coefficient $Z_N Z_O(Z-F)_O/(Z-F)_N$ is essentially constant; Table 15

shows that it is approximately equal to Z_O^2 for $s \geq 7.00$. An

$I_E^T(s)_{Theor}$ curve was calculated according to equation (I, 44) using

the final refined parameter values (Table 22) and is shown in Figure 2

and tabulated in Table 5. The agreement between the experimental

and theoretical curves is good.

In addition to the final composite intensity function $I_E^T(s)_{Exp}$,

several other $I_E(s)_{Exp}$ curves were calculated which included (1)

only data from plates taken at a single camera distance and (2) data

---

[1]This term has an important effect on the Fourier transform
only when the atomic number differences of the atoms in the molecule
are large.

taken from single plates at a single camera distance. The purpose
of these curves was to help with an understanding of the errors as-
sociated with the parameter values determined. The various curves
and ranges of data they include are:

$$I_E^a(s); \quad 2.50 \le s \le 20.75$$

$$I_E^b(s); \quad 10.25 \le s \le 42.00$$

$$I_E^c(s); \quad 28.75 \le s \le 49.75 \text{ and } 18.50 \le s \le 49.75$$

$$I_E^{a(1)}(s), \ I_E^{a(2)}(s), \ I_E^{a(3)}(s), \ I_E^{a(4)}(s); \quad 2.50 \le s \le 20.75$$

$$I_E^{b(1)}(s), \ I_E^{b(2)}(s), \ I_E^{b(3)}(s), \ I_E^{b(4)}(s); \quad 10.25 \le s \le 42.00 .$$

The curves described above are given in Tables 6, 7, and 8 and
plotted[1] in Figure 3.

Radial Distribution Function and Preliminary Structure

The final radial distribution function $rD'(r)_{Exp}$ [see equation
(I, 11)], from the modified experimental molecular intensity curve
$I_E^T(s)_{Exp}$ ($\Delta s = 0.25$) was calculated according to the equation

$$rD'(r)_{Exp} = \sum_{s=0}^{s=49.75} I_E^T(s)_{Exp} \exp(-0.001s^2) \sin(rs); \qquad (I, 45)$$

the intensity data in the range $0 \le s \le 2.25$ was calculated from a
theoretical curve according to equation (I, 44). The experimental
radial distribution curve (values are given in Table 9 and the curve

---

[1]Only $I_E^a(s)$, $I_E^b(s)$ and $I_E^c(s)$ are plotted in this figure.

is shown in Figure 4) shows two strong peaks attributed to the N-O

and O···O distances at about 1.2 and 2.2 Å, respectively. Careful

analysis of these peaks gave the following preliminary values for the

distance and amplitude parameters:

$$r(N\text{-}O) = 1.20_1 \text{ Å}, \quad l(N\text{-}O) = 0.0038_5 \text{ Å}$$

$$r(O\cdots O) = 2.21_0 \text{ Å}, \quad l(O\cdots O) = 0.043_8 \text{ Å}.$$

For comparison, a theoretical radial distribution curve calculated

using the final refined parameter values (Table 22) is shown in

Figure 4 and tabulated in Table 9. The calculation was carried out

according to the equation

$$rD'(r)_{Theor} = k'' \sum_{i,j}' n_{ij} Z_i Z_j r_{ij}^{-1} (l_{ij}^2 + .002)^{-\frac{1}{2}}$$

$$\times \exp\left[-(r-r_{ij})^2/(2l_{ij}^2 + .004)\right], \qquad (I, 46)$$

where the scale factor k'' was determined from the peak heights

in $rD'(r)_{Exp}$. The agreement between the experimental and theore-

tical curves is good.

Least-Squares Refinements

A large number of refinements, employing the Alwac III-E

digital computer, were carried out according to the procedures

already described. The results of several[1] of these refinements are summarized in Tables 16 through 19. In each refinement the starting model was obtained from the $rD'(r)_{Exp}$ curve. The information to be deduced from these tables will be discussed in the following paragraphs.

Non-Systematic Errors

The error matrix, M, derived from least-squares refinement is given by

$$M = s^2 D B^{-1} D',$$ (I, 47)

where the transformation matrix D is obtained from

$$U = D X.$$ (I, 48)

In the nitrogen dioxide case, the only additional parameter of interest is the bond angle: equation (I, 48) thus becomes

$$\begin{bmatrix} r(N-O) \\ r(O\cdots O) \\ <(O-N-O) \\ l(N-O) \\ l(O\cdots O) \end{bmatrix} = D \begin{bmatrix} r(N-O) \\ r(O\cdots O) \\ l(N-O) \\ l(O\cdots O) \end{bmatrix},$$ (I, 48')

and D is easily seen to be given by

---

[1]Additional refinements were carried out investigating the effect on the parameter values of such things as the various background corrections, selection of suitable s ranges for separate composites, determination of the overlap ranges, et cetera.

$$D = \begin{bmatrix} 1 & 0 & 0 & 0 \\ 0 & 1 & 0 & 0 \\ a' & b' & 0 & 0 \\ 0 & 0 & 1 & 0 \\ 0 & 0 & 0 & 1 \end{bmatrix} \, . \qquad (I, 49)$$

Combining the parameter values given in the first column of Table 19 with the corresponding $\bar{s}^2 B^{-1}$ matrix, M was evaluated[1] and is shown in Table 20. The off-diagonal elements, $(M)_{ij}$, of this matrix are the average products of the errors σ_i^{LS} and σ_j^{LS} (often denoted[2] by $\rho_{ij} \sigma_i^{LS} \sigma_j^{LS}$); the square roots of the diagonal elements, $(M)_{ii}$, are the standard error (σ_i^{LS}) associated with each parameter.

Though the error matrix, M, provides a means of estimating the random errors arising from the discrepancy of the composite observations from the theoretical modified molecular intensity curve [equation (I, 44)], Morino[3] has pointed out that another source of non-systematic error arises from variations in the most probable parameters as obtained from the individual photographic plates for a given camera distance (see Table 17). For the parameters r(N-O),

---

[1]From equations (I, 47) and (I, 49), the error,
$(M)_{<O-N-O, <O-N-O'}$ is defined by

$$\bar{s}^2 [(a')^2 (B^{-1})_{r_{N-O}, \, r_{N-O}} + 2a'b'(B^{-1})_{r_{N-O'} \, r_{O \ldots O}}$$
$$+ (b')^2 (B^{-1})_{r_{O \ldots O'} \, r_{O \ldots O}}] \, . \qquad (I, 50)$$

[2]ρ_{ij} is usually referred to as the correlation coefficient.

[3]Morino, Yonezo. Private communication. Tokyo, Japan. University of Tokyo, 1964.

$r(O\cdots O)$, $l(N-O)$ and $l(O\cdots O)$, $\sigma_2(x_j)^2$ was estimated as follows.

Let

$$\sigma_2^{a(i)}(x_j) = x_j^a - x_j^{a(i)} \tag{I, 51}$$

and

$$\sigma_2^{b(i)}(x_j) = x_j^b - x_j^{b(i)} . \tag{I, 51'}$$

The final values of $\sigma_2(x_j)$ were then calculated as

$$\sigma_2(x_j)^2 = (1/8-1)(0.365 \sum_{i=1}^{4} [\sigma_2^{a(i)}(x_j)]^2$$

$$+ 0.635 \sum_{i=1}^{4} [\sigma_2^{b(i)}(x_j)]^2) , \tag{I, 52}$$

where the weights 0.365 and 0.635 were obtained by consideration of the total s ranges contributed by each of the two camera distances (478 and 192 mm) relative to $I_E^T(s)_{Exp}$. The additional information that might have been obtained by a similar analysis of the 120 mm plates did not seem justified. The corresponding standard deviation for the bond angle was estimated[1] as

$$\sigma_2(<O-N-O)^2 = (a')^2 \sigma_2(r_{N-O})^2 + (b')^2 \sigma_2(r_{O\cdots O})^2. \tag{I, 53}$$

Systematic Errors

Uncertainties arising from the measurement of camera

---

[1]Equation (I, 53) neglects the negative cross term, $2a'b' <\sigma_2(r_{N-O})\,\sigma_2(r_{O\cdots O})>$ [see equation (I, 50)].

distance, electron wavelength and the position coordinate (uncertainty

Δx_T in the designation of the correct obscissa for a predetermined

s scale) principally effect the size of the molecule and are negligible

in their effect on the vibrational amplitudes. In terms of interatomic

distances, the error associated with the first two of these parameters

(h and λ) can be estimated as follows. Recalling that $s = 4\pi\lambda^{-1} \sin \theta$

where $\sin \theta = x_p/(h^2 + x_p^2)^{\frac{1}{2}}$,

$$-ds/s = [d\lambda/\lambda + h\,dh/(h^2 + x_p^2)] . \qquad (I, 54)$$

Since, for a given ring spacing

$$s \propto r_{ij}^{-1} , \qquad (I, 55)$$

then

$$ds/s = -dr_{ij}/r_{ij} , \qquad (I, 56)$$

and combining equations (I, 54) and (I, 56), we obtain

$$dr_{ij}/r_{ij} = [d\lambda/\lambda + h\,dh/(h^2 + x_p^2)]. \qquad (I, 57)$$

Setting x_p equal to zero and noting that λ and h are independent

parameters, the desired estimate is given by

$$dr_{ij}' = [(d\lambda/\lambda)^2 + (dh/h)^2]^{\frac{1}{2}} r_{ij} . \qquad (I, 58)$$

Using the values[1] $\lambda \pm d\lambda = 0.06458 \pm .00002$ Å and $h \pm dh = 263.3$

± 0.1 mm (obtained by simple averaging of 478, 192, and 120 mm

camera distances), equation (I, 58) gives a value of $0.0005\, r_{ij}$ for

———————

[1]$d\lambda$ and dh were obtained from an examination of the variation
of wavelength and camera distance over a period of several months.

dr'_{ij} which agrees with the corresponding estimate given by Hedberg

and Iwasaki (16, p. 592-593). In comparison, the error in the posi-

tion coordinate can be neglected.

Uncertainties in the blackness correction and the atomic form

factors affect largely the vibrational amplitudes. This error has been

estimated as 0.021_{ij} (16, p. 593). Since this investigation sought to

establish the reliability of these amplitudes, the significance of the

earlier remarks pertaining to the fact that only a very small fraction

of the densities used required a correction for blackness, should now

be clear.

If the data on which the determinations are based are not all

independent, the error estimates σ_{LS} are too small for all para-

meters. Very little is known about correlation among the data, but

a rough, plausible guess might be that about one-half the observations

are independent; this estimate would lead to standard errors σ_{LS}

greater by about $2^{\frac{1}{2}}$ than those calculated.

No attempt was made to estimate the systematic errors

arising from uncertainties in the sector correction[1] and in the ex-

perimental background, finite size of scattering region, deflection

of the electrons resulting from interaction with the magnetic field of

the earth which would give asymmetric rings, and the effect of

---

[1]Recent work in this laboratory indicates that sensible errors
from this source have very little effect on the final structure para-
meters.

anharmonicity.

Overall Standard Errors

The overall standard errors for the final structural para-
meters were estimated as follows:[1]

1. $\sigma_T(r_{ij}) = [2 \, \sigma_{LS}(r_{ij})^2 + \sigma_2(r_{ij})^2 + (0.0005 \, r_{ij})^2]^{\frac{1}{2}}$

2. $\sigma_T(<O-N-O) = [2 \, \sigma_{LS}(<O-N-O)^2 + \sigma_2 \, (<O-N-O)^2]^{\frac{1}{2}}$

3. $\sigma_T(l_{ij}) = [2 \, \sigma_{LS}(l_{ij})^2 + \sigma_2(l_{ij})^2 + (0.02 \, l_{ij})^2]^{\frac{1}{2}}$.

The complete error analysis is summarized in Table 21,

it should be noted that if the random errors σ_{LS} and σ_2 were not as-

sumed to be independent (that is, if the observations on several photo-

graphic plates did not belong to a single statistical population), it

would seem appropriate to only include the larger of the two in

evaluating σ_T. Further, it might very well be that σ_2 reflects the

presence of hidden systematic errors in the individual observations.

The results in Table 21 thus represent conservative estimates.

---

[1]The factor two associated with the term $2\sigma_{LS}^2$ arises from
considerations of data correlation discussed earlier. The value
1.0012 r_{ij} was used in evaluating the term $(0.0005 \, r_{ij})^2$.

Final Results

The final values[1] of the structural parameters (including estimated standard errors) are given in Table 22. These values were derived from those given in the first column in Table 19 and the r_{ij} parameters have been multiplied by 1.0012. The comparison of these results with the corresponding microwave work (5, p. 1040-1043) is pleasing. It should be noted that in neither case do the parameters represent true equilibrium values (2, p. 1219-1222; 23, p. 2961-2963; 29, 1945-1949; 37, p. 644-648; 38, p. 1108-1109), though the microwave parameters represent a closer approximation than those of electron diffraction.

---

[1]The effect of weighing the observations which emphasized the intermediate and inner data (but not innermost) led to an increase in l_{N-O}, $r_{O...O}$ and $l_{O...O}$.

PART II

QUADRATIC POTENTIAL CONSTANTS

POTENTIAL CONSTANT INVESTIGATION

List of Symbols (In order of appearance in Part II of the text)[1]

n	p. d.
Δr_1	internal bond stretching coordinate.
Δr_2	same as Δr_1.
$\Delta \alpha$	internal valence angle bending coordinate.
Δr_3	internal non-bonded stretching coordinate.
r^e_{X-Y}	equilibrium bond distance in non-linear XY_2 molecule.
$<Y-X-Y$	equilibrium valence angle in non-linear XY_2 molecule.
$r^e_{Y \cdots Y}$	equilibrium non-bonded distance in non-linear XY_2 molecule.
t	$t = r^e_{X-Y} \sin (<Y-X-Y)/r^e_{Y \cdots Y}$.
u	$u = r^e_{X-Y} [1-\cos (<Y-X-Y)]/r^e_{Y \cdots Y}$.
r_{ij}	p. d.
l_{ij}	p. d.
r^i_{ij}	p. d.
r^e_{ij}	p. d.
$\mathbb{R}$	column matrix of internal coordinate set.
$\mathbb{S}$	column matrix of symmetry coordinate set.

---

[1]p. d. will denote symbols previously defined.

$\mathbb{Q}$ column matrix of normal coordinate set.

$\bar{V}$ transformation matrix from S to R. $R = \bar{V} S$.

$\mathbb{L}$ transformation matrix from Q to S. $S = L Q$.

G_S symmetrized G matrix.

$\mathbb{F}_S$ symmetrized $\mathbb{F}$ matrix.

ν_k frequency of kth vibrational mode.

Λ eigenvalue matrix. $\lambda_k = 4\pi^2 \nu_k^2$.

V potential energy of vibration.

T kinetic energy of vibration.

X column matrix of Cartesian displacement coordinates.

$\bar{A}$ transformation matrix from $\mathbb{R}$ to X. $X = \bar{A}\mathbb{R}$.

$\bar{M}$ diagonal matrix of the atomic masses.

G_R internal G matrix. $G_R = \bar{V} G_S \bar{V}'$.

$\mathbb{E}$ unit matrix. $(\mathbb{E})_{ij} = \delta_{ij}$.

Δ diagonal matrix of the mean-square amplitudes of normal vibration. $\Delta = <Q Q'>$.

h p. d.

k p. d.

T absolute temperature (° K).

$\underline{\Sigma}_R$ the mean-square vibrational amplitude matrix in internal coordinates.

r^e same as r^e_{N-O}.

S_1 $S_1 = (\Delta r_2 + \Delta r_2)/2^{\frac{1}{2}}.$

S_2 $S_2 = r^e \Delta a .$

S_3 $S_3 = (\Delta r_1 - \Delta r_2)/2^{\frac{1}{2}}.$

Δr $\Delta r = \Delta r_1$ or $\Delta r_2 .$

a equilibrium O-N-O angle.

F_{11} $F_{11} = f_r + f_{rr} .$

F_{12} $F_{12} = 2^{\frac{1}{2}}f_{r a} .$

F_{22} $F_{22} = f_a .$

F_{33} $F_{33} = f_r - f_{rr}.$

μ_i $\mu_i = m_i^{-1}$ where m_i is the mass of the ith atom.

G_{11} $G_{11} = 2\mu_N \cos^2 (a/2) + \mu_O .$

G_{12} $G_{12} = -2^{3/2} \mu_N \sin (a/2) \cos (a/2).$

G_{22} $G_{22} = 2 [2\mu_N \sin^2 (a/2) + \mu_O].$

G_{33} $G_{33} = G_{22}/2.$

β $\beta = F_{11}F_{22} - F_{12}^2.$

$\overline{\gamma}$ $\overline{\gamma} = G_{11}G_{22} - G_{12}^2.$

C $C = F^{-1}.$

K $K = G^{-1}.$

ϕ $\phi = \lambda^{-1}.$

C_S $C_S = F_S^{-1}.$

C_{11} $C_{11} = F_{22}/\beta.$

C_{12} $C_{12} = -F_{22}/\beta.$

C_{22} $C_{22} = F_{11}/\beta.$

C_{33} $C_{33} = F_{33}^{-1}$.

ν_i observed fundamental frequency of the ith vibrational

        mode.

ω_i harmonic frequency of the ith vibrational mode.

P_{Ot} diagonal weight matrix used in least-squares deter-

        mination of symmetrized compliance constants.

f_i ith internal potential constant.

$\sigma(f_i)$ estimated error in f_i due to uncertainties in

        l_{N-O} and $l_{O\cdots O}$.

$\sigma_T(l_{ij})$ p. d.

$\sigma_{LS}(l_{ij})$ p. d.

Molecular Potential Functions

In the harmonic approximation, a non-linear polyatomic mole-
cule can be viewed as an aggregation of 3n-6 (3n-5 for a linear mole-
cule) independent simple harmonic oscillators. As internal coordi-
nates one normally selects either "valence" or "central force" co-
ordinates [various choices are possible (46, p. 223)]. The former
set consists of bond distance and bond angle displacements from
equilibrium and the latter solely of internuclear distance displace-
ments. For example, for a non-linear XY_2 molecule the valence
force coordinates would be the two equivalent X-Y stretches and the
Y-X-Y angle distortion, which may be denoted by Δr_1, Δr_2 and $\Delta\alpha$[1],
respectively; the corresponding central force coordinates would then
be Δr_1 and Δr_2 and the Y$\cdots$Y distance displacement Δr_3. By
geometric means, it is easily shown that (assuming small displace-
ments)

$$\Delta r_3 = (\Delta r_1 + \Delta r_2) \sin (< Y\text{-}X\text{-}Y/2) + r^e_{X\text{-}Y} \Delta\alpha \cos (< Y\text{-}X\text{-}Y/2). \quad (II, 1)$$

With the coordinates defined above one may consider many
vibrational models. Some of the more common are the simple cen-
tral force, simple valence force, generalized central force, gener-
alized valence force, and the Urey-Bradley force field which may be

---

[1] For dimensional reasons it is often convenient to replace the
internal bending coordinate $\Delta\alpha$ by $r^e_{X\text{-}Y} \Delta\alpha$.

abbreviated by SCF, SVF, GCF, GVF, and UBF, respectively. For

a bent XY_2 molecule the vibrational potentials corresponding to

these models have the forms (in the harmonic approximation)

$$SCF;\ 2V = A_r\ [(\Delta r_1)^2 + (\Delta r_2)^2] + A_{r'}\ (\Delta r_3)^2, \tag{II, 2}$$

$$SVF;\ 2V = B_r\ [(\Delta r_1)^2 + (\Delta r_2)^2] + B_a(r^e_{X-Y}\ \Delta a)^2, \tag{II, 3}$$

$$GCF;\ 2V = D_r\ [(\Delta r_1)^2 + (\Delta r_2)^2] + D_{r'}(\Delta r_3)^2$$

$$+ 2D_{rr}\ (\Delta r_1\ \Delta r_2) + 2D_{rr'}\ (\Delta r_1 + \Delta r_2)\ \Delta r_3, \tag{II, 4}$$

$$GVF;\ 2V = H_r\ [(\Delta r_1)^2 + (\Delta r_2)^2] + H_a\ (r^e_{X-Y}\ \Delta a)^2$$

$$+ 2H_{rr}\ (\Delta r_1\ \Delta r_2) + 2H_{ra}\ (\Delta r_1 + \Delta r_2)\ r^e_{X-Y}\ \Delta a, \tag{II, 5}$$

$$UBF;\ 2V = (K + t^2F' + u^2F)[(\Delta r_1)^2 + (\Delta r_2)^2] + (H - u^2F' + t^2F)(r^e_{X-Y}\ \Delta c)^2$$

$$+ 2(-t^2F' + u^2F)\ \Delta r_1\ \Delta r_2 + 2tu\ (F' + F)(\Delta r_1 + \Delta r_2)\ r^e_{X-Y}\Delta c. \tag{II, 6}$$

In equation (II, 6), K and H denote the stretching and bending potential

constants and F and F', the repulsive potential constants between

non-bonded atoms. F' is often approximated as $-(1/10)F$, which

follows from taking the potential energy proportional to $(r^e_{Y \cdots Y})^{-9}$.

Furthermore, the potential constants defined in equations (II, 4),

(II, 5) and (II, 6) can be simply related. Equating corresponding

coefficients in equations (II, 5) and (II, 6),

$$H_r = K + t^2F' + u^2F,$$

$$H_a = H - u^2F' + t^2F,$$

$$H_{rr} = -t^2F' + u^2F, \tag{II, 7}$$

$$H_{ra} = tu\ (F' + F)\ .$$

Since the potential and kinetic energy expressions must be invariant

with respect to the coordinate system, one has

$$H_r = D_r + 2D_{rr'} \sin (< Y-X-Y/2) + D_{r'} \sin^2 (< Y-X-Y/2),$$

$$H_\alpha = D_{r'} \cos^2 (< Y-X-Y/2), \qquad\qquad (II, 8)$$

$$H_{rr} = D_{rr} + 2D_{rr'} \sin (< Y-X-Y/2) + D_{r'} \sin^2 (< Y-X-Y/2),$$

$$H_{r\alpha} = D_{rr'} \cos (< Y-X-Y/2) + D_{r'} \cos (< Y-X-Y/2) \sin (< Y-X-Y/2).$$

Finally, a comparison of equations (II, 7), and (II, 8) gives

$$K + t^2 F' + u^2 F = D_r + 2D_{rr'} \sin (< Y-X-Y/2) + D_{r'} \sin^2 (< Y-X-Y/2),$$

$$H - u^2 F' + t^2 F = D_{r'} \cos^2 (< Y-X-Y/2), \qquad\qquad (II, 9)$$

$$-t^2 F' + u^2 F = D_{rr} + 2D_{rr'} \sin (< Y-X-Y/2) + D_{r'} \sin^2 (< Y-X-Y/2),$$

$$tu(F' + F) = D_{rr'} \cos (< Y-X-Y/2) + D_{r'} \cos (< Y-X-Y/2) \sin (< Y-X-Y/2).$$

Since the applicability of these models has been discussed by many

authors [see (19, p. 142-191; 40, p. 57-59; 49, p. 169-182) and

bibliographies therein cited], it suffices to mention here that the

usual problem met in evaluating all the potential constants of the

GCF or GVF is that generally there is insufficient data from spec-

troscopy alone: for example, for a bent XY_2 molecule, there are

three frequencies and four generalized quadratic potential constants.

Isotopic substitution provides a solution to this problem, but this

method is not always easy or satisfactory.

Potential and Compliance Constants of Nitrogen Dioxide from Mean-
Square Amplitudes and Vibrational Frequencies

The early work of James (26, p. 737-754) established the con-
nection between molecular vibration and the intensity of scattering
from molecules. Although this work was specifically concerned with
x-ray scattering, the results are also applicable to electrons, and
have been successfully applied to the interpretation of electron dif-
fraction patterns for many years. Recently, a good deal of attention
has been devoted to exploring the connection between amplitudes of
vibration, frequencies of vibration, and force constants [see (10,
p. 1-200; 11, p. 1121-1122; 22, p. 594-598; 33, p. 395; 34, p. 726-
733; 35, p. 1927-1933; 36, p. 737-747; 37, p. 643-652) and biblio-
graphies therein cited]; the work by James provides the theoretical
backbone for the interpretation of the diffraction results. It is the
intention here to present only an outline of those ideas and equations
needed to relate potential constants to mean amplitudes and normal
frequencies of vibration.

Morino and Hirota (36, p. 737-747) distinguish three types of
generalized vibrational amplitudes with respect to a specific atom
pair (i, j) in a molecule. Let the coordinates x_1, x_2 and x_3 denote
the Cartesian axes parallel and perpendicular, respectively, to r_{ij};
then Δx_1, Δx_2 and Δx_3 will denote the net displacement coordinates

of the i, j atomic pair along each of these axial directions. The

various amplitudes are then defined as follows:

$< \Delta x_1^2 >$; the mean-square parallel amplitude,

$< \Delta x_2^2 >, < \Delta x_3^2 >$; the mean-square perpendicular amplitudes,

$< \Delta x_1 \Delta x_2 >, <\Delta x_2 \Delta x_3 >, < \Delta x_2 \Delta x_1 >$; the mean cross products.

It has been shown (36, p. 743) that symmetry considerations allow

one to conclude that for a non-linear XY_2 molecule the only non-zero

amplitudes for the atomic pair Y-X are $< \Delta x_1^2 >$ and $< \Delta x_1 \Delta x_2 >$, and

for Y···Y, $< \Delta x_1^2 >$; the diagram shows the orientation of coordinates.
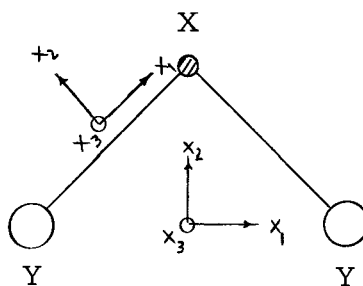
Now, in the usual definition (10, p. 1) of the mean amplitude

of vibration for an atom pair i, j one has

$$l_{ij} = <(r_{ij}^i - r_{ij}^e)^2 >^{\frac{1}{2}} . \qquad (II, 10)$$

As a first approximation l_{ij} is equivalent to the square root of the

mean-square parallel amplitude discussed earlier. That is,

$$r_{ij}^i - r_{ij}^e = \sum_{k=1}^{3} (\partial r_{ij}^i / \partial x_k)_e \Delta x_k + \text{higher order terms} = \sum_{k=1}^{3} (x_k / r_{ij}^e) \Delta x_k$$

+ higher order terms; neglecting the higher order terms, squaring

and averaging gives equation (II, 10). The various relationships de-

fining the basic framework of the potential constant calculation may

be summarized as follows.

Let the column matrices $\mathbb{R}$, $\mathbb{S}$, and $\mathbb{Q}$ represent respectively sets of internal coordinates, symmetry coordinates, and the normal coordinates. The relations between these sets of coordinates are

$$R = \bar{V} \, S \qquad\qquad (\text{II, 11})$$

and

$$S = L \, Q \, . \qquad\qquad (\text{II, 12})$$

The matrix L is determined by the equations (47, p. 1047-1052; 48, p. 76-84)

$$G_S \, F_S \, L = L \, \Lambda \, , \qquad\qquad (\text{II, 13})$$

$$L' \, F_S \, L = \Lambda \, , \qquad\qquad (\text{II, 14})$$

and

$$L \, L' = G_S \, . \qquad\qquad (\text{II, 15})$$

The matrix F_S, of course, is defined in terms of the potential energy

$$2V = S' \, F_S \, S \, . \qquad\qquad (\text{II, 16})$$

The matrix G_S is connected to the kinetic energy, as may be seen by the following equations:

$$X = \bar{A} \, R \, , \qquad\qquad (\text{II, 17}$$

$$2T = \dot{\mathbf{X}}' \, \overline{\mathbf{M}} \, \dot{\mathbf{X}}$$

$$= \dot{\mathbf{R}}' \, \overline{\mathbf{A}}' \, \overline{\mathbf{M}} \, \overline{\mathbf{A}} \, \dot{\mathbf{R}}$$

$$= \dot{\mathbf{R}}' \, \mathbf{G}_R^{-1} \, \dot{\mathbf{R}}$$

$$= \dot{\mathbf{S}}' \, \overline{\mathbf{V}}' \, \mathbf{G}_R^{-1} \, \overline{\mathbf{V}} \, \dot{\mathbf{S}}$$

$$= \dot{\mathbf{S}}' \, \mathbf{G}_S^{-1} \, \dot{\mathbf{S}}. \tag{II, 18}$$

The matrix $\boldsymbol{\Lambda}$ is a diagonal matrix the elements of which are given

by

$$\lambda_k = 4\pi^2 \nu_k^2 \; ; \tag{II, 19}$$

they are related to the $\mathbf{G}$ and $\mathbf{F}$ matrices by the secular equations

(47, p. 1047-1052)

$$| \, \mathbf{G}_S \, \mathbf{F}_S - \lambda \, \mathbf{E} \, | = 0 \tag{II, 20}$$

and

$$| \, \mathbf{G}_R \, \mathbf{F}_R - \lambda \, \mathbf{E} \, | = 0 \; . \tag{II, 21}$$

The mean square amplitudes of a normal vibration defined by

the diagonal matrix

$$< \mathbf{Q} \, \mathbf{Q}' > \; = \; < \mathbf{Q}^2 >^1 \; = \; \boldsymbol{\Delta} \tag{II, 22}$$

and in the harmonic approximation are given by (6, p. 309; 26,

p. 737-754)

$$< \mathbf{Q}_k^2 > = h/8\pi^2 \nu_k \; \coth \, (h\nu_k/2kT) \; . \tag{II, 23}$$

The mean square vibrational matrix in internal coordinates (Σ_R)

(34, p. 726-727) is given by

---

[1] $< \mathbf{Q} \, \mathbf{Q}' >$ is diagonal due to the non-mixing character of the normal coordinates.

$$\Sigma_R = <R\ R'> = <\bar{V}\ L\ Q\ Q'\ L'\ \bar{V}'>$$

$$= \bar{V}\ L\ <Q\ Q'>\ L'\ \bar{V}' = \bar{V}\ L\ \Delta\ L'\ \bar{V}' . \tag{II, 24}$$

The solution to the vibrational problem is contained in equations

(II, 13) and (II, 24). The V and G matrices can be written down by

inspection, and by eliminating the L matrix elements from these

two equations [with the aid of the normalization conditions expressed

in equations (II, 14) and (II, 15)] one obtains expressions for the

potential constants in terms of the measured mean-square vibrational

amplitudes and vibrational frequencies.

For nitrogen dioxide the general quadratic potential function in

terms of the internal valence force coordinates, Δr_1, Δr_2, and

$r^e\ \Delta a$ is [see equation (II, 5)]

$$2V = f_r\ [(\Delta r_1)^2 + (\Delta r_2)^2] + 2f_{rr}\ (\Delta r_1 \Delta r_2) + f_a(r^e\ \Delta a)^2$$

$$+ 2f_{ra}\ (\Delta r_1 + \Delta r_2)\ r^e\ \Delta a . \tag{II, 25}$$

The molecular point group of nitrogen dioxide is C_{2v}. The symmetry

species (49, p. 146-162) as obtained by standard procedures are

$$\Gamma\ (NO_2) = \Gamma\ (r) + \Gamma\ (a)$$

$$= (A_1 + B_1) + A_1$$

$$= 2A_1 + B_1 , \tag{II, 26}$$

where A_1 and B_1 denote symmetric and antisymmetric modes,

respectively. The selection rules thus predict two infrared and

Raman active A_1 modes (symmetric stretch and bend, respectively)

and one active B_1 mode (antisymmetric stretch) for nitrogen dioxide.

Representing the column matrices $\mathbb{R}$ and $\mathbf{S}$ as

$$\mathbb{R} = \{ \Delta r_1, \; r^e \Delta a, \; \Delta r_2 \} \qquad \text{(II, 27)}$$

and

$$\mathbf{S} = \{ S_1, \; S_2, \; S_3 \} \; , \qquad \text{(II, 28)}$$

the transformation matrix $\bar{V}$ can be obtained as follows. Let the subscripts 1 and 2 denote the totally symmetric N-O stretch and <O-N-O bend, respectively, and the subscript 3, the antisymmetric N-O stretch. Then the symmetry coordinates are given by (42, p. 902)

$$S_1 = S_r^{(A_1)} = 2^{-\frac{1}{2}} (\Delta r_1 + \Delta r_2) \; , \qquad \text{(II, 29)}$$

$$S_2 = S_a^{(A_1)} = r^e \; \Delta a \qquad \text{(II, 30)}$$

and

$$S_3 = S_r^{(B_1)} = 2^{-\frac{1}{2}} (\Delta r_1 - \Delta r_2) \; . \qquad \text{(II, 31)}$$

The orthogonality of $\bar{V}$ is easily demonstrated in this case. Since an orthogonal transformation leaves the sum of squares of both sets of coordinates invariant, the following relationship should and does exist:

$$(\Delta r_1)^2 + (\Delta r_2)^2 + (r^e \Delta a)^2 = S_1^2 + S_2^2 + S_3^2 \; . \qquad \text{(II, 32)}$$

Hence, $\bar{V}^{-1} = \bar{V}'$ and we have

$$\bar{V} = \begin{bmatrix} 2^{-\frac{1}{2}} & 0 & 2^{-\frac{1}{2}} \\[2mm] & 1 & 0 \\[2mm] & & -2^{-\frac{1}{2}} \end{bmatrix} \; . \qquad \text{(II, 33)}$$

One may now write the column matrix $\mathbb{Q}$ as

$$\mathbb{Q} = \{ Q_1, Q_2, Q_3 \} = \{ Q_r^{(A_1)}, Q_a^{(A_1)}, Q_r^{(B_1)} \} \ , \qquad (II, 34)$$

the transformation matrix $\mathbb{L}$ [see equation (II, 12)] as

$$\mathbb{L} = \begin{bmatrix} L_{11} & L_{12} & 0 \\ L_{21} & L_{22} & 0 \\ 0 & 0 & L_{33} \end{bmatrix} , \qquad (II, 35)$$

and the mean-square normal coordinate matrix, Δ [see equation (II, 22)], as

$$\Delta = \begin{bmatrix} \Delta_1 & 0 & 0 \\ & \Delta_2 & 0 \\ & & \Delta_3 \end{bmatrix} . \qquad (II, 36)$$

From the expression for Σ_R [equation (II, 24)] we can relate the mean-square vibrational amplitudes l_{N-O}^2 and $l_{O \cdots O}^2$ to the elements of the $\bar{V}$, L and Δ matrices as follows. Using the first expression in equation (II, 24)

$$< \mathbb{R} \ \mathbb{R}' > = \begin{bmatrix} l_{N-O}^2 & r^e < \Delta r \, \Delta a> & < \Delta r_1 \, \Delta r_2 > \\ & (r^e)^2 < \Delta a^2 > & r^e < \Delta r \, \Delta a> \\ & & l_{N-O}^2 \end{bmatrix} , \qquad (II, 37)$$

from which

$$\bar{V} \ \mathbb{L} \ \Delta \ L' \ \bar{V}' =$$

$$\begin{bmatrix} 2^{-1}(\Delta_1 L_{11}^2 + \Delta_2 L_{12}^2 + \Delta_3 L_{33}^2), & 2^{\frac{1}{2}}(\Delta_1 L_{11} L_{12} + \Delta_2 L_{12} L_{22}), & 2^{-1}(\Delta_1 L_{11}^2 + \Delta_2 L_{12}^2 - \Delta_3 L_{33}^2) \\ & \Delta_1 L_{21}^2 + \Delta_2 L_{22}^2 & , \ 2^{\frac{1}{2}}(\Delta_1 L_{11} L_{12} + \Delta_2 L_{12} L_{22}) \\ & & 2^{-1}(\Delta_1 L_{11}^2 + \Delta_2 L_{12}^2 + \Delta_3 L_{33}^2) \end{bmatrix} .$$

$$(II, 38)$$

If one squares both sides of equation (II, 1) and takes the time average

$$l^2_{O\cdots O} = <\Delta r^2_3> = 2(l^2_{N-O} + <\Delta r_1 \Delta r_2>) \sin^2 (a/2)$$

$$+ (r^e)^2 <\Delta a^2> \cos^2 (a/2) + 2r^e <\Delta r \Delta a> \sin a \ . \ (II, 39)$$

Combining equations (II, 37), (II, 38) and (II, 39), one obtains

$$l^2_{N-O} = 2^{-1} (\Delta_1 L^2_{11} + \Delta_2 L^2_{22} + \Delta_3 L^2_{33}) \qquad (II, 40)$$

and

$$l^2_{O\cdots O} = 2(\Delta_1 L^2_{11} + \Delta_2 L^2_{12}) \sin^2 (a/2) + (\Delta_1 L^2_{21} + \Delta_2 L^2_{22}) \cos^2 (a/2)$$

$$+ 2^{\frac{1}{2}} (\Delta_1 L_{11} L_{21} + \Delta_2 L_{12} L_{22}) \sin a \ . \qquad (II, 41)$$

The $\mathbb{F}_S$ and G_S matrices may be written down immediately

(42, p. 902)

$$\mathbb{F}_S = \begin{bmatrix} f_r + f_{rr} & 2^{\frac{1}{2}} f_{ra} & 0 \\ & f_a & 0 \\ & & f_r - f_{rr} \end{bmatrix} = \begin{bmatrix} F_{11} & F_{12} & 0 \\ & F_{22} & \\ & & F_{33} \end{bmatrix} \qquad (II, 42)$$

and

$$G_S = \begin{bmatrix} 2\mu_N \cos^2 (a/2) + \mu_O \ , & -2^{3/2} \mu_N \sin(a/2) \cos(a/2) & 0 \\ & 2(2\mu_N \sin^2 (a/2) + \mu_O & \\ & & 2\mu_N \sin^2 (a/2) + \mu_O \end{bmatrix}$$

$$= \begin{bmatrix} G_{11} & G_{12} & 0 \\ & G_{22} & 0 \\ & & G_{33} \end{bmatrix} \ . \qquad (II, 43)$$

Solving equation (II, 14) for $\mathbb{F}^{-1}_S$, one obtains

$$\mathbb{F}^{-1}_S = \mathbb{L} \ \Lambda^{-1} \ \mathbb{L}' \ . \qquad (II, 44)$$

Since

$$\mathbb{F}_S^{-1} = \begin{bmatrix} F_{22}/\beta & -F_{12}/\beta & 0 \\ & F_{11}/\beta & 0 \\ & & F_{33}^{-1} \end{bmatrix} \qquad (II, 45)$$

and

$$\Lambda^{-1} = \begin{bmatrix} 1/\lambda_1 & 0 & 0 \\ & 1/\lambda_2 & 0 \\ & & 1/\lambda_3 \end{bmatrix} , \qquad (II, 46)$$

one obtains with equations (II, 35) and (II, 43),

$$\begin{bmatrix} G_{11} & G_{12} & 0 \\ & G_{22} & 0 \\ & & G_{33} \end{bmatrix} = \begin{bmatrix} L_{11}^2 + L_{12}^2 & L_{11}L_{21} + L_{12}L_{22} & 0 \\ & L_{21}^2 + L_{22}^2 & 0 \\ & & L_{33}^2 \end{bmatrix} \qquad (II, 47)$$

and

$$\begin{bmatrix} F_{22}/\beta & -F_{12}/\beta & 0 \\ & F_{11}/\beta & 0 \\ & & F_{33}^{-1} \end{bmatrix}$$

$$= \begin{bmatrix} L_{11}^2\lambda_1^{-1} + L_{12}^2\lambda_2^{-1}, & L_{11}L_{21}\lambda_1^{-1} + L_{12}L_{22}\lambda_2^{-1}, & 0 \\ & L_{21}^2\lambda_1^{-1} + L_{22}^2\lambda_2^{-1}, & 0 \\ & & L_{33}^2\lambda_3^{-1} \end{bmatrix} . \quad (II, 48)$$

The solution of equation (II, 20) can be written down by inspection

(30, p. 3) giving

$$\lambda_1 + \lambda_2 = G_{11}F_{11} + G_{22}F_{22} + 2G_{12}F_{22} , \qquad (II, 49)$$

$$\lambda_1 \lambda_2 = \beta(G_{11}G_{22} - G_{12}^2) = \beta\bar{\gamma} , \qquad \text{(II, 50)}$$

and

$$\lambda_3 = G_{33}F_{33} . \qquad \text{(II, 51)}$$

Combining equations (II, 47) and (II, 48), one obtains

$$L_{11}^2 = [\lambda_1/\beta(\lambda_1 - \lambda_2)] (-\lambda_2 F_{22} + \beta G_{11}) , \qquad \text{(II, 52)}$$

$$L_{22}^2 = [\lambda_2/\beta(\lambda_1 - \lambda_2)] (\lambda_1 F_{11} - \beta G_{22}) , \qquad \text{(II, 53)}$$

$$L_{33}^2 = G_{33} = \lambda_3/F_{33} , \qquad \text{(II, 54)}$$

$$L_{12}^2 = [\lambda_2/\beta(\lambda_1 - \lambda_2)] (\lambda_1 F_{22} - \beta G_{11}) , \qquad \text{(II, 55)}$$

$$L_{21}^2 = [\lambda_1/\beta(\lambda_1 - \lambda_2)] (-\lambda_2 F_{11} + \beta G_{22}) , \qquad \text{(II, 56)}$$

$$L_{11}L_{21} = [\lambda_1/\beta(\lambda_1 - \lambda_2)] (\lambda_2 F_{12} + \beta G_{12}) , \qquad \text{(II, 57)}$$

$$L_{12}L_{22} = [-\lambda_2/\beta(\lambda_1 - \lambda_2)] (\lambda_1 F_{12} + \beta G_{12}) . \qquad \text{(II, 58)}$$

Finally, by condensing the various relationships one has

$$l_{N-O}^2 = A_1 F_{22} + A_2(F_{11}F_{22} - F_{12}^2) + A_3 , \qquad \text{(II, 59)}$$

$$l_{O\cdots O}^2 = A_4 F_{22} + A_5 F_{11} + A_6 F_{12} + A_7 , \qquad \text{(II, 60)}$$

$$A_8 = A_9 F_{22} + A_{10} F_{11} + A_{11} F_{12} , \qquad \text{(II, 61)}$$

and

$$F_{33} = \lambda_3/G_{33} , \qquad \text{(II, 62)}$$

where

$$A_1 = \bar{c}f/2g, \quad A_2 = G_{11}\bar{bc}/2dg, \quad A_3 = G_{33}e/2, \quad A_4 = 2\bar{i} \sin^2(a/2) ,$$

$$A_5 = \bar{i} \cos^2(a/2) , \quad A_6 = -2^{3/2}\bar{i} \sin(a/2) \cos(a/2) ,$$

$$A_7 = (\bar{b}/g)[2G_{11} \sin^2 a/2 + (G_{22} \cos a/2 + 2^{3/2}G_{12} \sin a/2) \cos a/2] ,$$

$$A_8 = \bar{h}, \quad A_9 = G_{22}, \quad A_{10} = G_{11}, \quad A_{11} = 2G_{12} \qquad \text{(II, 63)}$$

with

$$\bar{b} = \Delta_1 \lambda_1 - \Delta_2 \lambda_2, \quad \bar{c} = \bar{\gamma}, \quad d = \lambda_1 \lambda_2, \quad e = \Delta_3, \quad f = \Delta_2 - \Delta_2 ,$$

$$g = \lambda_1 - \lambda_2, \quad \bar{h} = \lambda_1 + \lambda_2, \quad \bar{i} = \bar{c} f / g = 2A_1 . \qquad \text{(II, 64)}$$

Since equation (II, 59) is quadratic in F_{12}, two sets of solutions are

possible. The most physically reasonable is selected.

During the course of this work J. C. Decius (12, p. 241-248)

introduced the notion of a compliance matrix. With this approach the

secular equation takes the form

$$| \mathbb{C} \mathbb{K} - \phi \mathbb{E} | = 0 , \qquad \text{(II, 65)}$$

where $\mathbb{K} = G^{-1}$, $\mathbb{C} = \mathbb{F}^{-1}$, and $\phi = \lambda^{-1}$. Since this paper de-

scribes the determination of compliance constants from normal fre-

quencies and mean-square amplitudes (or centrifugal distortion data),

treating among other molecules, nitrogen dioxide as an example,[1]

no attempt will be made here to duplicate this development. Since

the compliance constants to be reported in this thesis correspond to

the inverse of the $\mathbb{F}_S$ matrix defined in equation (II, 45), the sym-

metrized compliance matrix $\mathbb{C}_S$ (defined in terms of valence force

symmetry coordinates) will take the form

---

[1]The values of l^2_{N-O} and $l^2_{O \cdots O}$ used by Professor Decius
correspond to preliminary values obtained during the course of this
thesis work.

$$\mathbb{C}_S = \begin{bmatrix} C_{11} & C_{12} & 0 \\ & C_{22} & 0 \\ & & C_{33} \end{bmatrix} = \begin{bmatrix} F_{22}/\beta & -F_{12}/\beta & 0 \\ & F_{11}/\beta & 0 \\ & & F_{33}^{-1} \end{bmatrix}.$$

$$(\text{II, 66})$$

The compliance matrix of nitrogen dioxide reported by Decius is

defined in terms of central force coordinates, it differs numerically

from $\mathbb{C}_S$ of equation (II, 66).

Computation of Potential and Compliance Constants

The numerical solutions of equations (II, 59) - (II, 61) were ob-

tained by the use of the university Alwac III-E digital computer. Since

the computer program is rather specialized (non-linear XY_2 mole-

cules), it will not be reproduced here though a brief description will

be given. The vibrational frequencies (1, p. 413-427) used are

given[1] in Table 24. The computer output gave elliptical contours

(22, p. 596-598) corresponding to the observed values of l_{N-O} and

$l_{O\cdots O}$, respectively, such that on each of the two contours (cor-

responding to l_{N-O} and $l_{O\cdots O}$), all real combinations of the sym-

metrized potential constants F_{11}, F_{22} and F_{12} were represented.

Systematic investigation of the output contours identified their ap-

proximate intersections (ideally, there are two of them); these

---

[1]Separate calculations were made using first the ν_i's and
then the ω_i's.

intersections were subsequently calculated exactly. Since the inter-

sections represented two combinations of symmetrized potential

constants compatible with both electron diffraction and spectroscopic

data, they are the solutions of equations (II, 59) - (II, 61). Figure 5

is a plot of these contours. Finally, these solutions were transformed

to the corresponding ones in terms of the internal potential constants

f_r, f_{rr}, f_α and $f_{r\alpha}$ [see equation (II, 42)].

In addition to the potential constants obtained by the method

described above, various combinations of frequencies (see Table 30a)

and vibrational amplitudes were investigated using a newly devised

least-squares program of R. Ottinger.[1] The elements of the diagonal

weight matrix used were given by

$$(\mathbb{P}_{Ot})_{\nu_i} = 1 \quad \text{and} \quad (\mathbb{P}_{Ot})_{l_{ij}^2} = 2500. \tag{II, 67}$$

These results are expressed in terms of the symmetrized compliance

constants defined in equation (II, 66).

Errors in the Internal Potential Constants Derived from the Inter-

sections of Elliptical Contours

A complete error analysis should include uncertainties arising

from the determination of the vibrational amplitudes, normal fre-

quencies, interatomic distances, physical constants and the errors

---

[1]Ottinger, Robert. Private communication. Corvallis,
Oregon. Oregon State University, 1964.

arising from the method of calculation employed. The effect in the potential constants arising from the uncertainties in the vibrational amplitudes were estimated as follows. Let f_i denote one of the internal potential constants f_r, f_{rr}, f_α, and $f_{r\alpha}$, then

$$f_i = f_i \, (r_{N-O}, \; r_{O\ldots O}, \; l_{N-O}, \; l_{O\ldots O}, \; \nu_1, \; \nu_2, \; \nu_3). \qquad \text{(II, 68)}$$

Further, let $\sigma(f_i)$ be defined as

$$2\sigma(f_i) = f_i [\, r_{N-O}, \; r_{O\ldots O}, \; l_{N-O} + m\sigma_T(l_{N-O}), \; l_{O\ldots O} + n\sigma_T(l_{O\ldots O}), \; \nu_1, \nu_2, \nu_3]$$

$$-f_i(r_{N-O}, \; r_{O\ldots O}, \; l_{N-O}, \; l_{O\ldots O}, \; \nu_1, \nu_2, \nu_3). \qquad \text{(II, 69)}$$

It is clear that $\sigma(f_i)$ (as a very rough approximation) will reflect the uncertainty in f_i arising from those in the vibrational amplitudes. The values of the coefficients m and n were obtained from the error matrix given in Table 24. The correlation between l_{N-O} and $l_{O\ldots O}$ is positive indicating that the error which increases one mean amplitude also increases the other, hence, m and n should have the same algebraic signs. Arbitrarily, m was taken as two, and n as one-half. The results are given in Tables[1] 26a and 26b.

No attempt was made to estimate the errors arising from the determination of normal frequencies, internuclear distances, and physical constants. From the form of equations (II-59) to (II-64), it was felt that these errors would be negligible by comparison to those

---

[1] Similar estimates were obtained for the set of potential constants derived from the ω_i's instead of the ν_i's. The effect of $\sigma_{LS}(l_{ij})$ in place of $\sigma_T(l_{ij})$ was also investigated.

of the vibrational amplitudes.

Errors in the Symmetrized Compliance Constants Obtained from Least-Squares Fitting

The only errors estimated here were the standard errors obtained from least-squares fitting (Table 30a). The significance of these errors is mainly that of indicating the compatibility of the vibrational amplitudes and the normal frequencies with respect to the compliance constants.

Final Results

The constants used in the various calculations are given in Tables 23-25. The final results are given in Tables 27-30b. Comparison of the internal potential constants determined in this work with those obtained by isotopic spectroscopy (1, p. 413-427) shows the agreement to be good (Table 27). The comparison of the observed and calculated frequencies (derived from the final internal potential constants), as given in Table 29, is pleasing, especially so in the case of the ω_i's. The comparison of the observed vibrational amplitudes from this work with those calculated by Cyvin (10, p. 117) from potential constants derived from isotopic spectroscopy, is

given in Table 29. Again the agreement[1] is good. The numerous

compliance constant results given in Tables 30a and 30b are discussed

in the next section.

---

[1]Though the observed amplitudes and calculated ones cor-
respond to two different temperatures (380° and 298° K, respectively),
the temperature effect in this case is surely very small since the
vibrational frequencies are high.

SUMMARY

Part I

The molecular geometry of nitrogen dioxide was determined. The parameter values of r_{N-O}, $r_{O\cdots O}$, and $<O-N-O$ agree well with the corresponding microwave results (5, p. 1040-1043). Conservative estimates of standard errors lead to probable accuracies of 0.1, 0.2, and 0.5 percent for r_{N-O}, $r_{O\cdots O}$, and $<O-N-O$, respectively. Corresponding conservative estimates for the root-mean-square amplitudes of vibration lead to seven percent for l_{N-O} and 11 percent for $l_{O\cdots O}$.

Part II

The two sets of internal quadratic potential constants determined from $\{l_{N-O}, l_{O\cdots O}, r_{N-O}, r_{O\cdots O}, \nu_1, \nu_2, \nu_3\}$ and from $\{l_{N-O}, l_{O\cdots O}, r_{N-O}, r_{O\cdots O}, \omega_1, \omega_2, \omega_3\}$ agree well with those obtained from isotopic spectroscopy. The comparison of calculated and observed frequencies indicated that there is probably very little anharmonicity in the $O\cdots O$ motion. Further, the observed vibrational amplitudes agree well with those calculated by Cyvin.

The numerous least-squares fitting for symmetrized compliance constants indicated that (1) the results are essentially

insensitive to the bond angle[1] parameter used within reasonable

limits, (2) the off-diagonal compliance constants are quite sensitive

to input data combinations, where the diagonal elements are not. The

agreement between the various sets of compliance constants and in-

ternal potential constants suggest very strongly that vibrational

amplitudes from electron diffraction (at least for small polyatomics

composed of similar atoms) are compatible with spectroscopy data

(vibrational frequencies) with respect to either potential or com-

pliance constant determinations. This statement is further rein-

forced by the various comparisons of observed and calculated fre-

quencies.

In conclusion, the reliability and consistency of the vibrational

amplitudes from electron diffraction for potential or compliance

constant determinations can be regarded as favorable, at least for

small polyatomic molecules composed of similar atoms.

---

[1]As determined from r_{N-O} and $r_{O \cdots O}$.

BIBLIOGRAPHY

1. Arakawa, Edward T. and Alvin H. Nielsen. Infrared spectra and molecular constants of $N^{14}O_2$ and $N^{15}O_2$. Journal of Molecular Spectroscopy 2:413-427. 1958.

2. Bartell, L. S. Effects of anharmonicity of vibration on the diffraction of electrons by free molecules. The Journal of Chemical Physics 23:1219-1222. 1955.

3. Bastiansen, O. , O. Hassel, and Eilif Risberg. The Oslo electron diffraction units for gas work. Acta Chemica Scandinavica 9:232-238. 1955.

4. Bewilogua, L. Uber die inkoharente Streuung der Rontgen-strahlen. Physikalische Zeitschrift 32:470-474. 1931.

5. Bird, George R. Microwave spectrum of NO_2: A rigid rotor analysis. The Journal of Chemical Physics 25:1040-1043. 1956.

6. Bloch, F. Zur Theorie des Austauschproblems und der Remanenzerscheinung der Ferromagnetika. Zeitschrift für Physik 74:295-335. 1932.

7. Bonham, R. A. and L. S. Bartell. Rapid procedure for rigorous analysis of electron diffraction data. The Journal of Chemical Physics 31:702-708. 1959.

8. Brockway, L. O. Electron diffraction by gas molecules. Reviews of Modern Physics 8:231-266. 1936.

9. Claesson, Stig, Jerry Donohue, and Verner Schomaker. The molecular structure of nitrogen dioxide. A reinvestigation by electron diffraction. The Journal of Chemical Physics 16:207-210. 1948.

10. Cyvin, Sven J. Mean amplitudes of vibration in molecular struc-ture studies. Acta Polytechnica Scandinavica, Physics including Nucleonics, ser 6, 279:1-226. 1960.

11. Decius, J. C. Classical limit of mean thermal vibrational am-plitudes. The Journal of Chemical Physics 21:1121-1122. 1953.

12. Decius, J. C. Compliance matrix and molecular vibrations. The Journal of Chemical Physics 38:241-248. 1963.

13. Glauber, R. and V. Schomaker. The theory of electron diffraction. Physical Review 89:667-671. 1953.

14. Haine, M. E. and P. A. Einstein. Characteristics of the hot cathode electron microscope gun. British Journal of Applied Physics 3:40-46. 1952.

15. Harris, Louis and G. W. King. The rotational structure of the ultraviolet bands of NO_2. The Journal of Chemical Physics 8:775-784. 1940.

16. Hedberg, Kenneth and Machio Iwasaki. Effect of temperature on the structure of gaseous molecules. Molecular structure of PCl_3 at 300° and 500° K. The Journal of Chemical Physics 36:589-594. 1962.

17. Hedberg, Kenneth and Machio Iwasaki. Least-quares refinement of molecular structures from gaseous electron-diffraction sector-microphotometer intensity data. I. Method. Acta Crystallographica 17:529-533. 1964.

18. Heisenberg, W. Uber die inkoharente Streuung der Rontstrahlen. Physikalische Zeitschrift 32:737-740. 1931.

19. Herzberg, Gerhard. Infrared and Raman spectra of polyatomic molecules. Princeton, D. Van Nostrand, 1945. 632 p.

20. Hillier, James and R. F. Baker. On the improvement of resolution in electron diffraction cameras. Journal of Applied Physics 17:12-22. 1946.

21. Hoerni, Jean A. and James A. Ibers. Some calculations of atomic form factors. Acta Crystallographica 7:744-746. 1954.

22. Iwasaki, Machio and Kenneth Hedberg. Potential constants of PCl_3 from amplitudes of vibration and normal vibrational frequencies. The Journal of Chemical Physics 36:594-598. 1962.

23. Iwasaki, Machio and Kenneth Hedberg. Centrifugal distortion of bond distances and bond angles. The Journal of Chemical Physics 36:2961-2963. 1962.

24. Iwasaki, Machio, F. N. Fritsch, and Kenneth Hedberg. Least-squares refinement of molecular structures from gaseous electron-diffraction sector-microphotometer intensity data. II. Adaptation to automatic computation. Acta Crystallographica 17:533-537. 1964.

25. James, R. W. and G. W. Brindley. Some numerical calculations of atomic scattering factors. Philosophical Magazine and Journal of Science, ser. 7, 12:81÷111. 1931.

26. James, R. W. Uber der Einfluss der Temperatur auf die Streuung der Rontgenstrahlen durch Gas Molekule. Physikalische Zeitschrift 33:737-754. 1932.

27. Karle, J. and I. L. Karle. Internal motion and molecular structure studies by electron diffraction. II. Interpretation and method. The Journal of Chemical Physics 18:957-962. 1950.

28. Keller, Fred L. and Alvin H. Nielsen. Grating measurement of $\bar{v}_2$ of NO_2 at 200° C. The Journal of Chemical Physics 24: 636-637. 1956.

29. Kuchitsu, Kozo and L. S. Bartell. Effects of anharmonicity of molecular vibrations on the diffraction of electrons. II. Interpretation of experimental structural parameters. The Journal of Chemical Physics 35:1945-1949. 1961.

30. Lomont, J. S. Applications of finite groups. New York, Academic Press, 1959. 346 p.

31. Maxwell, Louis R. and V. M. Mosley. Molecular structure of nitrogen dioxide and nitric acid by electron diffraction. The Journal of Chemical Physics 8:738-742. 1940.

32. Moore, Gordon E. The spectrum of nitrogen dioxide in the 1.4-3.4 μ region and the vibrational and rotational constants of the NO_2 molecule. Journal of the Optical Society of America 43:1045-1050. 1953.

33. Morino, Yonezo. On the mean amplitudes of thermal vibration in CO_2 molecule. The Journal of Chemical Physics 18: 395. 1950.

34. Morino, Yonezo, Kôzo Kuchitsu and Takehiko Shimanouchi. The mean amplitudes of thermal vibrations in polyatomic molecules. I. $CF_2 = CF_2$ and $CH_2 = CF_2$. The Journal of Chemical Physics 20:726-733. 1952.

35. Morino, Yonezo et al. The mean amplitudes of thermal vibrations in polyatomic molecules. II. An approximate method for calculating mean square amplitudes. The Journal of Chemical Physics 21:1927-1933. 1953.

36. Morino, Yonezo and Eizi Hirota. Mean amplitudes of thermal vibrations in polyatomic molecules. III. The generalized mean amplitudes. The Journal of Chemical Physics 23: 737-747. 1955.

37. Morino, Yonezo, Yasushi Nakamura, and Takao Iijima. Mean square amplitudes and force constants of tetrahedral molecules. I. Carbon tetrachloride and germanium tetrachloride. The Journal of Chemical Physics 32:643-652. 1960.

38. Morino, Yonezo, Kôzo Kuchitsu, and Takeshi Oka. Internuclear distance parameters. The Journal of Chemical Physics 36: 108-1109. 1962.

39. Mott, N. F. and H. S. W. Massey. The theory of atomic collisions. 2d ed. London, Oxford University Press, 1949. 388 p.

40. Nakamoto, Kazuo. Infrared spectra of inorganic and coordination compounds. New York, John Wiley and Sons, 1963. 328 p.

41. Pauling, Linus and L. O. Brockway. A study of the methods of electron-diffraction photographs of gas molecules, with results for benzene and carbon tetrachloride. The Journal of Chemical Physics 2:867-881. 1934.

42. Polo, Santiago R. and M. Kent Wilson. Infrared spectrum of $S^{16}O^{18}O$ and the potential constants of SO_2. The Journal of Chemical Physics 22:900-903. 1954.

43. Viervoll, H. and O. Ögrim. An extended table of atomic scattering factors. Acta Crystallographica 2:277-279. 1949.

44. Waser, Jürg and Verner Schomaker. The Fourier inversion of diffraction data. Reviews of Modern Physics 25:671-690. 1953.

45. Weston, Ralph E., Jr. Infrared spectrum of $N^{15}O_2$ and force constants of NO_2. The Journal of Chemical Physics 26: 1248-1251. 1957.

46. Wilson, E. Bright, Jr. and Bryce L. Crawford, Jr. The secular equation for molecular vibrations. Journal of Chemical Physics 6:223. 1938.

47. Wilson, E. Bright, Jr. A method of obtaining the expanded secular equation for the vibration frequencies of a molecule. The Journal of Chemical Physics 7:1047-1052. 1939.

48. Wilson, E. Bright, Jr. Some mathematical methods for the study of molecular vibrations. Journal of Chemical Physics 9:76-84. 1941.

49. Wilson, E. Bright Jr., J. C. Decius and Paul C. Cross. Molecular vibrations. New York, McGraw-Hill, 1955. 388 p.

50. Yost, Don M. and Horace Russel, Jr. Systematic inorganic chemistry. New York, Prentice-Hall, 1944. 421 p.

APPENDICES

APPENDIX I

TABLES

Table 1. Previous structure investigations of nitrogen dioxide.

r_{N-O}, Å	<O-N-O, deg.		Comments
1.21 ± .02	130	±2	electron diffraction (31).[a]
1.20 ± .02	132	±3	electron diffraction (9).[a]
1.21	141		Spurr (50, p. 27) reanalyzed the electron diffraction data of Maxwell and Mosley (31).
1.28	154		partial analysis of ultraviolet spectrum (15).
1.188± .004	134.07± .25		infrared (32).
1.189± .003	133.95± .10		calculated (45) from rotational data of Keller and Nielsen (28) and Moore (32).
1.186± .003	133.53± .15		electron diffraction.[b], 1
1.197	134.25		microwave (5).

[a] Visual method (8, p. 250-254; 41, p. 867-881).
[b] Sector-microphotometer method (27).

[1] Severinsson, Robert. Private communication. Oslo, Norway. Universitetets Kjemisk Institutt, 1955.

Table 2. Electron intensity incident on the photographic plate: h = 478.00 mm.

s	$I_p^{a(1)}$		$I_p^{a(2)}$		$I_p^{a(3)}$		$I_p^{a(4)}$	
	L	R	L	R	L	R	L	R
2.50	0.4570	0.5110	0.3820	0.4240	0.5050	0.5490	0.4220	0.4500
2.75	0.4470	0.4920	0.3730	0.4100	0.4930	0.5310	0.4110	0.4370
3.00	0.4370	0.4780	0.3640	0.3960	0.4820	0.5160	0.4030	0.4240
3.25	0.4310	0.4670	0.3580	0.3850	0.4710	0.5020	0.3960	0.4120
3.50	0.4170	0.4530	0.3490	0.3720	0.4620	0.4900	0.3880	0.4010
3.75	0.4060	0.4370	0.3390	0.3590	0.4480	0.4720	0.3770	0.3880
4.00	0.3920	0.4230	0.3270	0.3460	0.4340	0.4540	0.3620	0.3750
4.25	0.3820	0.4130	0.3200	0.3340	0.4250	0.4420	0.3530	0.3650
4.50	0.3840	0.4120	0.3200	0.3330	0.4250	0.4420	0.3500	0.3630
4.75	0.3930	0.4210	0.3270	0.3410	0.4360	0.4520	0.3610	0.3730
5.00	0.4120	0.4400	0.3440	0.3540	0.4540	0.4730	0.3780	0.3900
5.25	0.4350	0.4650	0.3640	0.3740	0.4790	0.4960	0.3980	0.4120
5.50	0.4580	0.4880	0.3870	0.3970	0.5050	0.5240	0.4220	0.4360
5.75	0.4780	0.5120	0.4040	0.4160	0.5280	0.5470	0.4420	0.4550
6.00	0.4900	0.5250	0.4140	0.4290	0.5440	0.5620	0.4550	0.4670
6.25	0.4910	0.5290	0.4170	0.4320	0.5480	0.5630	0.4590	0.4710
6.50	0.4820	0.5220	0.4110	0.4250	0.5410	0.5550	0.4520	0.4630
6.75	0.4670	0.5100	0.3990	0.4120	0.5250	0.5360	0.4350	0.4510
7.00	0.4470	0.4890	0.3830	0.3950	0.5050	0.5150	0.4180	0.4310
7.25	0.4180	0.4620	0.3590	0.3690	0.4800	0.4840	0.3920	0.4050
7.50	0.3950	0.4370	0.3340	0.3450	0.4520	0.4550	0.3670	0.3820
7.75	0.3730	0.4160	0.3170	0.3240	0.4280	0.4280	0.3490	0.3630
8.00	0.3560	0.3970	0.3020	0.3080	0.4090	0.4060	0.3320	0.3470
8.25	0.3420	0.3860	0.2920	0.2960	0.3990	0.3900	0.3210	0.3340

Table 2 (continued).

s	$I_p^{a(1)}$		$I_p^{a(2)}$		$I_p^{a(3)}$		$I_p^{a(4)}$	
	L	R	L	R	L	R	L	R
8.50	0.3350	0.3780	0.2850	0.2880	0.3920	0.3800	0.3140	0.3270
8.75	0.3280	0.3720	0.2790	0.2830	0.3850	0.3730	0.3090	0.3220
9.00	0.3230	0.3690	0.2770	0.2760	0.3810	0.3670	0.3030	0.3200
9.25	0.3190	0.3660	0.2740	0.2730	0.3770	0.3620	0.3010	0.3180
9.50	0.3160	0.3650	0.2710	0.2690	0.3740	0.3580	0.2970	0.3160
9.75	0.3130	0.3630	0.2680	0.2660	0.3730	0.3530	0.2940	0.3130
10.00	0.3110	0.3600	0.2670	0.2640	0.3720	0.3510	0.2920	0.3110
10.25	0.3080	0.3590	0.2660	0.2620	0.3720	0.3500	0.2910	0.3100
10.50	0.3070	0.3630	0.2680	0.2620	0.3720	0.3510	0.2920	0.3110
10.75	0.3110	0.3670	0.2690	0.2650	0.3770	0.3530	0.2930	0.3130
11.00	0.3130	0.3710	0.2720	0.2680	0.3800	0.3580	0.2980	0.3150
11.25	0.3170	0.3760	0.2750	0.2710	0.3850	0.3610	0.3000	0.3190
11.50	0.3160	0.3800	0.2760	0.2720	0.3880	0.3620	0.3010	0.3220
11.75	0.3150	0.3810	0.2770	0.2720	0.3900	0.3630	0.3000	0.3210
12.00	0.3110	0.3800	0.2740	0.2700	0.3850	0.3590	0.2960	0.3180
12.25	0.3040	0.3750	0.2670	0.2630	0.3790	0.3520	0.2890	0.3120
12.50	0.2950	0.3660	0.2600	0.2560	0.3680	0.3420	0.2800	0.3040
12.75	0.2860	0.3570	0.2520	0.2470	0.3570	0.3310	0.2700	0.2940
13.00	0.2750	0.3480	0.2420	0.2360	0.3450	0.3190	0.2580	0.2840
13.25	0.2660	0.3380	0.2350	0.2290	0.3340	0.3080	0.2500	0.2750
13.50	0.2610	0.3330	0.2300	0.2220	0.3270	0.2990	0.2430	0.2700
13.75	0.2560	0.3290	0.2290	0.2170	0.3230	0.2940	0.2400	0.2640
14.00	0.2530	0.3270	0.2270	0.2150	0.3220	0.2900	0.2370	0.2630
14.25	0.2520	0.3270	0.2270	0.2130	0.3200	0.2880	0.2370	0.2630

Table 2 (continued).

s	$I_p^{a(1)}$		$I_p^{a(2)}$		$I_p^{a(3)}$		$I_p^{a(4)}$	
	L	R	L	R	L	R	L	R
14.50	0.2520	0.3280	0.2290	0.2130	0.3220	0.2900	0.2370	0.2630
14.75	0.2530	0.3290	0.2310	0.2130	0.3230	0.2900	0.2370	0.2650
15.00	0.2530	0.3310	0.2320	0.2140	0.3240	0.2910	0.2390	0.2670
15.25	0.2530	0.3320	0.2330	0.2140	0.3240	0.2920	0.2390	0.2690
15.50	0.2540	0.3330	0.2340	0.2140	0.3240	0.2910	0.2370	0.2700
15.75	0.2540	0.3340	0.2350	0.2150	0.3250	0.2910	0.2370	0.2710
16.00	0.2550	0.3350	0.2380	0.2160	0.3260	0.2910	0.2370	0.2720
16.25	0.2550	0.3370	0.2390	0.2160	0.3260	0.2910	0.2370	0.2730
16.50	0.2540	0.3400	0.2400	0.2170	0.3280	0.2910	0.2380	0.2740
16.75	0.2550	0.3410	0.2420	0.2170	0.3290	0.2920	0.2370	0.2770
17.00	0.2550	0.3420	0.2430	0.2180	0.3300	0.2920	0.2370	0.2760
17.25	0.2550	0.3430	0.2430	0.2170	0.3290	0.2890	0.2360	0.2760
17.50	0.2520	0.3430	0.2420	0.2160	0.3280	0.2880	0.2350	0.2760
17.75	0.2490	0.3420	0.2390	0.2130	0.3270	0.2850	0.2320	0.2740
18.00	0.2450	0.3400	0.2360	0.2100	0.3220	0.2800	0.2270	0.2710
18.25	0.2410	0.3360	0.2330	0.2060	0.3170	0.2740	0.2220	0.2670
18.50	0.2360	0.3320	0.2280	0.2010	0.3120	0.2670	0.2190	0.2620
18.75	0.2320	0.3300	0.2250	0.1980	0.3070	0.2630	0.2120	0.2580
19.00	0.2270	0.3270	0.2220	0.1950	0.3030	0.2590	0.2110	0.2560
19.25	0.2260	0.3250	0.2210	0.1930	0.3000	0.2570	0.2100	0.2530
19.50	0.2250	0.3240	0.2210	0.1920	0.2990	0.2560	0.2100	0.2520
19.75	0.2250	0.3240	0.2210	0.1920	0.2980	0.2560	0.2080	0.2520
20.00	0.2260	0.3260	0.2220	0.1930	0.2990	0.2580	0.2100	0.2540
20.25	0.2270	0.3280	0.2220	0.1940	0.3010	0.2590	0.2110	0.2550

Table 2 (continued).

s	$I_p^{a(1)}$		$I_p^{a(2)}$		$I_p^{a(3)}$		$I_p^{a(4)}$	
	L	R	L	R	L	R	L	R
20.50	0.2280	0.3300	0.2240	0.1950	0.3030	0.2600	0.2120	0.2560
20.75	0.2310	0.3310	0.2240	0.1960	0.3050	0.2620	0.2120	0.2570

L Left branch
R Right branch

Table 3. Electron intensity incident on the photographic plate: h = 192.07 mm.

s	$I_p^{b(1)}$		$I_p^{b(2)}$		$I_p^{b(3)}$		$I_p^{b(4)}$	
	L	R	L	R	L	R	L	R
10.25	0.9401	1.0580	1.0959	1.2336	0.9249	1.0681	0.9356	1.0879
10.50	0.9200	1.0389	1.0658	1.2009	0.9031	1.0325	0.9103	1.0619
10.75	0.8998	1.0188	1.0514	1.1853	0.8870	1.0111	0.8902	1.0429
11.00	0.8868	1.0076	1.0311	1.1660	0.8740	0.9951	0.8786	1.0338
11.25	0.8739	0.9890	1.0150	1.1481	0.8636	0.9830	0.8670	1.0211
11.50	0.8621	0.9707	1.0027	1.1320	0.8520	0.9708	0.8485	1.0050
11.75	0.8402	0.9522	0.9780	1.1050	0.8335	0.9461	0.8322	0.9803
12.00	0.8177	0.9222	0.9538	1.0682	0.8083	0.9103	0.8097	0.9500
12.25	0.7839	0.8809	0.9118	1.0274	0.7780	0.8750	0.7859	0.9091
12.50	0.7409	0.8402	0.8796	0.9780	0.7398	0.8311	0.7441	0.8659
12.75	0.7080	0.8050	0.8360	0.9294	0.7050	0.7939	0.7110	0.8211
13.00	0.6719	0.7560	0.7904	0.8820	0.6728	0.7482	0.6760	0.7759
13.25	0.6384	0.7184	0.7518	0.8244	0.6383	0.7133	0.6443	0.7377
13.50	0.6090	0.6977	0.7259	0.7960	0.6110	0.6873	0.6150	0.7163
13.75	0.5900	0.6770	0.7008	0.7739	0.5920	0.6668	0.5920	0.6903
14.00	0.5760	0.6575	0.6905	0.7550	0.5790	0.6514	0.5790	0.6790
14.25	0.5670	0.6494	0.6780	0.7462	0.5720	0.6413	0.5740	0.6698
14.50	0.5600	0.6433	0.6728	0.7354	0.5660	0.6373	0.5670	0.6616
14.75	0.5560	0.6363	0.6677	0.7290	0.5630	0.6302	0.5600	0.6544
15.00	0.5510	0.6312	0.6626	0.7207	0.5590	0.6251	0.5560	0.6494
15.25	0.5460	0.6231	0.6565	0.7143	0.5550	0.6221	0.5510	0.6433
15.50	0.5420	0.6170	0.6504	0.7090	0.5490	0.6160	0.5450	0.6352
15.75	0.5360	0.6100	0.6443	0.7009	0.5470	0.6070	0.5410	0.6292
16.00	0.5320	0.6060	0.6413	0.6935	0.5420	0.6040	0.5350	0.6231

Table 3 (continued).

s	$I_p^{b(1)}$		$I_p^{b(2)}$		$I_p^{b(3)}$		$I_p^{b(4)}$	
	L	R	L	R	L	R	L	R
16.25	0.5280	0.5990	0.6362	0.6872	0.5380	0.6000	0.5310	0.6180
16.50	0.5240	0.5940	0.6302	0.6831	0.5330	0.5960	0.5270	0.6140
16.75	0.5190	0.5920	0.6272	0.6811	0.5290	0.5920	0.5230	0.6110
17.00	0.5160	0.5880	0.6211	0.6770	0.5280	0.5860	0.5180	0.6070
17.25	0.5110	0.5810	0.6130	0.6719	0.5210	0.5810	0.5140	0.6000
17.50	0.5040	0.5750	0.6070	0.6616	0.5140	0.5740	0.5090	0.5910
17.75	0.4970	0.5610	0.5930	0.6474	0.5030	0.5630	0.5000	0.5790
18.00	0.4870	0.5460	0.5840	0.6322	0.4940	0.5510	0.4890	0.5640
18.25	0.4740	0.5310	0.5700	0.6170	0.4800	0.5360	0.4770	0.5490
18.50	0.4630	0.5180	0.5520	0.6010	0.4670	0.5210	0.4640	0.5330
18.75	0.4510	0.5060	0.5370	0.5870	0.4590	0.5060	0.4530	0.5190
19.00	0.4420	0.4920	0.5250	0.5720	0.4460	0.4960	0.4440	0.5090
19.25	0.4360	0.4860	0.5170	0.5630	0.4410	0.4900	0.4360	0.5030
19.50	0.4310	0.4810	0.5130	0.5570	0.4370	0.4860	0.4320	0.4960
19.75	0.4300	0.4810	0.5110	0.5540	0.4350	0.4820	0.4310	0.4950
20.00	0.4290	0.4800	0.5110	0.5530	0.4350	0.4830	0.4300	0.4960
20.25	0.4300	0.4800	0.5120	0.5560	0.4360	0.4850	0.4320	0.4970
20.50	0.4310	0.4800	0.5140	0.5560	0.4370	0.4850	0.4330	0.4970
20.75	0.4310	0.4790	0.5150	0.5570	0.4370	0.4840	0.4340	0.4950
21.00	0.4310	0.4790	0.5150	0.5550	0.4390	0.4830	0.4340	0.4940
21.25	0.4300	0.4760	0.5140	0.5520	0.4390	0.4830	0.4320	0.4940
21.50	0.4270	0.4740	0.5120	0.5480	0.4380	0.4810	0.4330	0.4890
21.75	0.4260	0.4700	0.5100	0.5450	0.4360	0.4760	0.4310	0.4850
22.00	0.4240	0.4670	0.5090	0.5380	0.4360	0.4740	0.4290	0.4800

Table 3 (continued).

s	$I_p^{b(1)}$		$I_p^{b(2)}$		$I_p^{b(3)}$		$I_p^{b(4)}$	
	L	R	L	R	L	R	L	R
22.25	0.4200	0.4640	0.5070	0.5350	0.4340	0.4690	0.4260	0.4780
22.50	0.4170	0.4600	0.5030	0.5300	0.4310	0.4650	0.4250	0.4730
22.75	0.4140	0.4560	0.4990	0.5240	0.4280	0.4610	0.4230	0.4690
23.00	0.4110	0.4510	0.4930	0.5200	0.4250	0.4560	0.4200	0.4640
23.25	0.4060	0.4460	0.4870	0.5130	0.4210	0.4510	0.4140	0.4590
23.50	0.4000	0.4380	0.4820	0.5040	0.4150	0.4460	0.4090	0.4490
23.75	0.3940	0.4310	0.4740	0.4950	0.4110	0.4380	0.4040	0.4430
24.00	0.3890	0.4240	0.4670	0.4880	0.4040	0.4310	0.3980	0.4360
24.25	0.3810	0.4170	0.4600	0.4820	0.3980	0.4260	0.3920	0.4300
24.50	0.3780	0.4120	0.4560	0.4770	0.3930	0.4200	0.3890	0.4240
24.75	0.3750	0.4100	0.4520	0.4710	0.3910	0.4160	0.3850	0.4210
25.00	0.3730	0.4060	0.4500	0.4680	0.3900	0.4130	0.3840	0.4180
25.25	0.3710	0.4060	0.4490	0.4670	0.3880	0.4120	0.3810	0.4160
25.50	0.3710	0.4060	0.4510	0.4670	0.3890	0.4120	0.3820	0.4170
25.75	0.3720	0.4070	0.4540	0.4690	0.3890	0.4140	0.3820	0.4180
26.00	0.3730	0.4080	0.4550	0.4680	0.3900	0.4140	0.3830	0.4190
26.25	0.3720	0.4080	0.4560	0.4680	0.3890	0.4140	0.3810	0.4190
26.50	0.3730	0.4080	0.4580	0.4660	0.3890	0.4150	0.3810	0.4180
26.75	0.3710	0.4080	0.4560	0.4660	0.3880	0.4150	0.3800	0.4170
27.00	0.3700	0.4070	0.4540	0.4640	0.3860	0.4130	0.3780	0.4150
27.25	0.3670	0.4030	0.4530	0.4610	0.3830	0.4110	0.3760	0.4120
27.50	0.3650	0.3990	0.4500	0.4580	0.3790	0.4090	0.3740	0.4090
27.75	0.3610	0.3960	0.4470	0.4540	0.3770	0.4060	0.3710	0.4060
28.00	0.3590	0.3950	0.4450	0.4500	0.3740	0.4030	0.3700	0.4030

Table 3 (continued).

s	$I_p^{b(1)}$		$I_p^{b(2)}$		$I_p^{b(3)}$		$I_p^{b(4)}$	
	L	R	L	R	L	R	L	R
28.25	0.3560	0.3920	0.4420	0.4470	0.3710	0.4010	0.3670	0.4000
28.50	0.3540	0.3870	0.4380	0.4420	0.3680	0.3970	0.3630	0.3950
28.75	0.3510	0.3840	0.4360	0.4390	0.3650	0.3940	0.3590	0.3920
29.00	0.3480	0.3800	0.4320	0.4340	0.3630	0.3920	0.3560	0.3890
29.25	0.3450	0.3760	0.4270	0.4300	0.3600	0.3880	0.3530	0.3840
29.50	0.3410	0.3720	0.4240	0.4250	0.3570	0.3850	0.3490	0.3800
29.75	0.3380	0.3680	0.4200	0.4210	0.3530	0.3810	0.3460	0.3780
30.00	0.3360	0.3650	0.4170	0.4170	0.3500	0.3790	0.3430	0.3750
30.25	0.3320	0.3620	0.4150	0.4140	0.3460	0.3770	0.3400	0.3720
30.50	0.3310	0.3600	0.4140	0.4130	0.3440	0.3760	0.3380	0.3710
30.75	0.3310	0.3600	0.4150	0.4120	0.3420	0.3750	0.3380	0.3690
31.00	0.3300	0.3590	0.4160	0.4120	0.3420	0.3750	0.3380	0.3690
31.25	0.3310	0.3600	0.4160	0.4120	0.3410	0.3750	0.3370	0.3680
31.50	0.3310	0.3590	0.4170	0.4130	0.3410	0.3750	0.3370	0.3680
31.75	0.3300	0.3600	0.4170	0.4120	0.3420	0.3760	0.3380	0.3690
32.00	0.3300	0.3600	0.4160	0.4120	0.3410	0.3750	0.3370	0.3680
32.25	0.3290	0.3580	0.4150	0.4100	0.3410	0.3730	0.3380	0.3650
32.50	0.3280	0.3560	0.4140	0.4080	0.3400	0.3720	0.3360	0.3630
32.75	0.3260	0.3550	0.4120	0.4060	0.3370	0.3710	0.3340	0.3610
33.00	0.3250	0.3510	0.4090	0.4030	0.3350	0.3690	0.3320	0.3580
33.25	0.3230	0.3500	0.4070	0.4010	0.3320	0.3660	0.3290	0.3560
33.50	0.3210	0.3480	0.4040	0.3980	0.3280	0.3640	0.3260	0.3530
33.75	0.3180	0.3450	0.4000	0.3950	0.3280	0.3620	0.3240	0.3500
34.00	0.3160	0.3420	0.3990	0.3920	0.3240	0.3610	0.3220	0.3480

Table 3 (continued).

s	$I_p^{b(1)}$		$I_p^{b(2)}$		$I_p^{b(3)}$		$I_p^{b(4)}$	
	L	R	L	R	L	R	L	R
34.25	0.3150	0.3410	0.3950	0.3900	0.3230	0.3590	0.3200	0.3450
34.50	0.3140	0.3370	0.3940	0.3870	0.3210	0.3570	0.3200	0.3430
34.75	0.3120	0.3340	0.3920	0.3850	0.3190	0.3550	0.3180	0.3390
35.00	0.3110	0.3330	0.3900	0.3820	0.3180	0.3540	0.3160	0.3370
35.25	0.3100	0.3300	0.3890	0.3810	0.3170	0.3510	0.3140	0.3350
35.50	0.3080	0.3290	0.3870	0.3770	0.3140	0.3500	0.3120	0.3330
35.75	0.3060	0.3280	0.3850	0.3760	0.3130	0.3480	0.3110	0.3310
36.00	0.3050	0.3270	0.3830	0.3740	0.3110	0.3470	0.3100	0.3300
36.25	0.3040	0.3270	0.3820	0.3730	0.3110	0.3470	0.3090	0.3280
36.50	0.3040	0.3260	0.3830	0.3720	0.3100	0.3470	0.3090	0.3270
36.75	0.3040	0.3260	0.3830	0.3720	0.3090	0.3470	0.3090	0.3270
37.00	0.3030	0.3260	0.3820	0.3720	0.3090	0.3480	0.3080	0.3270
37.25	0.3020	0.3250	0.3820	0.3720	0.3080	0.3480	0.3080	0.3280
37.50	0.3020	0.3240	0.3800	0.3710	0.3090	0.3470	0.3070	0.3260
37.75	0.3010	0.3230	0.3790	0.3690	0.3080	0.3470	0.3070	0.3250
38.00	0.3000	0.3220	0.3780	0.3670	0.3070	0.3460	0.3050	0.3240
38.25	0.2990	0.3200	0.3770	0.3640	0.3060	0.3440	0.3040	0.3230
38.50	0.2970	0.3180	0.3740	0.3620	0.3040	0.3430	0.3020	0.3210
38.75	0.2950	0.3160	0.3720	0.3610	0.3010	0.3410	0.3000	0.3200
39.00	0.2940	0.3140	0.3700	0.3590	0.3000	0.3400	0.2990	0.3190
39.25	0.2920	0.3120	0.3670	0.3570	0.2990	0.3380	0.2970	0.3170
39.50	0.2910	0.3100	0.3660	0.3550	0.2980	0.3370	0.2960	0.3150
39.75	0.2900	0.3080	0.3650	0.3540	0.2960	0.3360	0.2950	0.3140
40.00	0.2900	0.3070	0.3640	0.3520	0.2950	0.3340	0.2940	0.3130

Table 3 (continued).

s	$I_p^{b(1)}$		$I_p^{b(2)}$		$I_p^{b(3)}$		$I_p^{b(4)}$	
	L	R	L	R	L	R	L	R
40.25	0.2890	0.3070	0.3630	0.3500	0.2940	0.3330	0.2930	0.3120
40.50	0.2880	0.3060	0.3620	0.3490	0.2920	0.3330	0.2930	0.3110
40.75	0.2870	0.3040	0.3620	0.3470	0.2910	0.3330	0.2930	0.3110
41.00	0.2860	0.3030	0.3620	0.3460	0.2890	0.3330	0.2920	0.3110
41.25	0.2850	0.3020	0.3620	0.3450	0.2890	0.3310	0.2910	0.3100
41.50	0.2850	0.3020	0.3610	0.3450	0.2880	0.3310	0.2890	0.3090
41.75	0.2850	0.3010	0.3600	0.3440	0.2880	0.3310	0.2890	0.3090
42.00	0.2840	0.3010	0.3590	0.3430	0.2870	0.3310	0.2880	0.3090

L Left branch
R Right branch

Table 4. Electron intensity incident on the photographic plate: h = 120.00 mm.

s	$I_p^{c(1)}$ L	$I_p^{c(1)}$ R	$I_p^{c(2)}$ L	$I_p^{c(2)}$ R	$I_p^{c(3)}$ L	$I_p^{c(3)}$ R	$I_p^{c(4)}$ L	$I_p^{c(4)}$ R
18.50	1.0997	1.2665	0.8618	0.9983	0.8293	0.9454	0.8108	0.9092
18.75	1.0695	1.2320	0.8308	0.9628	0.8009	0.9106	0.7860	0.8856
19.00	1.0249	1.1837	0.8102	0.9265	0.7729	0.8788	0.7617	0.8612
19.25	0.9926	1.1495	0.7865	0.8991	0.7466	0.8522	0.7380	0.8394
19.50	0.9681	1.1265	0.7709	0.8861	0.7348	0.8362	0.7250	0.8188
19.75	0.9498	1.1090	0.7600	0.8745	0.7241	0.8247	0.7135	0.8097
20.00	0.9474	1.0957	0.7502	0.8641	0.7199	0.8190	0.7041	0.7995
20.25	0.9377	1.0891	0.7458	0.8572	0.7136	0.8156	0.7020	0.7950
20.50	0.9245	1.0852	0.7426	0.8526	0.7085	0.8099	0.6926	0.7905
20.75	0.9125	1.0721	0.7373	0.8468	0.7033	0.8065	0.6916	0.7826
21.00	0.9054	1.0630	0.7297	0.8399	0.6981	0.7964	0.6843	0.7748
21.25	0.8960	1.0527	0.7244	0.8330	0.6908	0.7930	0.6812	0.7671
21.50	0.8854	1.0337	0.7171	0.8239	0.6845	0.7806	0.6709	0.7584
21.75	0.8737	1.0262	0.7098	0.8114	0.6763	0.7717	0.6617	0.7497
22.00	0.8622	1.0098	0.7025	0.8012	0.6701	0.7630	0.6556	0.7389
22.25	0.8541	0.9975	0.6942	0.7910	0.6630	0.7532	0.6454	0.7303
22.50	0.8484	0.9815	0.6848	0.7787	0.6517	0.7455	0.6384	0.7187
22.75	0.8334	0.9693	0.6745	0.7676	0.6426	0.7380	0.6273	0.7093
23.00	0.8220	0.9547	0.6612	0.7611	0.6366	0.7295	0.6222	0.6989
23.25	0.8050	0.9414	0.6500	0.7458	0.6265	0.7136	0.6121	0.6833
23.50	0.7914	0.9197	0.6389	0.7297	0.6163	0.7001	0.5961	0.6740
23.75	0.7735	0.8971	0.6257	0.7139	0.5973	0.6908	0.5871	0.6597
24.00	0.7604	0.8772	0.6166	0.6973	0.5883	0.6763	0.5731	0.6485
24.25	0.7440	0.8576	0.6046	0.6848	0.5763	0.6609	0.5621	0.6303

Table 4 (continued)

s	$I_p^{c(1)}$		$I_p^{c(2)}$		$I_p^{c(3)}$		$I_p^{c(4)}$	
	L	R	L	R	L	R	L	R
24.50	0.7280	0.8392	0.5966	0.6714	0.5683	0.6477	0.5551	0.6212
24.75	0.7185	0.8266	0.5866	0.6632	0.5623	0.6386	0.5451	0.6131
25.00	0.7070	0.8186	0.5836	0.6561	0.5563	0.6335	0.5391	0.6071
25.25	0.7029	0.8152	0.5806	0.6500	0.5543	0.6265	0.5341	0.6031
25.50	0.6987	0.8118	0.5776	0.6500	0.5523	0.6245	0.5321	0.6011
25.75	0.6977	0.8084	0.5776	0.6429	0.5503	0.6234	0.5331	0.6001
26.00	0.6946	0.8061	0.5756	0.6409	0.5513	0.6224	0.5331	0.5971
26.25	0.6935	0.8050	0.5736	0.6399	0.5503	0.6214	0.5301	0.5951
26.50	0.6914	0.8027	0.5726	0.6369	0.5463	0.6163	0.5271	0.5911
26.75	0.6862	0.7936	0.5706	0.6328	0.5413	0.6113	0.5261	0.5861
27.00	0.6810	0.7846	0.5656	0.6278	0.5343	0.6063	0.5201	0.5821
27.25	0.6707	0.7768	0.5596	0.6196	0.5293	0.5983	0.5131	0.5711
27.50	0.6656	0.7713	0.5526	0.6136	0.5263	0.5923	0.5081	0.5671
27.75	0.6533	0.7614	0.5466	0.6086	0.5193	0.5863	0.5031	0.5621
28.00	0.6453	0.7560	0.5416	0.6046	0.5143	0.5803	0.4981	0.5581
28.25	0.6382	0.7473	0.5346	0.5946	0.5083	0.5723	0.4911	0.5531
28.50	0.6301	0.7397	0.5296	0.5896	0.5013	0.5673	0.4861	0.5461
28.75	0.6230	0.7333	0.5236	0.5846	0.4963	0.5613	0.4821	0.5401
29.00	0.6179	0.7226	0.5186	0.5796	0.4903	0.5523	0.4761	0.5351
29.25	0.6099	0.7174	0.5136	0.5716	0.4843	0.5483	0.4701	0.5301
29.50	0.6059	0.7091	0.5096	0.5656	0.4783	0.5433	0.4671	0.5221
29.75	0.5969	0.7018	0.5036	0.5606	0.4733	0.5363	0.4571	0.5171
30.00	0.5909	0.6945	0.4996	0.5516	0.4703	0.5313	0.4531	0.5121
30.25	0.5859	0.6883	0.4966	0.5506	0.4673	0.5283	0.4471	0.5081

Table 4 (continued).

s	$I_p^{c(1)}$		$I_p^{c(2)}$		$I_p^{c(3)}$		$I_p^{c(4)}$	
	L	R	L	R	L	R	L	R
30.50	0.5809	0.6831	0.4946	0.5466	0.4663	0.5223	0.4471	0.5041
30.75	0.5776	0.6779	0.4926	0.5446	0.4623	0.5213	0.4451	0.5021
31.00	0.5769	0.6758	0.4916	0.5436	0.4623	0.5203	0.4431	0.5011
31.25	0.5759	0.6789	0.4906	0.5426	0.4613	0.5183	0.4431	0.5001
31.50	0.5749	0.6789	0.4906	0.5396	0.4593	0.5173	0.4421	0.4981
31.75	0.5719	0.6789	0.4896	0.5406	0.4583	0.5163	0.4401	0.4871
32.00	0.5699	0.6748	0.4876	0.5396	0.4573	0.5163	0.4391	0.4961
32.25	0.5649	0.6717	0.4856	0.5356	0.4553	0.5113	0.4381	0.4941
32.50	0.5619	0.6687	0.4826	0.5336	0.4523	0.5113	0.4351	0.4901
32.75	0.5599	0.6655	0.4796	0.5316	0.4493	0.5063	0.4321	0.4851
33.00	0.5549	0.6605	0.4756	0.5276	0.4443	0.5013	0.4301	0.4821
33.25	0.5489	0.6544	0.4706	0.5226	0.4423	0.4943	0.4221	0.4781
33.50	0.5449	0.6503	0.4666	0.5186	0.4393	0.4903	0.4211	0.4751
33.75	0.5419	0.6422	0.4616	0.5156	0.4343	0.4873	0.4141	0.4721
34.00	0.5369	0.6382	0.4566	0.5126	0.4313	0.4813	0.4121	0.4661
34.25	0.5309	0.6324	0.4546	0.5096	0.4283	0.4763	0.4091	0.4631
34.50	0.5279	0.6281	0.4526	0.5066	0.4273	0.4723	0.4081	0.4591
34.75	0.5229	0.6250	0.4516	0.5026	0.4223	0.4693	0.4041	0.4551
35.00	0.5179	0.6220	0.4486	0.4996	0.4193	0.4663	0.4001	0.4511
35.25	0.5109	0.6159	0.4426	0.4976	0.4163	0.4613	0.3991	0.4471
35.50	0.5079	0.6119	0.4406	0.4936	0.4143	0.4583	0.3951	0.4451
35.75	0.5049	0.6079	0.4396	0.4916	0.4123	0.4553	0.3931	0.4411
36.00	0.5019	0.6049	0.4376	0.4906	0.4113	0.4543	0.3911	0.4401
36.25	0.4999	0.6029	0.4366	0.4886	0.4103	0.4533	0.3901	0.4371

Table 4 (continued).

s	$I_p^{c(1)}$		$I_p^{c(2)}$		$I_p^{c(3)}$		$I_p^{c(4)}$	
	L	R	L	R	L	R	L	R
36.50	0.4999	0.6009	0.4356	0.4896	0.4093	0.4533	0.3901	0.4381
36.75	0.4989	0.5999	0.4346	0.4886	0.4073	0.4513	0.3891	0.4361
37.00	0.4969	0.5979	0.4336	0.4876	0.4083	0.4503	0.3891	0.4351
37.25	0.4949	0.5959	0.4316	0.4876	0.4063	0.4483	0.3861	0.4321
37.50	0.4919	0.5939	0.4306	0.4846	0.4043	0.4463	0.3851	0.4331
37.75	0.4899	0.5909	0.4276	0.4836	0.4013	0.4463	0.3821	0.4301
38.00	0.4859	0.5879	0.4246	0.4806	0.3993	0.4423	0.3801	0.4281
38.25	0.4809	0.5839	0.4216	0.4786	0.3973	0.4403	0.3781	0.4251
38.50	0.4769	0.5799	0.4196	0.4756	0.3943	0.4373	0.3751	0.4231
38.75	0.4739	0.5759	0.4166	0.4736	0.3913	0.4343	0.3721	0.4211
39.00	0.4709	0.5729	0.4136	0.4706	0.3893	0.4323	0.3701	0.4181
39.25	0.4669	0.5669	0.4116	0.4666	0.3873	0.4293	0.3671	0.4161
39.50	0.4649	0.5639	0.4076	0.4646	0.3843	0.4263	0.3641	0.4141
39.75	0.4619	0.5619	0.4066	0.4616	0.3813	0.4243	0.3621	0.4121
40.00	0.4589	0.5599	0.4036	0.4597	0.3793	0.4223	0.3601	0.4101
40.25	0.4569	0.5579	0.4026	0.4586	0.3773	0.4203	0.3571	0.4091
40.50	0.4549	0.5559	0.3996	0.4566	0.3763	0.4203	0.3541	0.4071
40.75	0.4519	0.5549	0.3976	0.4546	0.3743	0.4173	0.3531	0.4051
41.00	0.4489	0.5539	0.3966	0.4536	0.3733	0.4153	0.3511	0.4041
41.25	0.4479	0.5479	0.3956	0.4526	0.3713	0.4143	0.3501	0.4031
41.50	0.4449	0.5469	0.3936	0.4516	0.3683	0.4143	0.3491	0.4021
41.75	0.4429	0.5439	0.3926	0.4516	0.3673	0.4143	0.3471	0.4021
42.00	0.4409	0.5429	0.3916	0.4496	0.3663	0.4133	0.3451	0.4011
42.25	0.4409	0.5429	0.3896	0.4496	0.3643	0.4113	0.3441	0.4001

Table 4 (continued)

s	$I_p^{c(1)}$		$I_p^{c(2)}$		$I_p^{c(3)}$		$I_p^{c(4)}$	
	L	R	L	R	L	R	L	R
42.50	0.4409	0.5429	0.3896	0.4496	0.3633	0.4113	0.3421	0.4001
42.75	0.4379	0.5429	0.3876	0.4486	0.3623	0.4113	0.3411	0.3971
43.00	0.4359	0.5429	0.3866	0.4466	0.3613	0.4093	0.3401	0.3971
43.25	0.4339	0.5399	0.3846	0.4456	0.3583	0.4083	0.3381	0.3971
43.50	0.4309	0.5349	0.3816	0.4446	0.3563	0.4063	0.3371	0.3951
43.75	0.4269	0.5329	0.3806	0.4416	0.3533	0.4053	0.3351	0.3931
44.00	0.4239	0.5309	0.3776	0.4406	0.3513	0.4043	0.3321	0.3921
44.25	0.4199	0.5299	0.3756	0.4396	0.3493	0.4033	0.3311	0.3911
44.50	0.4179	0.5269	0.3746	0.4376	0.3483	0.4023	0.3301	0.3891
44.75	0.4129	0.5249	0.3716	0.4356	0.3443	0.4023	0.3271	0.3871
45.00	0.4109	0.5239	0.3706	0.4336	0.3433	0.4013	0.3251	0.3871
45.25	0.4099	0.5209	0.3686	0.4336	0.3413	0.3993	0.3241	0.3851
45.50	0.4069	0.5199	0.3666	0.4316	0.3403	0.3963	0.3231	0.3831
45.75	0.4059	0.5189	0.3656	0.4306	0.3383	0.3933	0.3221	0.3821
46.00	0.4059	0.5169	0.3636	0.4296	0.3373	0.3913	0.3201	0.3821
46.25	0.4049	0.5159	0.3626	0.4276	0.3363	0.3903	0.3181	0.3811
46.50	0.4019	0.5159	0.3616	0.4276	0.3333	0.3883	0.3171	0.3801
46.75	0.3999	0.5159	0.3606	0.4266	0.3323	0.3883	0.3161	0.3781
47.00	0.3989	0.5159	0.3596	0.4246	0.3313	0.3883	0.3151	0.3791
47.25	0.3969	0.5139	0.3586	0.4246	0.3303	0.3883	0.3141	0.3781
47.50	0.3959	0.5119	0.3566	0.4236	0.3283	0.3873	0.3131	0.3771
47.75	0.3939	0.5129	0.3566	0.4226	0.3283	0.3873	0.3121	0.3771
48.00	0.3929	0.5119	0.3536	0.4226	0.3263	0.3863	0.3111	0.3771
48.25	0.3909	0.5119	0.3526	0.4216	0.3253	0.3863	0.3101	0.3761

Table **4** (continued).

s	$I_p^{c(1)}$		$I_p^{c(2)}$		$I_p^{c(3)}$		$I_p^{c(4)}$	
	L	R	L	R	L	R	L	R
48.50	0.3889	0.5099	0.3516	0.4206	0.3243	0.3853	0.3081	0.3761
48.75	0.3879	0.5089	0.3506	0.4196	0.3233	0.3843	0.3071	0.3751
49.00	0.3849	0.5069	0.3496	0.4196	0.3203	0.3833	0.3051	0.3741
49.25	0.3819	0.5059	0.3486	0.4196	0.3193	0.3823	0.3051	0.3751
49.50	0.3809	0.5049	0.3466	0.4176	0.3183	0.3823	0.3031	0.3741
49.75	0.3789	0.5019	0.3446	0.4166	0.3163	0.3813	0.3011	0.3731

L Left branch
R Right branch

Table 5. Experimental and theoretical $I_E^T(s)$ curves.

s	$I_E^T(s)_{Exp}$	$I_E^T(s)_{Theor}$	s	$I_E^T(s)_{Exp}$	$I_E^T(s)_{Theor}$
0.00		0.0	10.50	-151.0	-126.5
0.25		240.7	10.75	-8.0	21.6
0.50		441.2	11.00	154.0	198.6
0.75		593.0	11.25	316.0	380.1
1.00		645.9	11.50	454.0	534.4
1.25		622.0	11.75	547.0	630.4
1.50		530.0	12.00	557.0	645.3
1.75		394.2	12.25	447.0	571.4
2.00		242.2	12.50	293.0	418.0
2.25		97.3	12.75	110.0	210.1
2.50	-41.0	-25.0	13.00	-145.0	-16.9
2.75	-179.0	-121.8	13.25	-352.0	-226.4
3.00	-316.0	-199.9	13.50	-501.0	-387.6
3.25	-369.0	-269.2	13.75	-590.0	-482.1
3.50	-448.0	-337.9	14.00	-598.0	-507.5
3.75	-493.0	-408.7	14.25	-549.0	-474.2
4.00	-530.0	-473.8	14.50	-473.0	-401.9
4.25	-556.0	-515.8	14.75	-395.0	-312.3
4.50	-528.0	-513.6	15.00	-291.0	-222.8
4.75	-450.0	-450.2	15.25	-216.0	-142.7
5.00	-317.0	-317.8	15.50	-141.0	-72.0
5.25	-127.0	-123.0	15.75	-54.0	-3.4
5.50	93.0	110.7	16.00	45.0	72.2
5.75	326.0	348.0	16.25	118.0	160.8
6.00	527.0	549.4	16.50	220.0	260.9
6.25	654.0	679.1	16.75	327.0	362.1
6.50	702.0	714.8	17.00	402.0	446.5
6.75	647.0	652.9	17.25	445.0	492.8
7.00	543.0	508.0	17.50	476.0	483.3
7.25	337.0	309.8	17.75	373.0	408.8
7.50	121.0	95.4	18.00	269.0	273.2
7.75	-58.0	-100.4	18.25	89.0	93.0
8.00	-212.0	-251.3	18.50	-124.0	-105.0
8.25	-316.0	-347.7	18.75	-303.0	-289.3
8.50	-355.0	-392.2	19.00	-455.0	-430.8
8.75	-374.0	-399.5	19.25	-514.0	-509.5
9.00	-368.0	-387.4	19.50	-514.0	-517.7
9.25	-354.0	-370.0	19.75	-459.0	-461.8
9.50	-347.0	-353.5	20.00	-367.0	-358.3
9.75	-327.0	-334.0	20.25	-244.0	-230.0
10.00	-288.0	-298.8	20.50	-116.0	-99.6
10.25	-231.0	-233.1	20.75	5.0	15.3

Table 5 (continued).

s	$I_E^T(s)_{Exp}$	$I_E^T(s)_{Theor}$	s	$I_E^T(s)_{Exp}$	$I_E^T(s)_{Theor}$
21.00	123.0	105.7	31.50	24.0	63.9
21.25	182.0	171.2	31.75	140.0	164.2
21.50	251.0	217.6	32.00	225.0	237.1
21.75	271.0	252.7	32.25	255.0	275.7
22.00	293.0	282.7	32.50	267.0	279.5
22.25	351.0	308.2	32.75	277.0	254.2
22.50	332.0	324.3	33.00	230.0	208.8
22.75	332.0	321.4	33.25	164.0	152.9
23.00	293.0	289.1	33.50	120.0	95.1
23.25	243.0	220.5	33.75	38.0	40.4
23.50	118.0	115.3	34.00	-14.0	-9.4
23.75	-9.0	-17.8	34.25	-83.0	-54.9
24.00	-128.0	-162.2	34.50	-106.0	-97.7
24.25	-276.0	-296.0	34.75	-172.0	-138.3
24.50	-370.0	-397.2	35.00	-206.0	-175.2
24.75	-403.0	-448.4	35.25	-250.0	-204.1
25.00	-416.0	-441.1	35.50	-276.0	-219.4
25.25	-365.0	-377.4	35.75	-290.0	-215.2
25.50	-231.0	-269.6	36.00	-259.0	-187.8
25.75	-81.0	-137.0	36.25	-240.0	-136.9
26.00	39.0	-1.3	36.50	-130.0	-66.8
26.25	140.0	118.2	36.75	-26.0	14.3
26.50	229.0	208.2	37.00	71.0	95.4
26.75	304.0	263.0	37.25	115.0	164.7
27.00	337.0	285.0	37.50	144.0	212.7
27.25	300.0	281.5	37.75	141.0	233.4
27.50	264.0	261.5	38.00	139.0	225.5
27.75	236.0	232.9	38.25	106.0	192.6
28.00	226.0	199.5	38.50	58.0	141.8
28.25	204.0	161.1	38.75	12.0	82.0
28.50	126.0	114.7	39.00	-23.0	21.8
28.75	84.0	56.3	39.25	-108.0	-31.9
29.00	17.0	-15.6	39.50	-160.0	-75.3
29.25	-62.0	-98.4	39.75	-194.0	-106.9
29.50	-146.0	-184.3	40.00	-203.0	-127.8
29.75	-236.0	-261.4	40.25	-205.0	-139.6
30.00	-296.0	-316.3	40.50	-184.0	-144.0
30.25	-328.0	-337.1	40.75	-184.0	-141.3
30.50	-318.0	-317.2	41.00	-168.0	-131.2
30.75	-274.0	-256.7	41.25	-147.0	-112.1
31.00	-179.0	-163.3	41.50	-112.0	-83.2
31.25	-69.0	-50.8	41.75	-68.0	-44.4

Table 5 (continued).

s	$I_E^T(s)_{Exp}$	$I_E^T(s)_{Theor}$	s	$I_E^T(s)_{Exp}$	$I_E^T(s)_{Theor}$
42.00	-47.0	2.0	46.00	-75.0	-102.8
42.25	21.0	52.0	46.25	-78.0	-85.4
42.50	83.0	99.5	46.50	-69.0	-64.4
42.75	131.0	138.1	46.75	-66.0	-40.9
43.00	188.0	162.0	47.00	1.0	-15.5
43.25	188.0	167.4	47.25	27.0	11.1
43.50	139.0	153.3	47.50	21.0	38.1
43.75	64.0	121.9	47.75	77.0	63.7
44.00	7.0	78.1	48.00	81.0	85.6
44.25	18.0	28.4	48.25	117.0	101.0
44.50	-18.0	-20.5	48.50	104.0	107.2
44.75	-107.0	-62.5	48.75	118.0	102.7
45.00	-74.0	-93.8	49.00	77.0	87.0
45.25	-66.0	-112.4	49.25	112.0	61.7
45.50	-85.0	-118.8	49.50	64.0	29.7
45.75	-79.0	-114.7	49.75	7.0	-5.0

Table 6. Experimental $I_E^a(s)$ and $I_E^{a(i)}(s)$ curves (h = 478.00 mm).

s	$I_E^a(s)_{Exp}$	$I_E^{a(1)}(s)_{Exp}$	$I_E^{a(2)}(s)_{Exp}$	$I_E^{a(3)}(s)_{Exp}$	$I_E^{a(4)}(s)_{Exp}$
2.50	-41.0	-11.2	-17.5	-77.7	-15.5
2.75	-179.0	-100.0	-91.1	-170.0	-96.0
3.00	-316.0	-188.0	-164.0	-257.0	-172.0
3.25	-369.0	-217.0	-193.0	-287.0	-205.0
3.50	-448.0	-266.0	-235.0	-323.0	-242.0
3.75	-493.0	-296.0	-258.0	-354.0	-269.0
4.00	-530.0	-317.0	-280.0	-376.0	-291.0
4.25	-556.0	-327.0	-292.0	-390.0	-305.0
4.50	-528.0	-305.0	-275.0	-368.0	-294.0
4.75	-450.0	-262.0	-237.0	-321.0	-246.0
5.00	-317.0	-174.0	-167.0	-232.0	-168.0
5.25	-127.0	-56.3	-67.4	-118.0	-65.1
5.50	93.0	80.3	56.4	21.9	60.6
5.75	326.0	213.0	178.0	173.0	189.0
6.00	527.0	329.0	284.0	312.0	302.0
6.25	654.0	402.0	354.0	392.0	379.0
6.50	703.0	428.0	383.0	427.0	402.0
6.75	647.0	402.0	359.0	386.0	367.0
7.00	543.0	334.0	309.0	325.0	309.0
7.25	337.0	211.0	199.0	210.0	192.0
7.50	121.0	91.7	74.9	70.0	68.8
7.75	-58.0	-15.2	-21.3	-58.0	-22.7
8.00	-212.0	-110.0	-99.0	-164.0	-110.0
8.25	-316.0	-175.0	-157.0	-226.0	-176.0
8.50	-355.0	-198.0	-187.0	-249.0	-198.0
8.75	-374.0	-216.0	-195.0	-264.0	-206.0
9.00	-368.0	-212.0	-194.0	-260.0	-207.0
9.25	-354.0	-205.0	-185.0	-257.0	-190.0
9.50	-346.0	-207.0	-183.0	-253.0	-187.0
9.75	-327.0	-181.0	-177.0	-238.0	-181.0
10.00	-288.0	-164.0	-152.0	-205.0	-159.0
10.25	-235.0	-142.0	-123.0	-161.0	-126.0
10.50	-133.0	-80.5	-65.5	-103.0	-66.1
10.75	-8.0	6.7	-6.4	-16.5	-7.9
11.00	152.0	88.8	79.9	86.4	87.5
11.25	333.0	202.0	170.0	198.0	185.0
11.50	461.0	266.0	234.0	279.0	266.0
11.75	557.0	312.0	285.0	356.0	306.0
12.00	573.0	327.0	300.0	349.0	314.0
12.25	486.0	281.0	226.0	304.0	269.0
12.50	323.0	214.0	167.0	190.0	183.0
12.75	131.0	70.6	69.3	63.2	71.4

Table 6 (continued).

s	$I_E^a(s)_{Exp}$	$I_E^{a(1)}(s)_{Exp}$	$I_E^{a(2)}(s)_{Exp}$	$I_E^{a(3)}(s)_{Exp}$	$I_E^{a(4)}(s)_{Exp}$
13.00	-124.0	-69.2	-77.8	-96.8	-75.5
13.25	-333.0	-196.0	-169.0	-242.0	-182.0
13.50	-485.0	-263.0	-258.0	-351.0	-263.0
13.75	-585.0	-328.0	-299.0	-406.0	-322.0
14.00	-607.0	-351.0	-321.0	-416.0	-334.0
14.25	-576.0	-327.0	-314.0	-407.0	-300.0
14.50	-495.0	-291.0	-277.0	-326.0	-273.0
14.75	-390.0	-231.0	-224.0	-261.0	-214.0
15.00	-292.0	-179.0	-181.0	-195.0	-141.0
15.25	-225.0	-145.0	-153.0	-151.0	-100.0
15.50	-148.0	-82.7	-110.0	-107.0	-71.4
15.75	-57.0	-34.2	-56.1	-45.6	-26.5
16.00	43.0	19.5	19.7	13.2	17.0
16.25	118.0	76.8	59.4	62.0	61.1
16.50	236.0	133.0	97.8	139.0	127.0
16.75	363.0	196.0	180.0	224.0	200.0
17.00	438.0	234.0	241.0	286.0	221.0
17.25	474.0	274.0	256.0	279.0	244.0
17.50	494.0	260.0	261.0	305.0	272.0
17.75	436.0	229.0	207.0	296.0	239.0
18.00	304.0	167.0	149.0	199.0	158.0
18.25	113.0	62.1	62.8	67.1	48.2
18.50	-101.0	-54.1	-67.4	-79.7	-46.0
18.75	-293.0	-140.0	-154.0	-198.0	-203.0
19.00	-441.0	-258.0	-231.0	-307.0	-232.0
19.25	-528.0	-303.0	-268.0	-372.0	-281.0
19.50	-535.0	-325.0	-268.0	-375.0	-279.0
19.75	-514.0	-309.0	-242.0	-371.0	-290.0
20.00	-395.0	-255.0	-191.0	-303.0	-201.0
20.25	-290.0	-197.0	-154.0	-233.0	-146.0
20.50	-163.0	-138.0	-82.7	-153.0	-85.3
20.75	-24.0	-45.7	-31.3	-41.7	-31.3

Table 7.   Experimental $I_E^b(s)$ and $I_E^{b(i)}(s)$ curves (h = 192.07 mm).

s	$I_E^b(s)_{Exp}$	$I_E^{b(1)}(s)_{Exp}$	$I_E^{b(2)}(s)_{Exp}$	$I_E^{b(3)}(s)_{Exp}$	$I_E^{b(4)}(s)_{Exp}$
10.25	-226	-658	-768	-520	-560
10.50	-168	-390	-586	-395	-390
10.75	-7	-10	0	5	-7
11.00	155	439	426	405	474
11.25	300	768	834	818	869
11.50	451	1122	1308	1236	1174
11.75	543	1364	1533	1436	1405
12.00	552	1403	1572	1371	1438
12.25	433	1038	1189	1106	1192
12.50	262	564	823	627	699
12.75	89	219	254	215	228
13.00	-166	-455	-457	-396	-389
13.25	-370	-909	-1190	-858	-831
13.50	-508	-1237	-1528	-1263	-1175
13.75	-592	-1404	-1735	-1455	-1482
14.00	-594	-1490	-1681	-1484	-1424
14.25	-537	-1354	-1544	-1376	-1234
14.50	-450	-1149	-1313	-1142	-1065
14.75	-405	-1016	-1130	-1013	-983
15.00	-291	-753	-854	-749	-690
15.25	-207	-594	-615	-492	-484
15.50	-134	-390	-370	-343	-352
15.75	-50	-221	-154	-146	-113
16.00	46	55	142	118	88
16.25	118	197	326	308	277
16.50	204	396	564	490	501
16.75	290	602	872	656	712
17.00	385	852	1110	880	916
17.25	432	955	1253	969	1054
17.50	468	1066	1356	1039	1146
17.75	343	804	940	729	881
18.00	234	479	698	495	542
18.25	65	60	301	31	151
18.50	-148	-348	-338	-500	-394
18.75	-313	-733	-820	-873	-809
19.00	-463	-1109	-1276	-1267	-1078
19.25	-506	-1188	-1450	-1320	-1208
19.50	-503	-1191	-1421	-1289	-1253
19.75	-430	-937	-1256	-1204	-1042
20.00	-339	-770	-1023	-952	-813
20.25	-198	-477	-602	-613	-462
20.50	-69	-166	-215	-315	-147

Table 7 (continued).

s	$I_E^b(s)_{Exp}$	$I_E^{b(1)}(s)_{Exp}$	$I_E^{b(2)}(s)_{Exp}$	$I_E^{b(3)}(s)_{Exp}$	$I_E^{b(4)}(s)_{Exp}$
20.75	40	68	156	-94	81
21.00	123	304	357	152	268
21.25	182	389	481	376	431
21.50	251	534	643	581	618
21.75	271	597	754	564	665
22.00	293	654	746	730	657
22.25	351	752	983	823	845
22.50	332	714	907	762	851
22.75	332	731	841	768	918
23.00	293	658	721	680	855
23.25	243	555	545	610	718
23.50	118	212	223	379	342
23.75	-9	-89	-208	115	142
24.00	-128	-332	-513	-233	-140
24.25	-276	-796	-860	-514	-453
24.50	-370	-974	-1066	-839	-669
24.75	-403	-959	-1250	-884	-743
25.00	-416	-1039	-1270	-885	-721
25.25	-365	-864	-1065	-775	-684
25.50	-231	-594	-674	-468	-308
25.75	-81	-244	-150	-132	-4
26.00	38	94	115	146	347
26.25	140	335	491	372	545
26.50	229	605	725	629	726
26.75	304	773	918	973	908
27.00	337	939	1009	886	975
27.25	300	766	1016	804	916
27.50	264	655	942	684	882
27.75	236	530	853	656	834
28.00	226	615	790	551	878
28.25	204	549	750	523	821
28.50	126	414	530	369	582
28.75	91	319	536	270	438
29.00	23	118	236	230	311
29.25	-65	-66	-46	32	72
29.50	-161	-321	-285	-113	-186
29.75	-236	-527	-531	-391	-256
30.00	-298	-641	-745	-516	-420
30.25	-360	-861	-803	-676	-560
30.50	-328	-829	-670	-649	-510
30.75	-262	-584	-403	-626	-396
31.00	-175	-500	-92	-416	-166

Table 7 (continued)

s	$I_E^b(s)_{Exp}$	$I_E^{b(1)}(s)_{Exp}$	$I_E^{b(2)}(s)_{Exp}$	$I_E^{b(3)}(s)_{Exp}$	$I_E^{b(4)}(s)_{Exp}$
31.25	-80	-125	205	-253	-42
31.50	25	38	601	-28	202
31.75	155	306	823	361	620
32.00	222	518	1011	435	723
32.25	256	567	1082	554	851
32.50	261	549	1091	610	775
32.75	259	581	1095	561	754
33.00	210	441	899	494	624
33.25	194	494	922	308	541
33.50	133	446	754	96	344
33.75	58	168	431	137	168
34.00	0	-34	336	-70	65
34.25	-56	-16	45	-152	-157
34.50	-94	-222	-59	-288	-101
34.75	-173	-441	-170	-425	-379
35.00	-182	-368	-338	-372	-467
35.25	-202	-470	-244	-484	-556
35.50	-245	-472	-482	-587	-620
35.75	-262	-527	-520	-663	-663
36.00	-244	-438	-577	-681	-558
36.25	-225	-350	-562	-526	-642
36.50	-166	-227	-318	-419	-515
36.75	-41	82	60	-212	-190
37.00	42	242	266	136	-24
37.25	121	275	543	251	295
37.50	143	404	527	465	238
37.75	141	372	431	520	298
38.00	138	401	401	545	223
38.25	109	339	262	448	242
38.50	29	128	-20	333	28
38.75	-26	-25	-33	25	-45
39.00	-45	-86	-182	38	-28
39.25	-128	-293	-456	-84	-229
39.50	-161	-407	-540	-133	-376
39.75	-213	-574	-569	-324	-456
40.00	-202	-398	-585	-411	-437
40.25	-209	-302	-674	-442	-481
40.50	-182	-241	-583	-416	-330
40.75	-165	-376	-568	-337	-142
41.00	-162	-389	-436	-373	-66
41.25	-127	-332	-210	-332	-35
41.50	-98	-110	-83	-241	-198

Table 7 (continued).

s	$I_E^b(s)_{Exp}$	$I_E^{b(1)}(s)_{Exp}$	$I_E^{b(2)}(s)_{Exp}$	$I_E^{b(3)}(s)_{Exp}$	$I_E^{b(4)}(s)_{Exp}$
41.75	-38	30	-35	13	48
42.00	-26	97	-70	78	89

Table 8. Experimental $I_E^c(s)$ curve (h = 120.00 mm).

s	$I_E^c(s)_{Exp}$	s	$I_E^c(s)_{Exp}$	s	$I_E^c(s)_{Exp}$
18.50	134.0	29.00	12.0	39.50	-150.0
18.75	-23.0	29.25	-59.0	39.75	-172.0
19.00	-207.0	29.50	-137.0	40.00	-195.0
19.25	-351.0	29.75	-236.0	40.25	-193.0
19.50	-361.0	30.00	-294.0	40.50	-176.0
19.75	-336.0	30.25	-306.0	40.75	-189.0
20.00	-228.0	30.50	-311.0	41.00	-164.0
20.25	-123.0	30.75	-282.0	41.25	-153.0
20.50	-55.0	31.00	-181.0	41.50	-113.0
20.75	50.0	31.25	-61.0	41.75	-81.0
21.00	142.0	31.50	24.0	42.00	-54.0
21.25	225.0	31.75	145.0	42.25	21.0
21.50	236.0	32.00	227.0	42.50	83.0
21.75	281.0	32.25	254.0	42.75	131.0
22.00	331.0	32.50	270.0	43.00	188.0
22.25	401.0	32.75	289.0	43.25	188.0
22.50	359.0	33.00	243.0	43.50	139.0
22.75	327.0	33.25	141.0	43.75	64.0
23.00	356.0	33.50	110.0	44.00	7.0
23.25	272.0	33.75	24.0	44.25	18.0
23.50	160.0	34.00	-24.0	44.50	-18.0
23.75	9.0	34.25	-100.0	44.75	-107.0
24.00	-95.0	34.50	-111.0	45.00	-74.0
24.25	-260.0	34.75	-168.0	45.25	-66.0
24.50	-412.0	35.00	-220.0	45.50	-85.0
24.75	-444.0	35.25	-280.0	45.75	-79.0
25.00	-415.0	35.50	-292.0	46.00	-75.0
25.25	-370.0	35.75	-305.0	46.25	-78.0
25.50	-276.0	36.00	-263.0	46.50	-69.0
25.75	-135.0	36.25	-245.0	46.75	-66.0
26.00	10.0	36.50	-97.0	47.00	1.0
26.25	166.0	36.75	-7.0	47.25	27.0
26.50	267.0	37.00	99.0	47.50	21.0
26.75	327.0	37.25	117.0	47.75	77.0
27.00	309.0	37.50	152.0	48.00	80.0
27.25	235.0	37.75	149.0	48.25	117.0
27.50	240.0	38.00	147.0	48.50	104.0
27.75	182.0	38.25	111.0	48.75	118.0
28.00	183.0	38.50	87.0	49.00	77.0
28.25	119.0	38.75	47.0	49.25	112.0
28.50	92.0	39.00	2.0	49.50	64.0
28.75	78.0	39.25	-85.0	49.75	-7.0

Table 9.   Experimental and theoretical $rD'(r)$ curves.

r	$rD'(r)_{Exp}$	$rD'(r)_{Theor}$	r	$rD'(r)_{Exp}$	$rD'(r)_{Theor}$
0.00	0.0	0.0	1.68	0.4	0.0
0.04	-9.9	0.0	1.72	2.5	0.0
0.08	-13.1	0.0	1.76	3.2	0.0
0.12	-13.7	0.0	1.80	2.0	0.0
0.16	-16.7	0.0	1.84	0.4	0.0
0.20	-15.6	0.0	1.88	-0.9	0.0
0.24	-2.1	0.0	1.92	-1.4	0.0
0.28	12.8	0.0	1.96	-2.1	0.0
0.32	13.8	0.0	2.00	-3.3	0.3
0.36	5.5	0.0	2.04	-2.5	2.1
0.40	-0.1	0.0	2.08	4.5	8.7
0.44	-3.9	0.0	2.12	20.9	24.8
0.48	-10.1	0.0	2.16	44.1	48.4
0.52	-15.4	0.0	2.20	60.3	64.5
0.56	-16.8	0.0	2.24	54.5	58.8
0.60	-15.3	0.0	2.28	30.9	36.6
0.64	-12.4	0.0	2.32	9.2	15.6
0.68	-9.3	0.0	2.36	-0.6	4.5
0.72	-4.3	0.0	2.40	-3.8	0.9
0.76	2.4	0.0	2.44	-5.4	0.1
0.80	6.0	0.0	2.48	-5.4	0.0
0.84	5.7	0.0	2.52	-4.7	0.0
0.88	6.1	0.0	2.56	-4.1	0.0
0.92	6.6	0.0	2.60	-2.9	0.0
0.96	4.9	0.1	2.64	-1.4	0.0
1.00	3.8	0.7	2.68	-0.8	0.0
1.04	6.6	5.5	2.72	-0.7	0.0
1.08	27.8	28.1	2.76	0.0	0.0
1.12	94.5	90.2	2.80	0.3	0.0
1.16	192.6	182.4	2.84	0.0	0.0
1.20	243.8	232.3	2.88	0.3	0.0
1.24	197.0	186.1	2.92	1.5	0.0
1.28	101.5	93.9	2.96	1.3	0.0
1.32	34.8	29.8	3.00	-0.4	0.0
1.36	11.9	6.0	3.04	-0.5	0.0
1.40	5.5	0.7	3.08	1.2	0.0
1.44	2.2	0.1	3.12	1.6	0.0
1.48	3.0	0.0	3.16	0.8	0.0
1.52	4.8	0.0	3.20	1.4	0.0
1.56	4.1	0.0	3.24	2.8	0.0
1.60	1.4	0.0	3.28	2.4	0.0
1.64	-0.5	0.0	3.32	0.7	0.0

Table 9 (continued).

r	$rD'(r)_{Exp}$	$rD'(r)_{Theor}$	r	$rD'(r)_{Exp}$	$rD'(r)_{Theor}$
3.36	-0.3	0.0	4.20	-1.1	0.0
3.40	-0.1	0.0	4.24	-0.3	0.0
3.44	0.0	0.0	4.28	-0.3	0.0
3.48	-0.1	0.0	4.32	-1.3	0.0
3.52	0.1	0.0	4.36	-1.6	0.0
3.56	1.1	0.0	4.40	-0.9	0.0
3.60	2.0	0.0	4.44	-0.1	0.0
3.64	1.7	0.0	4.48	0.1	0.0
3.68	0.5	0.0	4.52	0.1	0.0
3.72	-0.1	0.0	4.56	-0.1	0.0
3.76	-0.1	0.0	4.60	-0.7	0.0
3.80	-0.1	0.0	4.64	-1.1	0.0
3.84	0.1	0.0	4.68	-0.7	0.0
3.88	0.3	0.0	4.72	-0.5	0.0
3.92	0.9	0.0	4.76	-0.9	0.0
3.96	1.3	0.0	4.80	-1.1	0.0
4.00	0.8	0.0	4.84	-0.7	0.0
4.04	-0.2	0.0	4.88	-0.4	0.0
4.08	-0.7	0.0	4.92	-0.1	0.0
4.12	-0.8	0.0	4.96	-0.4	0.0
4.16	-1.2	0.0	5.00	0.0	0.0

Table 10. Blackness correction table (Oslo).

D	δ	D	δ	D	δ
0.6200	.0001	1.0400	.0624	1.4600	.2726
0.6300	.0002	1.0500	.0658	1.4700	.2790
0.6400	.0003	1.0600	.0693	1.4800	.2854
0.6500	.0004	1.0700	.0728	1.4900	.2919
0.6600	.0006	1.0800	.0764	1.5000	.2984
0.6700	.0008	1.0900	.0800	1.5100	.3050
0.6800	.0011	1.1000	.0838	1.5200	.3117
0.6900	.0015	1.1100	.0879	1.5300	.3185
0.7000	.0019	1.1200	.0921	1.5400	.3253
0.7100	.0023	1.1300	.0964	1.5500	.3321
0.7200	.0027	1.1400	.1007	1.5600	.3390
0.7300	.0034	1.1500	.1051	1.5700	.3460
0.7400	.0041	1.1600	.1095	1.5800	.3531
0.7500	.0050	1.1700	.1141	1.5900	.3602
0.7600	.0059	1.1800	.1187	1.6000	.3674
0.7700	.0069	1.1900	.1235	1.6100	.3747
0.7800	.0081	1.2000	.1283	1.6200	.3821
0.7900	.0094	1.2100	.1331	1.6300	.3895
0.8000	.0107	1.2200	.1380	1.6400	.3969
0.8100	.0121	1.2300	.1429	1.6500	.4043
0.8200	.0135	1.2400	.1479	1.6600	.4119
0.8300	.0150	1.2500	.1529	1.6700	.4195
0.8400	.0165	1.2600	.1580	1.6800	.4272
0.8500	.0180	1.2700	.1632	1.6900	.4350
0.8600	.0196	1.2800	.1684	1.7000	.4428
0.8700	.0213	1.2900	.1737	1.7100	.4506
0.8800	.0231	1.3000	.1790	1.7200	.4584
0.8900	.0250	1.3100	.1844	1.7300	.4663
0.9000	.0270	1.3200	.1898	1.7400	.4743
0.9100	.0290	1.3300	.1953	1.7500	.4825
0.9200	.0311	1.3400	.2008	1.7600	.4907
0.9300	.0333	1.3500	.2064	1.7700	.4989
0.9400	.0355	1.3600	.2121	1.7800	.5072
0.9500	.0377	1.3700	.2179	1.7900	.5156
0.9600	.0400	1.3800	.2237	1.8000	.5241
0.9700	.0424	1.3900	.2296	1.8100	.5326
0.9800	.0450	1.4000	.2356	1.8200	.5411
0.9900	.0476	1.4100	.2416	1.8300	.5497
1.0000	.0502	1.4200	.2477	1.8400	.5584
1.0100	.0531	1.4300	.2539	1.8500	.5671
1.0200	.0561	1.4400	.2601	1.8600	.5758
1.0300	.0592	1.4500	.2663	1.8700	.5846

Table 11. Sector function: h = 478. 00 mm.

s	g(θ)	s	g(θ)	s	g(θ)
2.50	41.29	8.75	303.62	15.00	525.21
2.75	50.85	9.00	312.73	15.25	533.16
3.00	59.21	9.25	321.54	15.50	542.39
3.25	70.07	9.50	329.92	15.75	551.28
3.50	80.39	9.75	338.62	16.00	559.79
3.75	92.39	10.00	347.69	16.25	568.32
4.00	105.28	10.25	356.92	16.50	577.43
4.25	118.36	10.50	366.17	16.75	586.77
4.50	131.66	10.75	374.45	17.00	595.34
4.75	143.71	11.00	383.48	17.25	604.12
5.00	155.41	11.25	392.81	17.50	613.11
5.25	166.97	11.50	401.63	17.75	622.13
5.50	177.75	11.75	410.18	18.00	631.28
5.75	189.01	12.00	419.30	18.25	639.79
6.00	200.41	12.25	428.16	18.50	648.87
6.25	211.24	12.50	436.88	18.75	657.32
6.50	222.19	12.75	446.07	19.00	665.99
6.75	231.41	13.00	454.82	19.25	674.68
7.00	240.85	13.25	464.05	19.50	683.83
7.25	250.28	13.50	472.51	19.75	693.47
7.50	259.05	13.75	480.47	20.00	702.22
7.75	268.22	14.00	489.25	20.25	710.98
8.00	277.15	14.25	498.55	20.50	719.86
8.25	285.40	14.50	507.03	20.75	729.50
8.50	294.55	14.75	516.71	21.00	739.07

Table 12.   Sector function: h = 192. 07 mm.

s	g(θ)	s	g(θ)	s	g(θ)
10.25	4744	21.00	13295	31.75	20707
10.50	4963	21.25	13444	32.00	20878
10.75	5226	21.50	13633	32.25	21063
11.00	5472	21.75	13792	32.50	21227
11.25	5705	22.00	13951	32.75	21412
11.50	5943	22.25	14159	33.00	21588
11.75	6184	22.50	14311	33.25	21788
12.00	6414	22.75	14488	33.50	21977
12.25	6613	23.00	14649	33.75	22144
12.50	6830	23.25	14836	34.00	22311
12.75	7049	23.50	14998	34.25	22466
13.00	7253	23.75	15169	34.50	22633
13.25	7494	24.00	15349	34.75	22803
13.50	7690	24.25	15503	35.00	22985
13.75	7907	24.50	15649	35.25	23168
14.00	8128	24.75	15822	35.50	23366
14.25	8338	25.00	15978	35.75	23538
14.50	8553	25.25	16161	36.00	23736
14.75	8725	25.50	16345	36.25	23899
15.00	8945	25.75	16521	36.50	24073
15.25	9147	26.00	16688	36.75	24288
15.50	9346	26.25	16876	37.00	24479
15.75	9559	26.50	17033	37.25	24657
16.00	9774	26.75	17211	37.50	24836
16.25	9963	27.00	17391	37.75	24990
16.50	10159	27.25	17541	38.00	25171
16.75	10340	27.50	17702	38.25	25353
17.00	10539	27.75	17882	38.50	25524
17.25	10734	28.00	18055	38.75	25720
17.50	10944	28.25	18238	39.00	25907
17.75	11090	28.50	18422	39.25	26092
18.00	11268	28.75	18606	39.50	26267
18.25	11448	29.00	18769	39.75	26428
18.50	11602	29.25	18946	40.00	26631
18.75	11776	29.50	19121	40.25	26808
19.00	11951	29.75	19298	40.50	27014
19.25	12128	30.00	19464	40.75	27194
19.50	12311	30.25	19643	41.00	27373
19.75	12489	30.50	19822	41.25	27585
20.00	12645	30.75	20001	41.50	27767
20.25	12808	31.00	20170	41.75	27966
20.50	12980	31.25	20353	42.00	28137
20.75	13145	31.50	20524	42.25	28337

Table 13. Sector function: h = 120.00 mm.

s	g(θ)	s	g(θ)	s	g(θ)
18.50	44984	29.00	89385	39.50	126704
18.75	46111	29.25	90250	39.75	127612
19.00	47308	29.50	91049	40.00	128522
19.25	48480	29.75	91957	40.25	129375
19.50	49689	30.00	92871	40.50	130380
19.75	50808	30.25	93737	40.75	131286
20.00	51998	30.50	94562	41.00	132194
20.25	53038	30.75	95438	41.25	133150
20.50	53964	31.00	96363	41.50	134196
20.75	55087	31.25	97249	41.75	135065
21.00	56213	31.50	98140	42.00	136023
21.25	57256	31.75	99123	42.25	137077
21.50	58283	32.00	100025	42.50	137871
21.75	59381	32.25	100939	42.75	138930
22.00	60556	32.50	101779	43.00	139951
22.25	61812	32.75	102752	43.25	140935
22.50	62690	33.00	103611	43.50	141920
22.75	63681	33.25	104484	43.75	142755
23.00	64851	33.50	105296	44.00	143598
23.25	65933	33.75	106155	44.25	144655
23.50	66980	34.00	107103	44.50	145482
23.75	68026	34.25	107847	44.75	146438
24.00	69156	34.50	108679	45.00	147483
24.25	70184	34.75	109494	45.25	148531
24.50	71014	35.00	110323	45.50	149597
24.75	72130	35.25	111301	45.75	150588
25.00	73264	35.50	112228	46.00	151565
25.25	74217	35.75	113072	46.25	152484
25.50	75144	36.00	113967	46.50	153506
25.75	76249	36.25	114755	46.75	154397
26.00	77312	36.50	115777	47.00	155428
26.25	78417	36.75	116808	47.25	156426
26.50	79496	37.00	117793	47.50	157441
26.75	80563	37.25	118657	47.75	158385
27.00	81470	37.50	119533	48.00	159352
27.25	82428	37.75	120376	48.25	160427
27.50	83397	38.00	121433	48.50	161414
27.75	84349	38.25	122314	48.75	162419
28.00	85348	38.50	123299	49.00	163453
28.25	86349	38.75	124223	49.25	164487
28.50	87397	39.00	125060	49.50	165380
28.75	88448	39.25	125894	49.75	166405

Table 14. $[(Z-F/Z]_N$ and $[(Z-F)/Z]_O$ table.

s	$[(Z-F)/Z]_N$	$[(Z-F)/Z]_O$	s	$[(Z-F)/Z]_N$	$[(Z-F)/Z]_O$
0.00	0.0000	0.0000	10.50	0.7985	0.8090
0.25	0.0093	0.0072	10.75	0.8013	0.8113
0.50	0.0240	0.0180	11.00	0.8039	0.8135
0.75	0.0460	0.0380	11.25	0.8064	0.8160
1.00	0.0770	0.0619	11.50	0.8090	0.8180
1.25	0.1140	0.0928	11.75	0.8117	0.8210
1.50	0.1595	0.1293	12.00	0.8140	0.8233
1.75	0.2031	0.1680	12.25	0.8166	0.8259
2.00	0.2495	0.2090	12.50	0.8193	0.8282
2.25	0.2959	0.2513	12.75	0.8217	0.8300
2.50	0.3421	0.2940	13.00	0.8242	0.8321
2.75	0.3880	0.3350	13.25	0.8267	0.8340
3.00	0.4300	0.3770	13.50	0.8287	0.8360
3.25	0.4694	0.4160	13.75	0.8314	0.8380
3.50	0.5030	0.4520	14.00	0.8335	0.8399
3.75	0.5340	0.4860	14.25	0.8360	0.8418
4.00	0.5650	0.5180	14.50	0.8385	0.8437
4.25	0.5928	0.5470	14.75	0.8410	0.8456
4.50	0.6160	0.5740	15.00	0.8435	0.8472
4.75	0.6373	0.5990	15.25	0.8462	0.8494
5.00	0.6550	0.6225	15.50	0.8484	0.8513
5.25	0.6719	0.6428	15.75	0.8510	0.8535
5.50	0.6875	0.6618	16.00	0.8535	0.8553
5.75	0.7003	0.6768	16.25	0.8559	0.8572
6.00	0.7110	0.6930	16.50	0.8580	0.8590
6.25	0.7220	0.7070	16.75	0.8600	0.8606
6.50	0.7310	0.7185	17.00	0.8620	0.8623
6.75	0.7387	0.7290	17.25	0.8645	0.8645
7.00	0.7447	0.7390	17.50	0.8665	0.8662
7.25	0.7509	0.7480	17.75	0.8690	0.8681
7.50	0.7560	0.7560	18.00	0.8715	0.8699
7.75	0.7613	0.7640	18.25	0.8738	0.8718
8.00	0.7660	0.7701	18.50	0.8760	0.8736
8.25	0.7700	0.7770	18.75	0.8785	0.8752
8.50	0.7740	0.7822	19.00	0.8810	0.8772
8.75	0.7780	0.7860	19.25	0.8830	0.8788
9.00	0.7820	0.7900	19.50	0.8855	0.8806
9.25	0.7850	0.7940	19.75	0.8875	0.8823
9.50	0.7877	0.7973	20.00	0.8895	0.8841
9.75	0.7900	0.8003	20.25	0.8917	0.8860
10.00	0.7930	0.8039	20.50	0.8935	0.8878
10.25	0.7958	0.8060	20.75	0.8955	0.8895

Table 14 (continued).

s	$[(Z-F)/Z]_N$	$[(Z-F)/Z]_O$	s	$[(Z-F)/Z]_N$	$[(Z-F)/Z]_O$
21.00	0.8977	0.8907	31.50	0.9555	0.9473
21.25	0.9000	0.8921	31.75	0.9560	0.9480
21.50	0.9020	0.8940	32.00	0.9567	0.9490
21.75	0.9040	0.8955	32.25	0.9575	0.9498
22.00	0.9062	0.8970	32.50	0.9582	0.9503
22.25	0.9080	0.8984	32.75	0.9592	0.9513
22.50	0.9102	0.9000	33.00	0.9600	0.9520
22.75	0.9120	0.9015	33.25	0.9606	0.9528
23.00	0.9140	0.9030	33.50	0.9614	0.9537
23.25	0.9157	0.9044	33.75	0.9620	0.9542
23.50	0.9168	0.9060	34.00	0.9624	0.9550
23.75	0.9185	0.9075	34.25	0.9632	0.9560
24.00	0.9202	0.9089	34.50	0.9639	0.9564
24.25	0.9220	0.9103	34.75	0.9642	0.9570
24.50	0.9237	0.9120	35.00	0.9647	0.9576
24.75	0.9252	0.9137	35.25	0.9655	0.9580
25.00	0.9268	0.9150	35.50	0.9660	0.9584
25.25	0.9281	0.9169	35.75	0.9663	0.9594
25.50	0.9297	0.9182	36.00	0.9670	0.9600
25.75	0.9316	0.9199	36.25	0.9675	0.9603
26.00	0.9325	0.9210	36.50	0.9680	0.9613
26.25	0.9338	0.9222	36.75	0.9684	0.9617
26.50	0.9347	0.9238	37.00	0.9691	0.9621
26.75	0.9360	0.9250	37.25	0.9699	0.9625
27.00	0.9374	0.9261	37.50	0.9702	0.9633
27.25	0.9382	0.9279	37.75	0.9708	0.9637
27.50	0.9395	0.9292	38.00	0.9714	0.9639
27.75	0.9403	0.9303	38.25	0.9720	0.9642
28.00	0.9418	0.9320	38.50	0.9723	0.9646
28.25	0.9425	0.9334	38.75	0.9727	0.9653
28.50	0.9438	0.9342	39.00	0.9735	0.9657
28.75	0.9445	0.9358	39.25	0.9739	0.9661
29.00	0.9457	0.9367	39.50	0.9741	0.9663
29.25	0.9468	0.9378	39.75	0.9743	0.9668
29.50	0.9480	0.9387	40.00	0.9748	0.9675
29.75	0.9491	0.9399	40.25	0.9754	0.9678
30.00	0.9500	0.9410	40.50	0.9758	0.9681
30.25	0.9516	0.9423	40.75	0.9760	0.9685
30.50	0.9522	0.9435	41.00	0.9762	0.9687
30.75	0.9532	0.9442	41.25	0.9765	0.9693
31.00	0.9540	0.9450	41.50	0.9771	0.9696
31.25	0.9545	0.9462	41.75	0.9776	0.9700

Table 14 (continued).

s	$[(Z-F)/Z]_N$	$[(Z-F)/Z]_O$	s	$[(Z-F)/Z]_N$	$[(Z-F)/Z]_O$
42.00	0.9779	0.9702	46.00	0.9816	0.9745
42.25	0.9780	0.9703	46.25	0.9818	0.9748
42.50	0.9783	0.9705	46.50	0.9820	0.9753
42.75	0.9785	0.9707	46.75	0.9821	0.9756
43.00	0.9790	0.9712	47.00	0.9823	0.9758
43.25	0.9795	0.9719	47.25	0.9824	0.9760
43.50	0.9798	0.9721	47.50	0.9826	0.9761
43.75	0.9800	0.9722	47.75	0.9831	0.9763
44.00	0.9802	0.9726	48.00	0.9835	0.9765
44.25	0.9804	0.9730	48.25	0.9836	0.9765
44.50	0.9805	0.9733	48.50	0.9839	0.9768
44.75	0.9807	0.9735	48.75	0.9840	0.9772
45.00	0.9810	0.9736	49.00	0.9841	0.9775
45.25	0.9810	0.9740	49.25	0.9843	0.9778
45.50	0.9812	0.9741	49.50	0.9845	0.9780
45.75	0.9814	0.9742	49.75	0.9846	0.9781

Table 15. $Z_N Z_O (Z-F)_O / (Z-F)_N$ table.

s	$A_{O\ldots O}$	s	$A_{O\ldots O}$	s	$A_{O\ldots O}$
0.25	49.5	10.75	64.8	21.25	63.4
0.50	48.0	11.00	64.8	21.50	63.4
0.75	52.9	11.25	64.8	21.75	63.4
1.00	51.4	11.50	64.7	22.00	63.3
1.25	52.1	11.75	64.7	22.25	63.3
1.50	51.9	12.00	64.7	22.50	63.3
1.75	52.9	12.25	64.7	22.75	63.3
2.00	53.6	12.50	64.7	23.00	63.2
2.25	54.4	12.75	64.6	23.25	63.2
2.50	55.0	13.00	64.6	23.50	63.2
2.75	55.3	13.25	64.6	23.75	63.2
3.00	56.1	13.50	64.6	24.00	63.2
3.25	56.7	13.75	64.5	24.25	63.2
3.50	57.5	14.00	64.5	24.50	63.2
3.75	58.2	14.25	64.4	24.75	63.2
4.00	58.7	14.50	64.4	25.00	63.2
4.25	59.1	14.75	64.3	25.25	63.2
4.50	59.6	15.00	64.3	25.50	63.2
4.75	60.2	15.25	64.3	25.75	63.2
5.00	60.8	15.50	64.2	26.00	63.2
5.25	61.2	15.75	64.2	26.25	63.2
5.50	61.6	16.00	64.1	26.50	63.3
5.75	61.8	16.25	64.1	26.75	63.2
6.00	62.4	16.50	64.1	27.00	63.2
6.25	62.7	16.75	64.1	27.25	63.3
6.50	62.9	17.00	64.0	27.50	63.3
6.75	63.2	17.25	64.0	27.75	63.3
7.00	63.5	17.50	64.0	28.00	63.3
7.25	63.8	17.75	63.9	28.25	63.4
7.50	64.0	18.00	63.9	28.50	63.3
7.75	64.3	18.25	63.9	28.75	63.4
8.00	64.3	18.50	63.8	29.00	63.4
8.25	64.6	18.75	63.8	29.25	63.4
8.50	64.7	19.00	63.7	29.50	63.4
8.75	64.6	19.25	63.7	29.75	63.4
9.00	64.6	19.50	63.6	30.00	63.4
9.25	64.7	19.75	63.6	30.25	63.4
9.50	64.8	20.00	63.6	30.50	63.4
9.75	64.8	20.25	63.6	30.75	63.4
10.00	64.9	20.50	63.6	31.00	63.4
10.25	64.8	20.75	63.6	31.25	63.4
10.50	64.8	21.00	63.5	31.50	63.4

Table 15 (continued)

s	$A_{O\cdots O}$	s	$A_{O\cdots O}$	s	$A_{O\cdots O}$
31.75	63.5	37.75	63.5	43.75	63.5
32.00	63.5	38.00	63.5	44.00	63.5
32.25	63.5	38.25	63.5	44.25	63.5
32.50	63.5	38.50	63.5	44.50	63.5
32.75	63.5	38.75	63.5	44.75	63.5
33.00	63.5	39.00	63.5	45.00	63.5
33.25	63.5	39.25	63.5	45.25	63.5
33.50	63.5	39.50	63.5	45.50	63.5
33.75	63.5	39.75	63.5	45.75	63.5
34.00	63.5	40.00	63.5	46.00	63.5
34.25	63.5	40.25	63.5	46.25	63.5
34.50	63.5	40.50	63.5	46.50	63.6
34.75	63.5	40.75	63.5	46.75	63.6
35.00	63.5	41.00	63.5	47.00	63.6
35.25	63.5	41.25	63.5	47.25	63.6
35.50	63.5	41.50	63.5	47.50	63.6
35.75	63.5	41.75	63.5	47.75	63.6
36.00	63.5	42.00	63.5	48.00	63.5
36.25	63.5	42.25	63.5	48.25	63.5
36.50	63.6	42.50	63.5	48.50	63.5
36.75	63.6	42.75	63.5	48.75	63.6
37.00	63.5	43.00	63.5	49.00	63.6
37.25	63.5	43.25	63.5	49.25	63.6
37.50	63.5	43.50	63.5	49.50	63.6
				49.75	63.6

$$A_{O\cdots O} = Z_N Z_O (Z-F)_O / (Z-F)_N.$$

Table 16. Results of least-squares refinements[a]: comparison of separate composites for different Δs intervals.

	I_E^a; $2.50 \leq s \leq 20.75$				I_E^b; $10.25 \leq s \leq 42.00$			I_E^c; $28.75 \leq s \leq 49.75$			I_E^c; $18.50 \leq s \leq 49.75$
	Δs				Δs			Δs			Δs
	.25	.50	.75	1.00	.25	.50	.75	.25	.50	.75	.25
r_{N-O}, Å	1.200	1.200	1.200	1.200	1.202	1.202	1.202	1.200	1.200	1.200	1.200
$\sigma_{LS}(r_{N-O})$, Å	± .0015	± .0023	± .0028	± .0034	± .0009	± .0013	± .0016	± .0008	± .0013	± .0017	± .0010
$r_{O \cdots O}$, Å	2.207	2.207	2.206	2.210	2.211	2.211	2.211	2.212	2.213	2.216	2.207
$\sigma_{LS}(r_{O \cdots O})$, Å	± .0058	± .0087	± .0111	± .0139	± .0036	± .0053	± .0068	± .0044	± .0067	± .0080	± .0043
l_{N-O}, Å	.0336	.0347	.0309	.0334	.0368	.0362	.0363	.0378	.0367	.0373	.0334
$\sigma_{LS}(l_{N-O})$, Å	± .0044	± ..0064	± .0087	± .0100	± .0014	± .0021	± .0026	± .0020	± .0032	± .0040	± .0017
$l_{O \cdots O}$, Å	.0504	.0511	.0526	.0547	.0444	.0447	.0449	.0464	.0447	.0443	.0420
$\sigma_{LS}(l_{O \cdots O})$, Å	± .0077	± .0116	± .0141	± .0167	± .0033	± .0049	± .0062	± .0032	± .0051	± .0063	± .0036

[a] $(\mathbb{P})_{ii} = 1$, $A_{N-O} = 2Z_N Z_O$, and $A_{O \cdots O} = Z_O^2$ were used in all refinements.

117

Table 17. Results of least-squares refinements[a]: comparison of individual photographic plates with their composites.

	2.50 ≤ s ≤ 20.75, Δs = .25					10.50 ≤ s ≤ 20.75, Δs = .25					10.25 ≤ s ≤ 42.00, Δs = .25				
	I_E^a	$I_E^{a(1)}$	$I_E^{a(2)}$	$I_E^{a(3)}$	$I_E^{a(4)}$	I_E^a	$I_E^{a(1)}$	$I_E^{a(2)}$	$I_{E'}^{a(3)}$	$I_E^{a(4)}$	I_E^b	$I_E^{b(1)}$	$I_E^{b(2)}$	$I_E^{b(3)}$	$I_E^{b(4)}$
r_{N-O}, Å	1.200	1.199	1.199	1.200	1.201	1.200	1.199	1.199	---	1.201	1.202	1.202	1.203	1.201	1.201
$\sigma_{LS}(r_{N-O})$, Å	±.0015	±.0016	±.0018	±.0022	±.0015	±.0018	±.0019	±.0023	---	±.0019	±.0009	±.0010	±.0012	±.0010	±.0014
$r_{O...O}$, Å	2.207	2.203	2.212	2.202	2.207	2.208	2.202	2.216	---	2.208	2.211	2.213	2.213	2.207	2.212
$\sigma_{LS}(r_{O...O})$, Å	±.0056	±.0068	±.0073	±.0085	±.0055	±.0071	±.0086	±.0099	---	±.0071	±.0036	±.0041	±.0051	±.0041	±.0055
l_{N-O}, Å	.0036	.0354	.0369	.0293	.0381	.0201	.0126	.0221	---	.0260	.0367	.0382	.0365	.0385	.0400
$\sigma_{LS}(l_{N-O})$, Å	±.0042	±.0044	±.0047	±.0072	±.0038	±.0137	±.0228	±.0163	---	±.0109	±.0014	±.0015	±.0019	±.0016	±.0020
$l_{O...O}$, Å	.0504	.0617	.0589	.0507	.0511	.0422	.0516	.0495	---	.0426	.0441	.0457	.0446	.0448	.0466
$\sigma_{LS}(l_{O...O})$, Å	±.0075	±.0077	±.0086	±.0113	±.0072	±.0115	±.0111	±.0138	---	±.0114	±.0033	±.0037	±.0046	±.0038	±.0049

[a] $(P)_{ii} = 1$, $A_{N-O} = 2 Z_N Z_O$, and $A_{O...O} = Z_N Z_O (Z-F)_O / (Z-F)_N$ were used in all refinements.

Table 18. Results of least-squares refinements[a]: comparison of different composites.

	I_E^a; $2.50 \le s \le 20.75$, $\Delta s = .25$		I_E^b; $10.25 \le s < 42.00$, $\Delta s = .25$		I_E^c; $28.75 < s < 49.75$, $\Delta s = .25$	I_E^T; $2.50 < s < 49.75$ $\Delta s = .25$
	C[b]	V[c]	C	V	C	V
r_{N-O}, Å	1.200	1.200	1.202	1.202	1.200	1.201
$\sigma_{LS}(r_{N-O})$, Å	± .0015	± .0015	± .0009	± .0009	± .0008	± .0007
$r_{O\cdots O}$, Å	2.207	2.207	2.211	2.211	2.212	2.210
$\sigma_{LS}(r_{O\cdots O})$, Å	± .0058	± .0056	± .0036	± .0036	± .0044	± .0030
l_{N-O}, Å	.0036	.0336	.0368	.0367	.0378	.0382
$\sigma_{LS}(l_{N-O})$, Å	± .0044	± .0042	± .0014	± .0014	± .0020	± .0080
$l_{O\cdots O}$, Å	.0504	.0504	.0444	.0441	.0464	.0470
$\sigma_{LS}(l_{O\cdots O})$, Å	± .0077	± .0075	± .0033	± .0033	± .0032	± .0025

(a) $(\mathbb{P})_{ii} = 1$ was used in all refinements.

(b) $A_{N-O} = 2Z_N Z_O$ and $A_{O\cdots O} = Z_O^2$

(c) $A_{N-O} = 2Z_N Z_O$ and $A_{O\cdots O} = Z_N Z_O (Z-F)_O / (Z-F)_N$.

Table 19. Results of least-squares refinements:[a] effect of variable weight matrix in analysis of $I_E^T(s)$.

| | $I_E^T(s)$; $2.50 \le s \le 49.75$, $\Delta s = .25$ | | |
| | $(P)_{ii}$ | | |
	1	const s_i exp $(-.0016\, s_i^2)$	const s_i exp $(-.002\, s_i^2)$
r_{N-O}, $\overset{\circ}{A}$	1.2009	1.2010	1.2012
$\sigma_{LS}(r_{N-O})$, $\overset{\circ}{A}$	$\pm$ .0007	$\pm$ .0007	$\pm$ .0007
$r_{O\cdots O}$, $\overset{\circ}{A}$	2.2102	2.2096	2.2095
$\sigma_{LS}(r_{O\cdots O})$, $\overset{\circ}{A}$	$\pm$ .0030	$\pm$ .0027	$\pm$ .0028
l_{N-O}, $\overset{\circ}{A}$	.03815	.03753	.03747
$\sigma_{LS}(l_{N-O})$, $\overset{\circ}{A}$	$\pm$ .00079	$\pm$ .00098	$\pm$ .00108
$l_{O\cdots O}$, $\overset{\circ}{A}$	.04698	.04701	.04714
$\sigma_{LS}(l_{O\cdots O})$, $\overset{\circ}{A}$	$\pm$ .00253	$\pm$ .00263	$\pm$ .00282

[a] $A_{N-O} = 2\, Z_N Z_O$ and $A_{O\cdots O}(s) = Z_N Z_O (Z-F)_O / (Z-F)_N$ were used in all refinements.

Table 20. Error matrix $(\times 10^6)$ obtained from third cycle of least-squares refinement[a] of $I_E^T(s)$: $2.50 \leq s \leq 49.75$ and $\Delta s = 0.25$.

r_{N-O}[b]	$r_{O\cdots O}$	$<O-N-O$[c]	l_{N-O}	$l_{O\cdots O}$
.4736	- .0002	-106.4285	- .0052	- .0097
	8.7908	1072.76	.0107	- .1374
		154815.8	2.4791	-14.5843
			.6223	.2792
				6.4444

[a] $(\mathbb{P})_{ii} = 1$, $A_{N-O} = 2\, Z_N Z_O$ and $A_{O\cdots O}(s) = Z_N Z_O\, (Z-F)_O/(Z-F)_N$.
[b] Distance and amplitude quantities in $(\text{Å})^2$.
[c] Angle quantities in $(\text{deg})^2$.

Table 21. Error analysis of structure parameters.

	r_{N-O}	$r_{O\cdots O}$	$<O-N-O$	l_{N-O}	$l_{O\cdots O}$
1) $(.0005 r_{ij})^2 \times 10^6$	.361	1.224	---	---	---
2) $(.02 l_{ij})^2 \times 10^6$	---	---	---	.582	.883
3) $\sigma^2_{LS} \times 10^6$	± .474	±8.791	±154816	± .622	±6.444
4) $\sigma^2_2 \times 10^6$	± .443	±5.867	±109700	±4.22	±11.34
5) σ^2_{LS}/σ^2_2	1.07	1.50	1.41	.15	.57
6) σ_T	± .0013	± .0050	±.65	± .0025	± .0050
7) $(\sigma^2_T - 2\sigma^2_{LS})^{\frac{1}{2}}$	± .0009	± .0027	±.33	± .0022	± .0035
8) $(\sigma^2_T - \sigma^2_2)^{\frac{1}{2}}$	± .0011	± .0043	±.56	± .0014	± .0037

(1) - (4) Distance and amplitude quantities in $(\overset{\circ}{A})^2$; angle quantities in $(deg)^2$.

(6) - (8) Distance and amplitude quantities in $\overset{\circ}{A}$; angle quantities in deg.

Table 22. Final results of structure analysis.

	r_{N-O}, Å	$r_{O\cdots O}$, Å	<O-N-O, deg	l_{N-O}, Å	$l_{O\cdots O}$, Å
This work	1.202±.0013	2.213±.0050	134.02±.65	.0382±.0025	.0470±.0050
Microwave (5)	1.197	(2.207)[a]	134.25	----	----

[a] Calculated from the relation $r_{O\cdots O} = 2 r_{N-O} \sin (< O-N-O/2)$.

Table 23. Numerical evaluation of G_S (x 10^{-28}/6. 02472) for $N^{14}O_2$ and $N^{15}O_2$.

	$N^{14}O_2$		$N^{15}O_2$	
	$I^{(a)}$	$II^{(b)}$	$III^{(a)}$	$IV^{(b)}$
G_{11}, Å/md sec^2	. 08407	. 08429	. 08264	. 08284
G_{12}	-. 07232	-. 07261	-. 06751	-. 06778
G_{22}	. 36741	. 36699	. 351298	. 35090
G_{33}	. 18371	. 18349	. 17565	. 17545

(a) $<$O-N-O = 134. 25 deg (5) was used.

(b) $<$O-N-O = 134. 02 deg (this work) was used.

Table 24. Vibrational frequencies (in cm^{-1}) of $N^{14}O_2$ and $N^{15}O_2$ (1, p. 413-427).

	$N^{14}O_2$	$N^{15}O_2$
ν_1	1319, 7	1306. 5
ν_2	749. 8	740. 15
ν_3	1617. 75	1580. 32
ω_1	1357. 8	1342. 5
ω_2	756. 8	747. 1
ω_3	1665. 5	1628. 0

Table 25. Numerical evaluation of Λ (x 10^{-28}) and Δ (x 10^{31}) for $N^{14}O_2$.

	$I^{(a)}$	$II^{(b)}$
λ_1, sec^{-2}	6. 17945	6. 54141
λ_2	1. 99476	2. 03218
λ_3	9. 28587	9. 84213
Δ_1, md $\overset{\circ}{A}$ sec^2	2. 149796	2. 08568
Δ_2	4. 197205	4. 14563
Δ_3	1. 73773	1. 68668

(a) ν_i's (observed fundamental frequencies) were used.

(b) ω_i's (harmonic frequencies) were used.

Table 26a. Error analysis of internal potential constants (in md/Å) obtained from intersections of elliptical contours.

	I[a]	II[b]	III[c]	IV[d]	V[e]
f_r	10.771	8.966	10.162	11.158	9.156
f_α	.969	2.167	1.274	1.094	2.447
f_{rr}	2.368	.563	1.758	2.251	.249
$f_{r\alpha}$	.520	1.176	.566	.533	1.303

[a] $<$O-N-O = 134.02 deg, l_{N-O} = .03815 Å, $l_{O\cdots O}$ = .04698 Å, T = 380.16° K, v_1 = 1319.7, v_2 = 749.8 and v_3 = 1617.75 cm^{-1} were used in this calculation.

[b] Same as (a) save for amplitudes: l_{N-O} + $2\sigma_T(l_{N-O})$ = .04309 Å and $l_{O\cdots O}$ + $\sigma_T(l_{O\cdots O})/2$ = .04949 Å.

[c] Same as (a) save for amplitudes: l_{N-O} + $2\sigma_{LS}(l_{N-O})$ = .03973 Å and $l_{O\cdots O}$ + $\sigma_{LS}(l_{O\cdots O})/2$ = .04825 Å.

[d] Same as (a) save for frequencies: ω_1 = 1357.8, ω_2 = 756.8 and ω_3 = 1665.5 cm^{-1}.

[e] $<$O-N-O = 134.02 deg, l_{N-O} + $2\sigma_T(l_{N-O})$ = .04309 Å, $l_{O\cdots O}$ + $\sigma_T(l_{O\cdots O})/2$ = .04949 Å, T = 380.16° K, ω_1 = 1357.8, ω_2 = 756.8 and ω_3 = 1665.5 cm^{-1}.

Table 26b. Errors in internal potential constants (in md/Å) derived from uncertainties in l_{N-O} and $l_{O \cdots O}$.

	$I^{(a)}$	$II^{(b)}$	$III^{(c)}$
$\sigma(f_r)$	$\pm.903$	$\pm.305$	±1.001
$\sigma(f_\alpha)$	$\pm.599$	$\pm.153$	$\pm.677$
$\sigma(f_{rr})$	$\pm.903$	$\pm.305$	±1.001
$\sigma(f_{r\alpha})$	$\pm.328$	$\pm.023$	$\pm.385$

$^{(a)}$Effect of $\sigma_T(l_{ij})$'s on internal potential constants derived from ν_i's and l_{ij}'s.

$^{(b)}$Effect of $\sigma_{LS}(l_{ij})$'s on internal potential constants derived from ν_i's and l_{ij}'s.

$^{(c)}$Effect of $\sigma_T(l_{ij})$'s on internal potential constants derived from ω_i's and l_{ij}'s.

Table 27. Final results of internal potential constants (GVF) for nitrogen dioxide (in md/Å).

	$\text{I}^{(a)}$	$\text{II}^{(b)}$	$\text{III}^{(c)}$	$\text{IV}^{(d)}$
f_r	$10.77_1 \pm .90_3$	$10.406 \pm .025$	$11.15_8 \pm 1.00_1$	$10.927 \pm .065$
f_a	$.96_9 \pm .59_9$	$1.0968 \pm .0009$	$1.09_4 \pm .67_7$	$1.125 \pm .003$
f_{rr}	$2.36_8 \pm .90_3$	$2.024 \pm .025$	$2.25_1 \pm 1.00_1$	$2.038 \pm .065$
f_{ra}	$.52_0 \pm .32_8$	$.535 \pm .005$	$.53_3 \pm .38_5$	$.390 \pm .020$

[a] $<$O-N-O = 134.02 deg, l_{N-O} = .03815 Å, $l_{O \cdots O}$ = .04698 Å, T = 380.16°K, ν_1 = 1319.7, ν_2 = 749.8 and ν_3 = 1617.75 cm^{-1} were used in this calculation (present work).

[b] $<$O-N-O = 134.25 deg, ν_1 = 1319.7, ν_2 = 749.8, ν_3 = 1617.75, ν_1^* = 1306.5, ν_2^* = 740.15 and ν_3^* = 1580.32 cm^{-1} were used in this calculation (1, p. 413-427).

[c] Same as (a) save for frequencies: ω_1 = 1357.8, ω_2 = 756.8 and ω_3 = 1665.5 cm^{-1} (present work).

[d] Same as (b) save for frequencies: ω_1 = 1357.8, ω_2 = 756.8, ω_3 = 1665.5, ω_1^* = 1342.5, ω_2^* = 747.1 and ω_3^* = 1628.0 cm^{-1} (1, p. 413-427).

*These frequencies correspond to $N^{15}O_2$.

Table 28. Comparison of the calculated and observed frequencies (in cm^{-1}) of $N^{14}O_2$.

	Calculated[a]	Observed[b]	Difference (Percent)
ν_1	1342.6	1319.7	-1.7
ν_2	707.2	749.8	+5.7
ν_3	1618.1	1617.75	-.0$_2$
ω_1	1360.7	1357.8	-.2
ω_2	750.8	756.8	+.8
ω_3	1665.9	1665.5	-.0$_2$

[a] Calculated from internal potential constants tabulated in columns I and III in Table 27 (this work).

[b] Arakawa and Nielsen (1, p. 413-427).

Table 29. Comparison of the calculated and observed root-mean-square amplitudes (in Å) of $N^{14}O_2$.

	Calculated[a]	Observed[b]
at 298° K		
l_{N-O}	.0382	---
$l_{O\cdots O}$	.0469	---
at 380° K		
l_{N-O}	---	.0382+.0025
$l_{O\cdots O}$	---	.0470+.0050

(a)Cyvin (10, p. 117).
(b)This work.

Table 30a. Symmetrized compliance constants (in Å/md) obtained from least-squares refinements.

	I (a)	II (b)	III (c)	IV (d)	V (e)	VI (f)	VII (g)	VIII (h)
C_{11}	.0835 ± .0003	.0836 ± .0003	.0792 ± .0002	.0793 ± .0002	.0822 ± .0002	.0779 ± .0001	.0829 ± .0005	.0787 ± .0004
C_{12}	-.0411 ± .0025	-.0423 ± .0025	-.0354 ± .0015	-.0365 ± .0016	-.0676 ± .0112	-.0542 ± .0016	-.0507 ± .0069	-.0427 ± .0044
C_{22}	.9253 ± .0053	.9252 ± .0053	.9009 ± .0033	.9007 ± .0033	.9750 ± .0197	.9374 ± .0030	.9424 ± .0134	.9137 ± .0089
C_{33}	.1193 ± .0001	.1192 ± .0001	.1125 ± .0001	.1124 ± .0001	.1190 ± .0005	.1123 ± .0001	.1192 ± .0004	.1124 ± .0002

(a) Input data: $<$O-N-O $=$ 134.25 deg, $\nu_1 = 1319.7$, $\nu_2 = 749.8$, $\nu_3 = 1617.75$, $\nu*_1 = 1306.5$, $\nu*_2 = 740.15$, and $\nu*_3 = 1580.32$ cm^{-1}.

(b) Input data: same as (a) save for $<$O-N-O $=$ 134.02 deg.

(c) Input data: $<$O-N-O $=$ 132.25 deg, $\omega_1 = 1357.8$, $\omega_2 = 756.8$, $\omega_3 = 1665.5$, $\omega*_1 = 1342.5$, $\omega*_2 = 747.1$, and $\omega*_3 = 1628.0$ cm^{-1}.

(d) Input data: same as (c) save for $<$O-N-O $=$ 134.02 deg.

(e) Input data: $<$O-N-O $=$ 134.02 deg, T = 380.16° K, $l^2_{N-O} = (.03815)^2$ Å^2, $l^2_{O\cdots O} = (.04698)^2$ Å^2, $\nu_1 = 1319.7$, $\nu_2 = 749.8$ and $\nu_3 = 1617.75$ cm^{-1}.

(f) Input data: same as (e) save for frequencies; $\omega_1 = 1357.8$, $\omega_2 = 756.8$ and $\omega_3 = 1665.5$ cm^{-1}.

(g) Input data: same as (e) plus $\nu*_1 = 1306.5$, $\nu*_2 = 740.15$ and $\nu*_3 = 1580.32$ cm^{-1}.

(h) Input data: same as (f) plus $\omega*_1 = 1342.5$, $\omega*_2 = 747.1$ and $\omega*_3 = 1628.0$ cm^{-1}.

Table 30b. Comparison of the observed and calculated frequencies (in cm^{-1}) and mean-square amplitudes (in $\overset{\circ}{A}{}^2$) for nitrogen dioxide.

	Observed	Calculated							
		$I^{(a)}$	$II^{(b)}$	$III^{(c)}$	$IV^{(d)}$	$V^{(e)}$	$VI^{(f)}$	$VII^{(g)}$	$VIII^{(h)}$
ν_1	1319.7	1320.1	1320.1	---	---	1319.7	---	1319.7	---
ν_2	749.8	749.8	749.8	---	---	749.8	---	750.1	---
ν_3	1617.75	1616.92	1616.90	---	---	1617.87	---	1616.97	---
ν^*_1	1306.5	1306.1	1306.1	---	---	---	---	1306.6	---
ν^*_2	740.15	740.13	740.13	---	---	---	---	739.90	---
ν^*_3	1580.32	1581.06	1581.07	---	---	---	---	1581.14	---
ω_1	1357.8	---	---	1357.7	1357.4	---	1357.8	---	1357.1
ω_2	756.8	---	---	756.8	756.8	---	756.8	---	756.9_7
ω_3	1665.5	---	---	1665.2	1665.2	---	1665.5	---	1665.2_7
ω^*_1	1342.5	---	---	1342.8	1342.8	---	---	---	1343.2
ω^*_2	747.1	---	---	747.1	747.1	---	---	---	746.9
ω^*_3	1628.0	---	---	1628.3	1628.3	---	---	---	1628.3
at 380°K									
l^2_{N-O}	$.001455^{(i)}$	---	---	---	---	$.001506_4$	$.001462_7$	$.001508_9$	$.001465_4$
$l^2_{O\cdots O}$	$.002207^{(j)}$	---	---	---	---	$.0022067$	$.002206_8$	$.002286_9$	$.002264_8$

(a) – (h) Same as Table 30a.

(i) $(.0381_5)^2 = .001455$

(j) $(.0469_8)^2 = .002207$

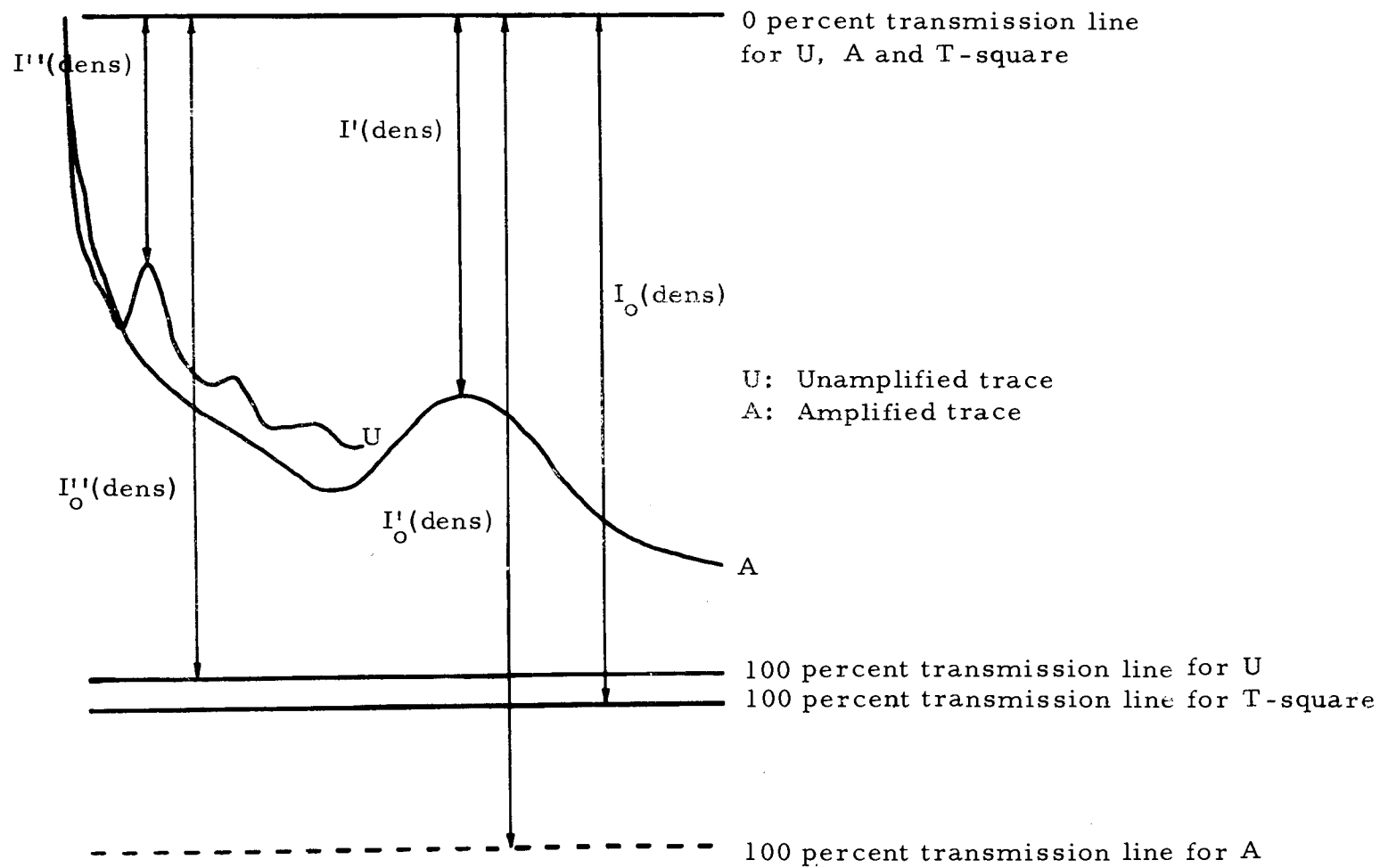* These frequencies correspond to $N^{15}O_2$.

APPENDIX II

FIGURES

Figure 1. Calibration of densitometer traces of a typical photographic plate.

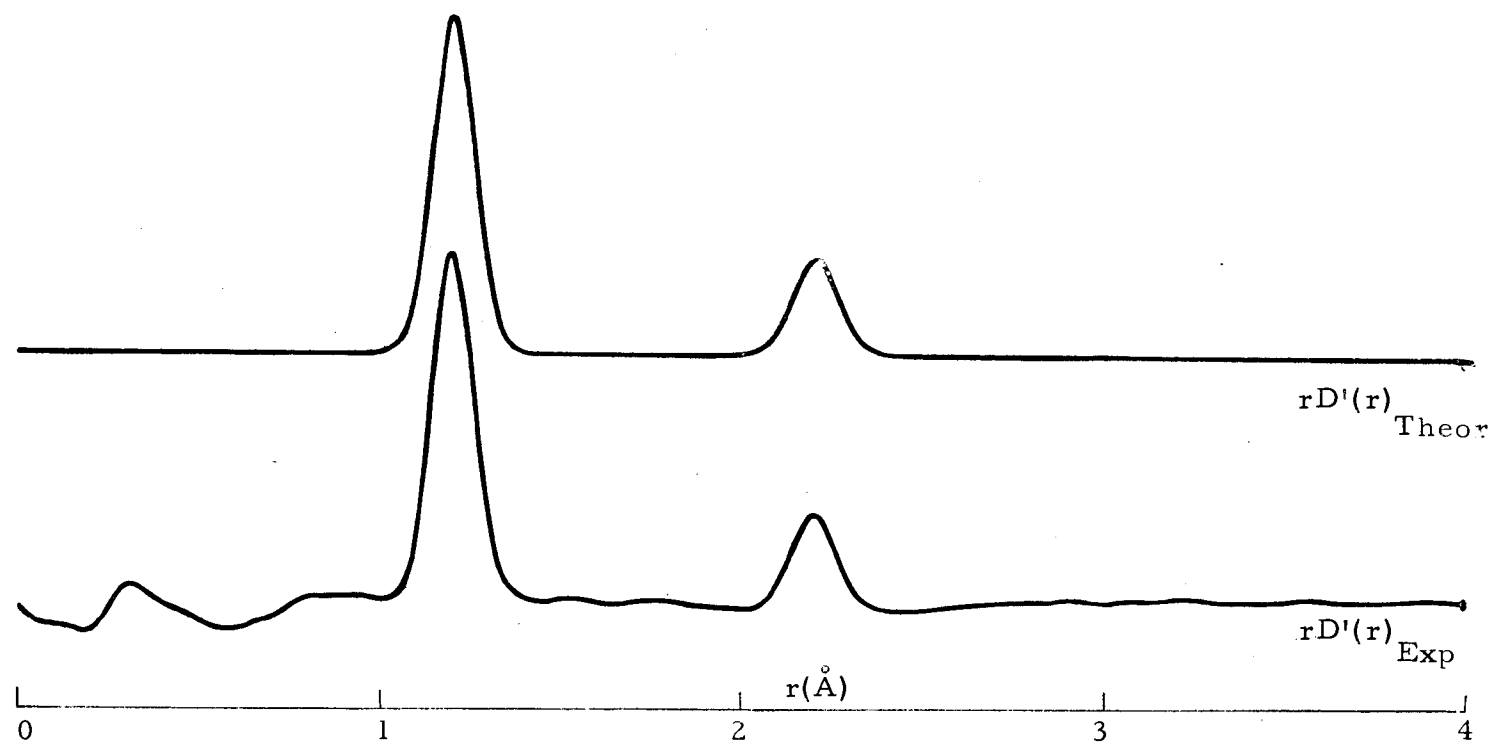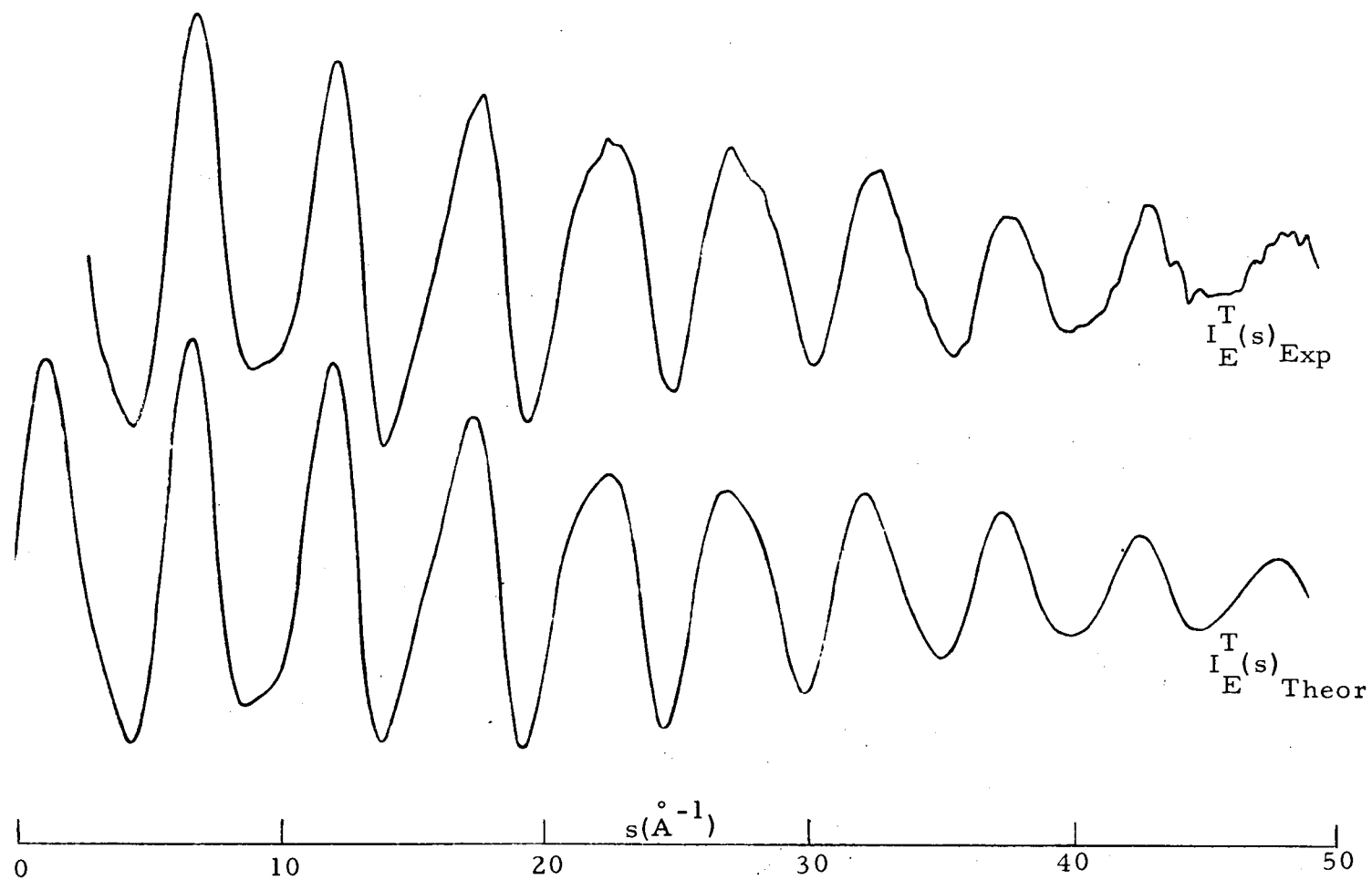Figure 2. Experimental and theoretical radial distribution curves for nitrogen dioxide,

$I_E^T(s)_{Exp}$

$I_E^T(s)_{Theor}$

$s(\overset{\circ}{A}^{-1})$

0   10   20   30   40   50

Figure 3. Experimental and theoretical modified molecular intensity curves for nitrogen dioxide.

A: $I_E^a(s)_{Exp}$; $2.50 \leq s \leq 20.75$

B: $I_E^b(s)_{Exp}$; $10.25 \leq s \leq 42.00$

C: $I_E^c(s)_{Exp}$; $18.50 \leq s \leq 49.75$

(dashed portion not used in $I_E^T(s)_{Exp}$)
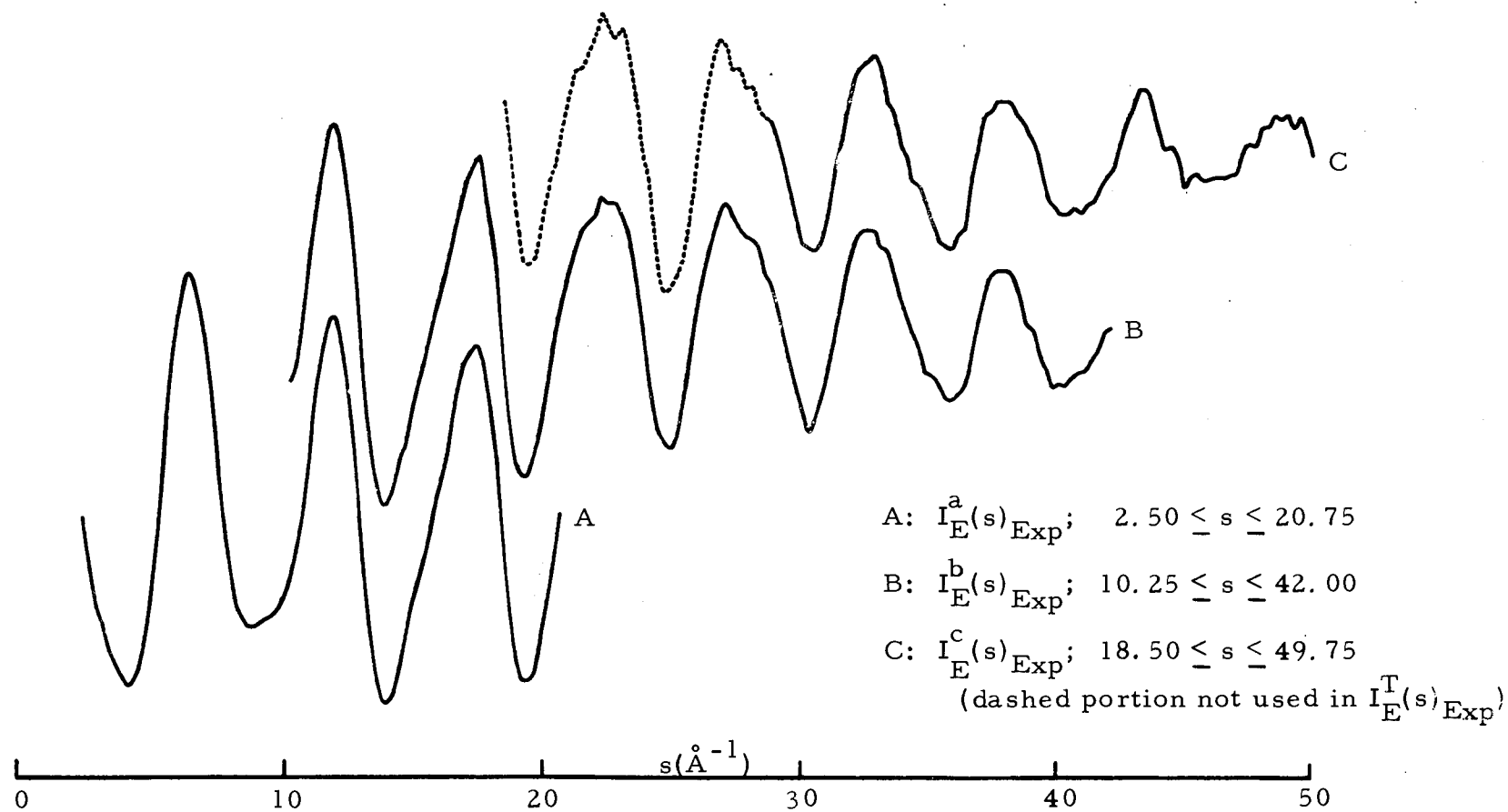
$s(\text{Å}^{-1})$

Figure 4. Experimental modified molecular intensity curves from separate camera distances for nitrogen dioxide.
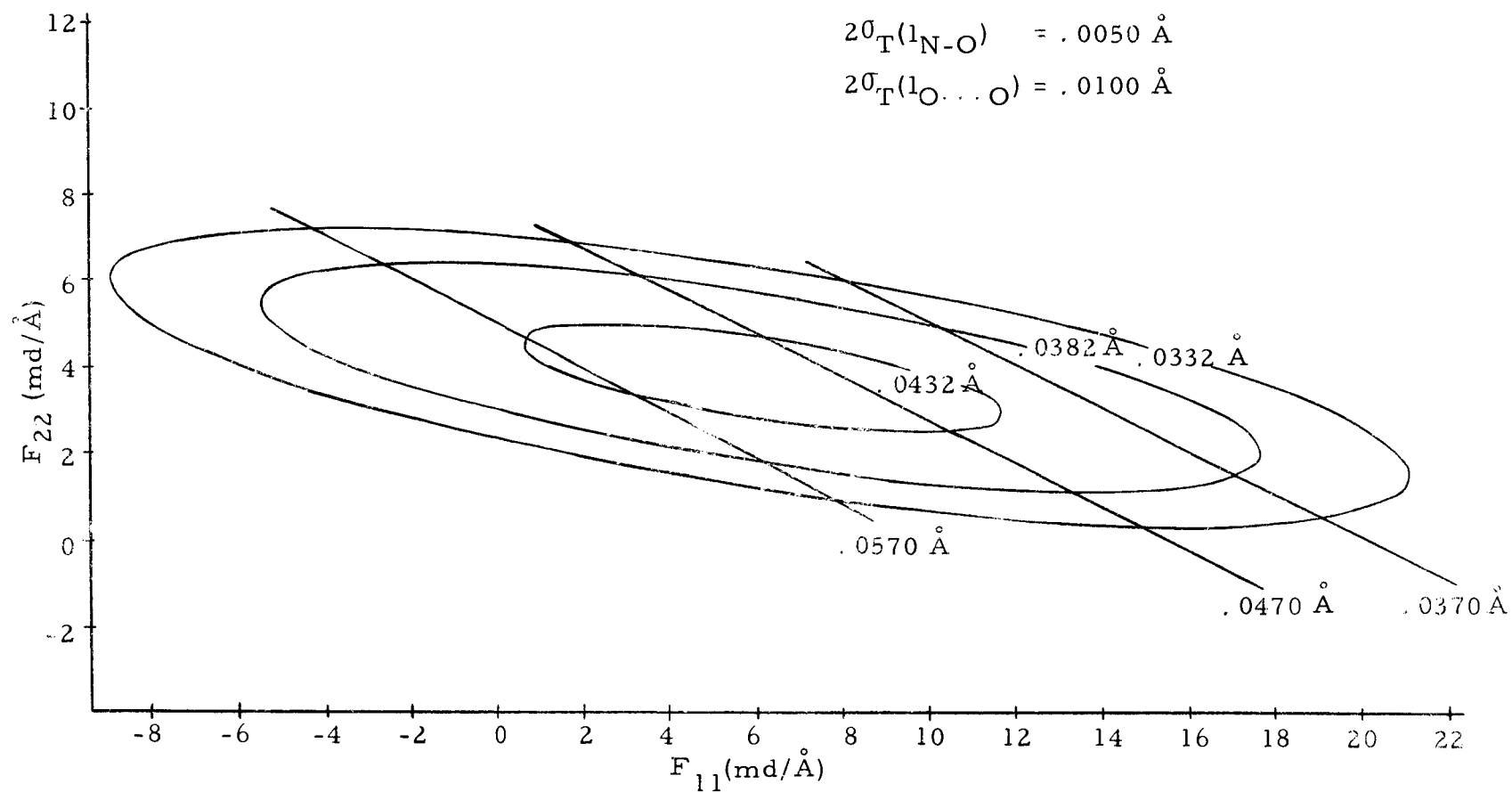
Figure 5. Relation between root-mean-square amplitudes and symmetrized potential constants for nitrogen dioxide.